PACS №: 84.70+p

C.M. Fowler*, L.L. Altgilbers**
*Los Alamos National Laboratory Los Alamos,
New Mexico USA 87545
** U.S. Army Space and Missile Defense Command,
P.O. Box 1500, Huntsville, AL 35807

Magnetic Flux Compression Generators: a Tutorial and Survey

Contents

Abstract

Explosive-driven magnetic-flux-compression generators have been around since the early 1950s, when they were independently invented in the United States and the Former Soviet Union. Interest in these generators has been cyclic over the years and we appear to be in the upswing of renewed interest, not only in the US and Russia but other countries as well. Therefore, it was decided that it was time to write a tutorial article based upon the experiences of one of the original founders of this technology and a co-author of this paper; that is, C.M. Fowler. In this paper, we will review some of the fundamental ideas behind magnetic flux compression, the types of flux compression generators, their characteristics, and the power conditioning required to make them practical power sources for various loads. Some of their applications will also be presented followed by brief reviews of current university and government/industrial programs.

1. Introduction

1.1. Generator Principles

Explosive-driven magnetic-flux-compression generators are devices that convert part of the energy contained in high explosives into electromagnetic energy. Owing to the large energy content, high-power capability and high pressures generated by the explosives, these devices have found wide application as pulsed-power sources, particularly where weight and volume are limited, and in the generation of ultra-high magnetic fields. In general, the explosives are used to compress an initial magnetic flux by driving part, or all, of a conducting surface which contains the flux. These conductors do work on the magnetic fields by moving against them, which results in an increase in electromagnetic energy. This additional energy comes originally from the chemical energy stored in the explosives, a part of which is transmitted to the conductors.

As in most fields of study, a special nomenclature has developed over the years for these devices. In common with conventional practice, the moving conductors are frequently called *armatures* (or *liners*), whereas, fixed elements basic to the devices are often called *stators*. When there is little chance of confusion, the devices are often simply called *generators*.

Other generic names found in the literature, together with appropriate abbreviations, include: Flux Compression Generators (FCG), Magnetic Flux Compression Generators (MFCG), and, particularly in the Soviet, and now Russian, literature, Magneto-Cumulative Generators (MCG). None of these abbreviated descriptions is perfect, but for the time being we appear to be stuck with them. As will be noted in the following sections, there are several classes of these devices in common use, each class having some characteristics that may make it more suitable for a specific application. The most commonly used generators usually carry a name descriptive of their class, often indicative of conductor components characteristic of that class. Examples are "coaxial generators", "plate generators", and "spiral or helical generators". Sketches of several generator types that will be discussed in more detail are shown on Fig. 1. While these generator classes may, externally, bear little resemblance to each other, they all operate on the same principles outlined below. In the remainder of this text, we will use FCG, or simply generator, in a generic sense, and class names, such as plate generator in specific cases.

A rather extensive FCG literature has accumulated over the years, including a substantial

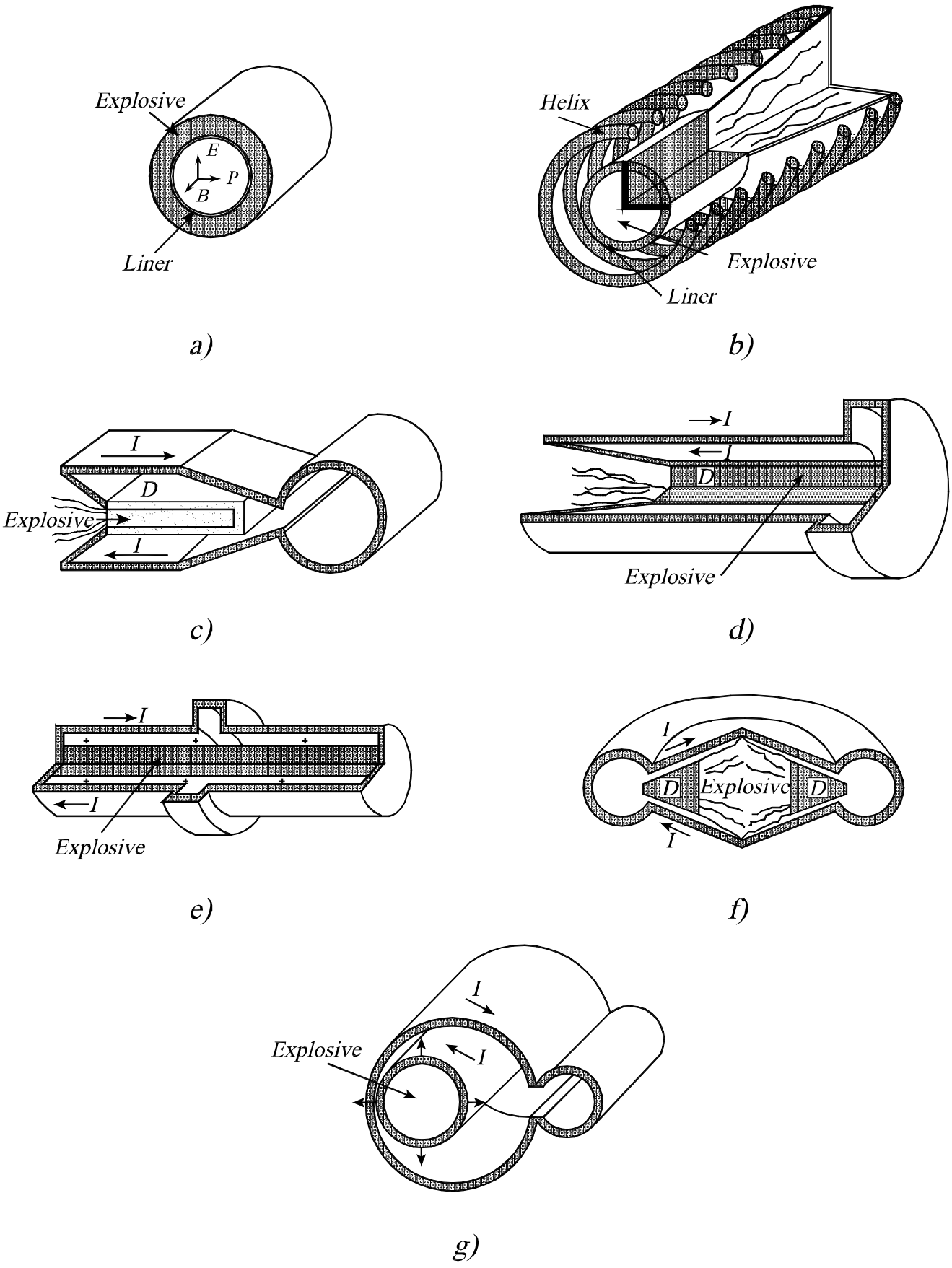

Fig. 1. Sketches of a number of generator types discussed in the text appear to be different, but all operate under the same basic principles.

amount in Russian journals. Rather than compiling a bibliography with hundreds of entries, we have adopted the following procedure. Individual papers will be referenced only if they elucidate some specific point or application discussed in the text. For a broader view, the reader may consult the first twelve references. These include the 7 published volumes [1–7] and one in publication [8] comprising the proceedings of the "Megagauss Conferences" that are devoted to this subject, two books [9,10], and two monographs [11,12], that are devoted to this subject. From the papers cited therein and the proceedings of the various IEEE Pulsed Power Conferences, that usually contain a number of related papers, a fairly complete view may be obtained of where such work has been done, as well as the key people involved. The reader will notice that there is a bias towards work done at Los Alamos. For this, we make no apologies, since the scope of the Los Alamos work is broad and we are, of course, more familiar with it. However, we should note that the All-Russian Scientific Research Institute of Experimental Physics (VNIIEF), also known as Arzamas-16, in Russia, in particular, and Loughborough University continue their excellent work in developing and applying FCGs and that there are relatively new, and in some cases aggressive, programs in Australia, Canada, China, France, Germany, Japan, The Netherlands, South Africa, South Korea, Sweden, and Ukraine. Also, a consortium of universities including Texas Tech, Texas A&M, University of Missouri in Rolla, and the University of Texas in Austin have spent 5 years working on a Multidisciplinary University Research Initiative (MURI) program to investigate the basic physics of FCGs as well as other explosive driven power sources. Additionally, Texas A&M University has initiated a program to develop very compact FCGs. Other Universities that have recently investigated FCGs are the University of Missouri in Columbia that investigated their use for mine detection and the University of Alabama in Huntsville that investigated their use for micro fusion propulsion. Most of these programs will be briefly summarized in Section 6.

1.1.1. General Principles

The basic principles of FCG operation [9–12] may be illustrated with the use of Fig. 2. The sketch is an idealized version of a plate generator, which will be discussed in more detail later. Basically, it consists of a conducting rectangular box, an input slot at the upper left, and a slab of high explosive on the upper plate. Current, usually supplied from a capacitor bank, is passed through the input slot to develop an initial magnetic flux within the box. The current is assumed to flow uniformly over the width of the box. The length l and width w of the box are assumed to be large

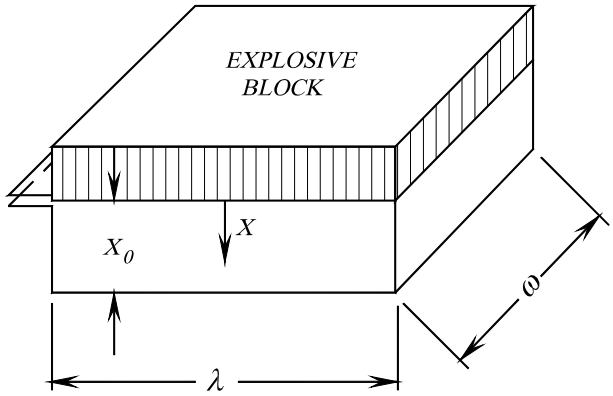

Fig. 2. Planar implosion system, illustrating principles of flux compression.

enough compared to the height x so that edge effects can be neglected. The current I is then assumed to be distributed uniformly over the box width w. The high explosive is detonated at such a time that it closes the input slot at peak current, or peak magnetic flux within the box, and then continues to drive the top metal plate downward. A fundamental result from Maxwell's equations is that magnetic flux is conserved when bounded by a perfect conductor regardless of the subsequent distortion or displacement of the conductors [13]. As a first approximation, we will assume that once the input slot is closed, the box is now a bounding perfect conductor.

Before embarking upon the common methods of analyzing FCG performance, we note that as the top plate of the generator is driven downward, the flux enclosing area is reduced, and thus, the average magnetic field must increase. The complete solution of most FCG problems is formidable indeed, usually requiring full three-dimensional (3D) magnetohydrodynamic (MHD) treatments, with knowledge of the constitutive relations under extreme conditions. Progress in code development continues to be good, as noted later in this report, but it will be some time before complete treatments of all but the simplest FCGs will be available. Consequently, varying degrees of simplification are employed in analyzing FCG performance. In Ref. 13, for example, it is shown that the magnetic fields, and their accompanying electric fields, actually build up by electromagnetic waves reflected back and forth from the top and bottom plates. However, in time scales long compared to the transit times (of order 10^{-9} to 10^{-10} seconds), the fields may be calculated from the current in an adiabatic fashion without undue error.

Under these conditions (no flux loss, negligible edge effects), we can calculate the new magnetic field B when the top plate moves from its initial height x_0 to a new, lower height x and when the initial field is

B_0. Conservation of magnetic flux gives[1]

$$\phi = B_0 l x_0 = \phi(x) = Blx. \quad (1)$$

In the examples treated in this section, such as the one discussed here, edge effects are usually ignored and the magnetic field B is parallel to the flux-compressing conductor. In this case, the magnetic stress on the conductor is compressive and normally treated as a magnetic pressure exerted on the conductor [14]. Here, the magnetic pressure and the energy density of the magnetic field are both equal to $B^2/2\mu$ (Pascals or joules/m^3). The magnetic energies, ($(B^2/2\mu)V$, using Eq. (1), are

$$E_0 = \frac{B_0^2}{2\mu} l w x_0, \quad E(x) = \frac{B^2}{2\mu} l w x = E_0 \frac{x_0}{x}. \quad (2)$$

The energy increase is easily shown to equal the work done by the top plate moving against the magnetic pressure

$$W = \int F ds = \int_{x_0}^{x} \frac{B^2}{2\mu} l w (-dx) = E(x) - E_0. \quad (3)$$

While it is perhaps somewhat more satisfying to work with magnetic fields, by far most of the analyses of generator circuits are carried out using an engineering or lumped parameter approach. Here, currents are usually used instead of magnetic fields and the geometry of the generators is accounted for by inductances, although instances encountered later such as flux losses and magnetic forces do employ the use of fields. The inductance, L, is so defined that when it is multiplied by the generator current, the magnetic flux linked to the current is obtained. For the parallel plate configuration of Fig. 2, the field and current are related by

$$B = \mu I / w. \quad (4)$$

Putting this expression into Eq. (1), the generator inductance is found to be

$$L(x) = \mu l x / w. \quad (5)$$

With these substitutions, Eqs. (1) and (2) become

$$\phi = L_0 I_0, \qquad \phi(x) = L(x) I, \quad (6)$$

$$E_0 = \frac{1}{2} L_0 I_0^2, \quad E(x) = \frac{1}{2} L(x) I^2 = E_0 \frac{L_0}{L(x)}. \quad (7)$$

More generally, Eqs. (1) and (6), which express the conservation of flux in perfectly conducting systems, can be written

$$\frac{d\phi}{dt} = \frac{d(BA)}{dt} = \frac{d(LI)}{dt} = 0. \quad (8)$$

[1] Unless specifically stated otherwise, rationalized MKS units are used throughout the text.

Equation (8) is also a statement that the voltage around the circuit, $d\phi/dt$, is zero. If we expand the last of these expressions and use Eqs. (4) and (5), we obtain

$$I\frac{dL}{dt} + L\frac{dI}{dt} = Blv + L\frac{dI}{dt} = 0. \quad (9)$$

These terms are readily identifiable as the motional voltage across the moving conductor, or generator armature, and the inductive voltage across the remaining inductance in the generator.

1.1.2. Field-line Stretching

Occasionally the literature contains expressions such as "the energy required to stretch field lines." This expression has a ready interpretation in terms of flux conservation concepts. Consider a cylinder of length W_0 and cross-sectional area A_0 enclosing a uniform magnetic field B_0 directed along the cylindrical axis. The flux enclosed by the cylinder is $B_0 A_0$ and the magnetic energy contained in the cylinder is $E_0 = W_0 A_0 B_0^2/2\mu$. If the cylinder is now forcibly changed to have new dimensions W_1 and A_1, the energy in the cylinder becomes $E_1 W_1 A_1 B_1^2/2\mu$. However, if flux is conserved, $B_1 A_1 = B_0 A_0$, the energy expression can be rewritten as $E_1 = E_0(W_1/W_0)(A_0/A_1)$. As can be seen, work is done on the magnetic field by decreasing the area (flux-compression) or by increasing the length (field-line stretching). This energy relation is not unexpected, since, with neglect of edge effects as above, the inductance of the cylinder is proportional to A/W, as in Eq. (5), and the energy relation is equivalent to $E_1 = E_0 L_0/L_1$, as in Eq. (7).

1.1.3. The Generator Impedance

Figure 3 is a schematic of a circuit containing a generator, with inductance L, and a fixed inductive load L_1 that is to be energized. The inductance symbol with an arrow is commonly used to indicate a generator. Allowance for source or waste inductance (from various external leads to the load, residual generator inductance, etc.) is indicated by l, and circuit resistance is shown as R. The equation governing the performance of this circuit is then:

$$\frac{d}{dt}[(L + l + L_1)I] + IR = 0. \quad (10)$$

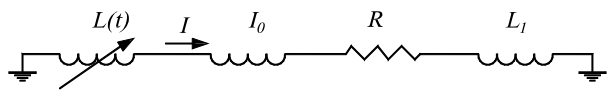

Fig. 3. Circuit schematic showing FCG (variable inductor) powering series load, L_1, source inductance, I_0, and resistance R.

Several consequences follow from Eq. (10)

- If $R = 0$, the circuit is perfectly conducting, and the circuit flux $(L+L_1+l)I$ is conserved. Clearly, as L decreases, the current I increases.

- When $R \neq 0$, we expand the equation as follows:

$$\left[\frac{dL}{dt} + R\right] I + (L + L_1 + l)\frac{dI}{dt} = 0. \qquad (11)$$

Since generator inductances are forcibly reduced, dL/dt is negative. The absolute value of dL/dt is usually called the internal impedance of the generator. It may vary widely during the generators operating time. However, it is clear from Eq. (11) that the impedance must exceed the resistance R, at least part of the time during generator operation, or the current will not amplify.

As noted earlier, IdL/dt is the voltage across the moving armature that serves to drive the entire system.

- Multiplication of Eq. (10) by I leads to

$$\frac{1}{2}\frac{dL}{dt}I^2 + \frac{d}{dt}\left(\frac{1}{2}LI^2\right) + \frac{1}{2}l\frac{dI^2}{dt} + \frac{1}{2}L_1\frac{dI^2}{dt} + I^2R = 0. \qquad (12)$$

Equation (12) is clearly a power equation whose last four terms are the rates at which energy is delivered to the remaining generator inductance, the source inductance, the load inductance, and in heating the resistance R. The negative first term, $(I^2/2)(DL/dt)$, clearly is the power delivered by the generator to the other circuit elements. As shown by Eq. (11), the generator impedance, on average, must exceed the circuit resistance for current amplification. As seen from Eq. (12), the generator impedance, on average, must exceed twice the circuit resistance for the inductance load energy to amplify.

In some cases, skin losses in the generator can be represented by a generator resistance. In such cases, the resistance depends upon the generator action in a complex way. Among the significant factors affecting the resistance are changes in conductor skin depth, temperature, and path length as generator action proceeds. For illustrative purposes, however, we consider the case where R of Eq. (10) can be considered a function of time, explicitly. If, further, the inductances in the generator circuit are also functions only of time, the solution of this equation is

$$I(t) = I_0\frac{L_T(0)}{L_T(t)}\exp\left[-\int_0^t \frac{R}{L_T(y)}dy\right]. \qquad (13)$$

Here, we have abbreviated the total circuit inductance $L + l + L_1$ by L_T.

The inductive energy E of the circuit becomes

$$E(t) = E_0\frac{L_T(0)}{L_T(t)}\exp\left[-\int_0^t \frac{R}{L_T(y)}dy\right]. \qquad (14)$$

1.1.4. Results for an Idealized Generator

For purposes of illustration, we consider the generator pictured in Fig. 2, whose inductance is taken to be given by Eq. (5). We will assume that the top plate moves with a constant velocity v, starting from an initial plate separation x_0, so that we have, then, from Eq. (5),

$$L = L_0(1 - t/\tau) \qquad (15)$$

where

$$L_0 = \mu l x_0/w \qquad (16)$$

and

$$\tau = x_0/v. \qquad (17)$$

At time τ, the top plate has contacted the fixed bottom plate, and generator action has been completed. The time τ is called the generator *burnout time*. With l, L_1, and R constant, Eqs. (13) and (14) reduce to

$$I(t) = I_0\left[\frac{L_T(0)}{L_T(t)}\right]^{1-Rt/L_0}, \qquad (18)$$

$$E(t) = E_0\left[\frac{L_T(0)}{L_T(t)}\right]^{1-2Rt/L_0}. \qquad (19)$$

Here, as before, we have abbreviated the total circuit inductance $L + l + L_1$ by L_T.

At burnout, $t = \tau$, the current and energy are at a maximum. The energy is distributed between the two inductances l_0 and L_1 in proportion to their inductances. The maximum current and energy, E, into the load L_l, therefore become

$$I(\tau) = I_0\left[\frac{L_T(0)}{L_T(\tau)}\right]^{1-R\tau/L_0}, \qquad (20)$$

$$E(\tau) = E_0\frac{L_1}{L_1 + l_0}\left[\frac{L_T(0)}{L_T(\tau)}\right]^{1-2R\tau/L_0}. \qquad (21)$$

The generator impedance $|dL/dt|$, from Eq. (15), is

$$|dL/dt| = L_0/\tau. \qquad (22)$$

As expected, Eqs. (20) and (21) show that the generator impedance must exceed R for current gain and must exceed 2R for energy gain.

To gain a feeling for the magnitudes involved, we assume the following values for the parallel plate generator under discussion:

Initial Inductance:	$L_0 = 0.3$ μH
Load Inductance:	$L_1 = 10$ nH
Source Inductance:	$l = 2$ nH
Resistance:	$R = 3$ mΩ
Burn Time:	$\tau = 10$ μs
Initial Current:	$I_0 = 1$ MA.

Thus,

Total Initial Inductance:	$L_T(0) = 0.312\ \mu$H
Total Final Inductance:	$L_T(t) = 0.012\ \mu$H
Generator Impedance:	$\lvert dL/dt\rvert = 0.03\ \Omega$
Exponent:	$R_\tau/L_0 = 0.100$.

From these values, we find the initial magnetic energy:

$$E_0 = \frac{1}{2}L_T(0)I_0^2 = \frac{1}{2}(0.312)\cdot 10^{-6}\cdot(10^6)^2 = 0.156 \text{ MJ}.$$

With $R_\tau/L_0 = 0.100$ we find the current and energy at generator burnout from Eqs. (20) and (21)

$$I(\tau) = 10^6\left(\frac{0.312}{0.012}\right)^{0.9} = 18.77 \text{ MA},$$

$$E_1(\tau) = (0.156\cdot 10^6)\cdot\left(\frac{0.010}{0.012}\right)\left(\frac{0.312}{0.012}\right)^{0.8} = 1.762 \text{ MJ}.$$

Finally, we note that at burnout, the internal armature voltage is

$$(\lvert dL/dt\rvert I)_\tau = (0.03)(18.77\cdot 10^6) = 563 \text{ kV}$$

and the power supplied by the generator is

$$\left(\frac{1}{2}\lvert dL/dt\rvert I^2\right)_\tau = \frac{1}{2}(0.03)(18.77\cdot 10^6)^2 = 5.28 \text{ TW}.$$

It is also clear that good generator practice calls for a minimum of stray circuit resistance and source inductance. If the resistance were negligible, the burnout current would increase to 26 MA and the load energy to 3.38 MJ. If the source inductance were also negligible, peak current and energy would be 31 MA and 4.81 MJ, respectively.

It is clear that a parallel plate generator of this type is not well suited to power loads that are resistive. Some generators, described later, can achieve burnout impedances in the low-ohm range and can be used to power directly some resistive loads. However, impedance matching techniques are usually more effective, particularly when the load exceeds a few ohms. These techniques will also be described later.

Much effort has been expended in developing approximate expressions for generator inductances. The difficulty arises, of course, because the concept of inductance is itself somewhat artificial. Generally speaking, when an inductance can be defined, it is a geometric quantity that relates circuit flux to the total circuit current, as determined from specific boundary conditions. Part of the complexity for generators arises because their geometric configurations vary with time, with a consequent redistribution of currents and varying current skin depths in the conductors. In some cases, particularly when very large currents are generated, some of the generator elements can be moved by magnetic forces and this also modifies the inductance.

We do not want to leave the impression that the inductance approach is fraught with insurmountable difficulties. Indeed, by approximate accounting for factors such as skin depth and current concentration, generator models have been developed that lead to almost quantitatively correct predictions. Even the simplest models usually lead to qualitatively correct results. In any event, until solutions can he obtained from first principles; we will have to be satisfied with these approximate treatments.

1.2. Explosive Properties

Chemical high explosives serve as the primary FCG energy source. Table I gives a list of commonly used explosives, together with some of their properties of interest. These data are extracted from Refs. 15 and 16, which contain extensive data tabulations of many explosives.

The explosives are tabulated in decreasing power levels, ranging from the plastic-bonded explosive PBX 9501 to the liquid explosive nitromethane. Values given in the table are representative of a given explosive but vary, sometimes considerably, with a number of factors. Among these are small variations in chemical composition, temperature at detonation, and for solids, grain size and initial density, which can vary with pressing or casting procedures.

The properties of interest in Table I are given in MKS units, but for the most part can be read directly in more commonly used units. Thus, the density of PBX is 1840 kg/m^3 or 1.84 gm/cm^3. Similarly, the detonation velocity is 8.8 mm/s, the detonation energy is 11 kJ/cm^3 and the power density (detonation velocity times detonation energy) is 9.7 GW/cm^2. The old, time-honored pressure unit of kilobars has now been largely replaced by pascals. Thus, the Chapman-Jouget pressure (immediately behind the detonation front) is 37 GPa or in older units, 370 kb or approximately 370,000 atmospheres. Among other factors of importance are stability (against accidental detonation) and in some cases mechanical strength. Generally speaking, cast and pressed explosives can be machined in various shapes to high tolerances, and for each type, show high reproducibility in performance. Explosive science and technology is, of course, very broad in scope with a very large body of literature available. For those interested in more details, [17–19] may be consulted with profit.

The means of controlled detonation of high explosives also has an extensive literature database, but few, if any, consolidated treatments exist, such as those referenced for high explosives. Most modern detonators consist of a small, sensitive explosive pellet

Table 1. Properties of Selected Explosives.

Explosive	Density kg/cm^3 x 10^{-3}	Detonation Velocity m/s x 10^3	CJ Pressure GPa	Energy Density GJ/m^3	Power Density GW/m^2 x 10^{-4}
PBX 9501	1.84	8.8	37	11.0	9.7
Composition B	1.72	8.0	29.5	8.6	6.8
TNT	1.6	7.0	21.5	7.8	5.5
EL5060*	1.48	7.0	20.5	7.0	4.9
Baratol	2.6	5.1	14.0	7.8	4.0
Nitromethane	1.13	6.2	12.5	6.4	4.0

*DuPont Trade Name, Detasheet C

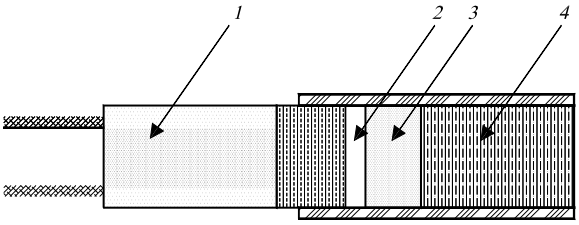

Fig. 4. Electric Bridge Wire Detonator: 1 – molded head, 2 – brigewire (gold), 3 – initiating explosive (e.g. PETMN), and 4 – high density explosive (e.g. RDX).

that is initiated at one end by an electrically exploded bridge wire in intimate contact with one face of the pellet (see Fig. 4). The other face of the pellet is in intimate contact with the main charge. Detonation of the main charge occurs when the explosive detonation front from the pellet reaches it. Examples of detonator fabrication can be found in [20].

Various techniques have been employed to extend the single-point initiation from a detonator to simultaneous initiation over a linear element [21], plane surfaces [22,23], and cylinders [24,25].

We will briefly mention another initiation technique that has been developed over the last several years, called the "slapper" system. Here, the pressure of the exploding bridge wire is used to drive small plastic pellets housed in short barrels. The pellets are driven fast enough to initiate the explosive. Single-point initiation, line initiation, and surface initiation with slapper systems are discussed in [26].

1.3. Other Flux Compression Techniques

Almost any method for moving a conductor fast enough can, in principle, be adapted as a power source for FCGs. To get an idea of what constitutes a good conductor and what speed is required, consider the exponent $R\tau/L_0$ of Eq. (18). As noted earlier, the smaller this value, the more effective the plate generator, to which it applies, operates. The reciprocal of this expression is related to a magnetic Reynolds number, R_e. For purposes of convenience, we will assume that the resistance in the plate generator circuit is all in the moving plate. With a conductivity σ and current sheet of thickness λ, the resistance is then

$$R = l/w\sigma\lambda$$

and with Eqs. (16) and (17), we obtain

$$R_e = L_0/R\tau = \mu\sigma\lambda v = \mu v/(\rho/\lambda). \qquad (23)$$

Expressions similar to Eq. (23) typically arise in flux-compression analysis. Generally, they assume the form $L_0/\tau R$ or a ratio of velocity to ohms per square of conductor. In many cases, as in the present case, flux compression occurs only when R_e is of order or greater than one. To get some fee1ing for magnitudes of R_e, consider a copper plate, $\sigma \sim 5{\cdot}10^7$ mho/m, $\lambda = 1$ mm, and $v = 4 \cdot 10^3$ m/s (typical of explosive-driven flux compressors). Here,

$$R_e = (1.26 \cdot 10^{-6})(5 \cdot 10^7)(1.0 \cdot 10^{-3})(4 \cdot 10^3) \doteq 250.$$

As another example, consider the explosive-driven MHD generator described by Jones and McKinnon [27]. Here, explosive products were driven down an MHD channel. The explosive front face was seeded with cesium nitrate to improve the conductivity of the front. In a typical experiment, the explosive front moved through the externally applied magnetic field with an average velocity of 8 km/s and had a resistance of 5.3 mΩ/sq. Thus,

$$R_e = (1.26 \cdot 10^{-6})(8 \cdot 10^3)/(5.3 \cdot 10^{-3}) \doteq 2.$$

It is not the purpose of this article to describe MHD generators, since these seem best adapted to long-pulse, low-voltage operation. However, attention should be paid to a couple of articles. Velikhov

and his collaborators [28] considered a generator where lithium plasma produced from a thermonuclear device is driven through an MHD channel in an externally supplied magnetic field. Although the Reynolds number is low (< 1.0), the overall efficiency of the device is high. Finally, we mention briefly the pulsed MHD generators built by Baum and Shimmin [29] and by Gill [30]. In these devices, specially configured high explosives shock Xenon or Argon gas, which is then driven at high speed through an MHD channel. The conductivities appear to be high, with resultant large Reynolds numbers (thought to be greater than ten).

Several other ways in which flux has been compressed will be mentioned briefly.

- Rotating Machinery. The initial energy source may be a rotating flywheel, such as a homopolar generator. The normal output pulse can be compressed in time with greater output power by employing special built-in circuitry and mechanical construction that involves flux compression. A number of generators of this type, called "compulsatore", have been designed and built by Weldon et al [31].

- Compressed Gases. In this concept, Velikhov and his collaborators [32] considered using high-pressure gas to implode a thin-walled copper cylinder that contains an initial magnetic flux. Here, the energy source is the stored gas, which can be quite high at the 1–2000 atmospheres suggested. To achieve the simultaneity required for good flux compression, the high-pressure gas is kept away from the liner by a thin metal-diaphragm system, chosen of such thickness as to be just below its yield strength. A current pulse is then applied to the diaphragm that should lead to simultaneous rupture. There appear to be several difficulties with this system, and we do not know if actual experiments were undertaken.

- Explosive Gases. Hahn [33], for his doctoral thesis, carried out flux-compression experiments where the energy source was contained in a stoichiometric mixture of hydrogen and oxygen. By operating at high pressure (60 atmospheres), the energy content of the explosive mixture was several percent of that contained in the explosives listed in Table 1. In his experiments, the gas was located in the center of a thin-walled metal cylinder. Initiation of the gas mixture was obtained by electrically exploding a thin wire placed axially in the cylinder. Magnetic flux was located between the metal cylinder and an outer fixed-cylindrical conductor. Flux compression was obtained when the inner cylinder expanded, after initiation of the gas.

- Magnetic Fields. The experiments we describe here use a capacitor bank as the initial energy source. In the first system we consider, developed by Cnare [34], the bank is discharged through a heavy, cylindrical one-turn coil. Inside this coil, there is a thin-walled concentric metal tube. Some flux leaks into the thin-walled tube by diffusion of the field produced by the heavy outer coil. Flux may also be inserted into the tube by an external coil pair. The pressure of the larger magnetic field on the outer surface of the thin-walled cylinder implodes it, with a consequent build-up of its field by flux compression. In this way, Cnare was able to develop magnetic fields exceeding a megagauss. Recently, Miura and his coworkers [35] have generated fields exceeding 6 MG in this manner and applied them to solid state investigations.

- Linus Concept. In this concept, a rotating liquid (NaK) liner surrounds a plasma contained by a magnetic field within the liner. Compressed gases, through ingenious piston arrangements, drive the liner inward to a minimum radius determined by the field-plasma pressure and the increasing liner rotational energy, after which it expands outward, with a further repetition of the cycle. The rotation of the liner overcomes the Raleigh-Taylor instabilities that would normally destroy it. Framing camera pictures of several different experiments confirm the integrity of the liner, at least as far as a complete cycle, and also show flux compression. Reviews of the program are given by Turchi and his associates [36] and by Robson [37].

- Plasma Compressors. While plasmas may be formed naturally during the latter stages of flux compression, in some concepts a plasma is purposely formed at the very outset for flux compression. Linhart [38] describes a system where an initial magnetic field was imploded by a surrounding plasma layer, formed by passing a Z-current through a very thin foil. An initial field of 2 kG was compressed to 60 kG. In later experiments, Felber and coworkers [39] obtained axial magnetic fields of 1.6 MG by employing a gas-puff Z-pinch plasma to compress the initial field.

- Metal Flyer Plates. Metal plates driven to high speeds by light gas guns have been suggested as flux compressors. One such concept is given in [40]. Figure 5 of this reference shows the principle involved, in which the flyer plate impinges upon an open triangular wedge that lies in a region of magnetic field. Upon striking the wedge, the enclosed flux is trapped. Further motion of the plate then compresses the trapped flux. (The authors have heard that an

experiment of this nature was done, but so far have been unable to identify the experimenters.)

- Proflux. This device, designed by Williams [41], consists of a cylindrical helical stator and a concentric central conductor that guides a projectile along the length of the stator, contacting the turns and thus compressing the initial flux, provided the output has low resistance. A novel feature is that propellants drive the projectile, or armature. Here, the contact of the projectile with the helical windings is supposed to be sufficiently benign that the system can be used again

- Inverse Railguns. As will be discussed later, FCGs have been used to power railguns. Here the FCG supplies the current to generate the magnetic fields that accelerate a projectile down the rails. The inverse railgun is opposite. Here, the original rails contain an initial field and an external agency drives the projectile against the field to compress the flux. Thus, in effect, firing the railgun backward. Marshall [42] has analyzed this technique as a power source for space launches. He proposes using a single stroke internal combustion heat engine. Powell and Jamison [43] analyzed inverse railguns as power sources for several different kinds of loads. They also used propellants for the projectile energy source. They concluded that the inverse railgun would be a useful power source for conventional railguns as well as other inductive loads, provided the load resistance is small.

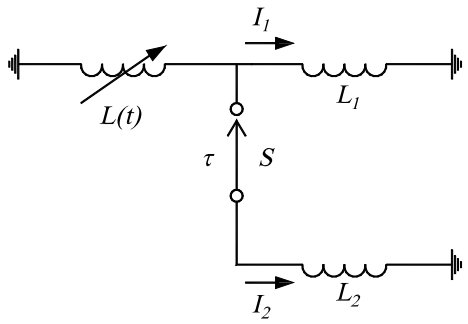

Fig. 5. Circuit schematic showing FCG powering parallel loads. the second load, L_2, is switched into the circuit at a later time, τ.

1.4. Advantages and Disadvantages

We will consider, mainly, the advantages of FCGs, since most of the disadvantages are rather obvious. The hazards of working with high explosives, both to personnel and nearby equipment, are clear. Even environmental effects such as loud noise must be considered. In some cases firing shots in containment vessels can mitigate these effects, but such vessels usually limit explosive charges to relatively small sizes. The normal electrical hazards associated with the initial energy sources, such as capacitor banks, are thus compounded. Experimental facilities devoted to explosive flux compression are specialized, usually requiring considerable isolation from nearby structures, and must be carefully controlled to avoid inadvertent access by outside people (as well as domestic animals). Access to highly sophisticated explosive facilities is a requirement for many systems. Even though such facilities may be available to outside users, the product costs could be high, in part because of the mandatory requirements put on shipping, accountability, and, in some cases, physical security. Finally, these devices are basically single shot. Although the loads themselves are not destroyed (such as a rail gun or electron beam diode), the basic generator power supplies or, at least, most of their components are destroyed.

In view of these disadvantages, it is clear that it would be foolish to use such sources if other more conventional sources could be used at comparable costs. There are, however, a number of advantages characteristic of these sources, some of which make their use very attractive. Among these are:

1.4.1. High Energy and Power Density

Reference to Table I shows that most of the explosives listed have an energy content of 2–3 MJ/lb. At explosive-to-electric conversion efficiencies of only 2–3 %, energies of many tens of kilojoules can be delivered per pound of explosive at very high power levels. Thus, these generators have applications where weight and volume are limited. The 'Birdseed' experiments, [44] done with over 30-year-old technology, illustrate this point. High energy, generator-powered plasma guns were installed is rockets and fired into the ionosphere ($\sim$ 200 km altitude). Energy ($\sim$ 400 kJ) was supplied by a flux compression generator system. A self-contained generator power system of the same total weight ($\sim$ 500 lbs) with 3-5 MJ output was designed and partly tested, but never flown.

1.4.2. Adaptability

Most generators can be altered to meet varying load requirements without extraordinary difficulty, particularly when contrasted with most other installed energy sources – capacitor banks, for example. Examples of this adaptability will be noted later.

1.4.3. Pulse Shape Effects

Equation (11) points out a basic difference between the pulse shape of a generator current pulse and that, for example, from a capacitor discharge. As noted from this equation, since dL/dt of the generator

is negative, current increase arises from a positive dI/dt. Thus, increases of voltage across the load, $L_1 dI/dt$, are accompanied over much of the generator run by increasing currents, and therefore, increasing magnetic fields. In other words, when the electric fields are large, the magnetic fields are also large. There have been a number of cases where potential electric breakdowns in generator-powered loads are thought to have been averted thanks to this built-in magnetic insulation effect. This may be contrasted with the typical capacitor discharge where maximum voltage occurs at zero current.

This pulse shape, in some cases, has a negative feature, in that it is sometimes difficult to get a large, initial dI/dt when it is required, as for some Z-pinch configurations [44]. For example, sheath formation in plasma focuses appears to be poor if the initial dI/dt is low [45].

The shape of the generator pulse also has advantages, for some applications, in reducing unwanted metal displacements or heating. Generators, being low-impedance devices, usually operate more effectively when powering loads to high currents. The resulting magnetic fields exert pressures on the conducting elements and can lead to unwanted displacements. To get a feeling for these displacements, consider the downward motion of the bottom plate of the generator shown in Fig. 2. We let M be the mass-per-unit area of the plate and assume that the magnetic field increases from a low value to a value B_M in time T. For simplicity, we represent the time variation of B as a power n of time:

$$B(t) = B_M(t/T)^n. \tag{24}$$

The equation of motion of the plate, with y in the downward direction, is

$$M(d^2y/dt^2) = B_M^2(t/T)^{2n}/2\mu.$$

The displacement, to time T, is then

$$\Delta y = B_M^2 T^2/(2\mu M)(2n+1)(2n+2). \tag{25}$$

Frequently, initial loading is supplied by capacitor discharge, to the quarter period. The value $n = 1/2$ is a good approximation for the current wave form. On the other hand, $n = 2$ is fairly representative of the wave form supplied by generators, at least over a substantial part of its operation. As seen from Eq. (25), the capacitor discharge would displace the plate about five times as much as the current supplied by the generator. To put this into perspective, if the generator of Fig. 2 was to be loaded to 50 T (about 400 kA/cm) in a time of 15 μs and if its density were 25 kg/m^2 ($\sim$ 1/8 in. thick copper), then the plate would be displaced by $\sim$ 0.3 mm with the generator supplying the current or by about 1.5 mm with the capacitor bank discharge. While this analysis is qualitative, the effects are real and good generator design requires careful attention to undesired component motion.

Other effects that are mitigated by the generator pulse shape include I^2R heating, the action integral, and flux diffusion. More details of the above analysis are available [46], and specifically for capacitor bank loadings [47]. Knoepfel [48] shows that flux penetration into a conductor is also reduced for the faster rising pulses, as would be expected.

1.4.4. Powering Parallel Loads

In many cases, a second inductive load may be switched into a generator circuit, such as shown in Fig. 5. In this figure, the generator L is series connected to the load L_1, with an initial current I_0. At a later time τ, a second inductance load L_2 is switched into the circuit. At this time, the generator inductance has been reduced to L_τ. For purposes of illustration, we consider an idealized circuit (no resistance), so that flux is conserved. Up to time τ, the current I flows only in the upper branch of the circuit and the current is given by

$$I = \frac{I_0(L_0 + L_1)}{L + L_1}, \quad t \le \tau. \tag{26}$$

At switch time, the second circuit is switched in. At this time, the flux in the upper circuit remains at $I_0(L_0 + L_1) = I(\tau)(L_\tau + L_1)$. In the second circuit, consisting of the generator and load L_2, the flux is that in the generator, $I_\tau L_\tau$, since current has not started to flow in L_2. At a later time, with currents I_1 and I_2, the flux relations are

$$\begin{aligned} &L(I_1 + I_2) + L_1 I_1 = I_0(L_0 + L_1), \quad t \ge \tau, \\ &L(I_1 + I_2) + L_2 I_2 = I_\tau L_\tau \\ &\qquad = I_0(L_0 + L_1)L_\tau/(L_\tau + L_1), \quad t \ge \tau. \end{aligned} \tag{27}$$

At burnout ($L = 0$), the final peak currents are

$$\begin{aligned} I_1 &= I_0(L_0 + L_1)L_1, \\ I_2 &= \frac{I_0(L_0 + L_1)L_\tau}{L_2(L_\tau + L_1)}. \end{aligned} \tag{28}$$

Interestingly, the peak current and the energy in L_1 is just the same as though L_2 had not been switched in. This points out another fundamental difference between flux compressors and other sources of fixed energy. In its effort to conserve flux, the generator will attempt to deliver the additional energy required to power other loads switched into the circuit. The assumption is, of course, that the available energy in the explosive far exceeds the magnetic energies involved. In practice, the situation is somewhat different. The presence of resistances in the circuit affects the peak currents obtained. Further, the generator conductors are forced to carry higher total current and this can adversely affect the generator performance. Still, on several occasions we have benefited from this effect when inadvertent

short circuits have arisen in generator systems. While the generator performance is usually significantly degraded in such cases, the short circuits do not always cause the catastrophic effect that would result had the source been a capacitor bank.

2. Specific Types of Generators

Many types of generators can be conceived and a number have been proposed, but relatively few are practical. Design limitations are set by the ability to machine or otherwise fabricate components, including the explosives, availability of explosive initiation systems, and avoiding excessive losses. We consider here the types in most common use and, for the most part, update the discussion in [49].

2.1. Helical or Spiral Generators

More has been written about this class of generators because of the high current and energy gains possible but also because the explosive system required is relatively simple and requires only single point initiation for a conventional generator.

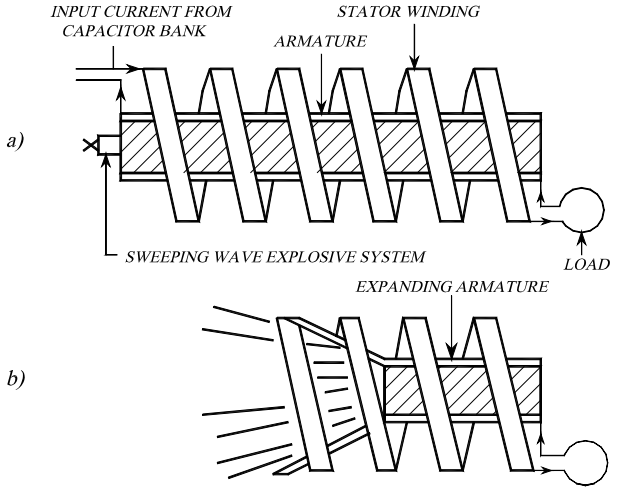

Fig. 6. Sketches of a helical generator and load coil, (a) before and (b) after explosive initiation.

Figure 6a shows the basic components of a class of generators of this type. At the lower right is a fixed external load coil, of inductance L1, which is to be energized by the generator. The generator itself consists of the external helical winding, together with the explosive-loaded metal cylinder, or armature. Initial flux may be supplied to the generator and series load coil from a capacitor bank. It can be seen that the armature itself serves as part of the conducting circuit. When the explosive is detonated, the armature expands, resulting in a conical metal front moving with explosive detonation velocity. The detonation is so timed that this conical front shorts out the generator input at or near peak current or, equivalently, peak flux in the generator. This also effectively isolates the capacitor bank from the system. After closure of the current input, the conical front proceeds down the armature making contact with the helical turns in a more or less wiping fashion. Figure 6b gives a view of the generator fairly late in the detonation stage. The inductance of the generator is roughly proportional to the square of the number of turns in the helix and inversely proportional to the remaining length over which the turns are spaced. The generator inductance thus varies more or less continuously with time from its initial value L_0 to zero after armature motion has ceased.

These generators are characterized by large initial inductance owing to the coupling between the many turns of the helix. Many models have been proposed to describe the operation of these generators, usually for a rather specific construction and range of operation. The magnetohydrodynamics involved is clearly three-dimensional, and there remain uncertainties in various material physical properties at very high energy density, such as electrical conductivities. However, code development progress is steady and a number of codes have been developed that, with suitable benchmarking with experimental results, have proved to be very useful. A list of some of these codes is given in Sec. 7.

Generally, the initial inductances of these generators are a few to a few tens of microhenrys, although some have been as high as several hundred microhenrys. Energy gain factors for appropriate inductance loads with very low initial loading may be several hundred or more, dropping to a few tens for very large outputs (greater than 10 MJ). Generator operation or "burn" times, largely controlled by the length of explosive in the armature, generally range from a few tens to a few hundred microseconds.

Controlling the current density is a primary factor in the design of these generators. Generally, current densities should be kept less than 1 MA/cm of conductor width for good operation for these time scales. Thus, a generator designed to generate a current of 25 MA should have an output turn width of at least 25 cm. At the input end of the generator, the turns can be narrow and closely packed, since the currents are small. At this stage of generator burn, inductance is reduced relatively rapidly and internal generator impedances can exceed an ohm. However, as the output is approached, the internal impedance drops rapidly owing to the rapidly decreasing inductance per stator length. Although, generator output currents continue to increase, the peak internal voltage, $|dL/dt|I$, generally peaks considerably before burnout. Of the many papers written on this class of generators, the following have been singled out as particularly instructive. The first description of this class of generators was given by Cummings and Morley [50], although these generators

were developed and used earlier at both American and Russian weapon laboratories and perhaps in other countries as well. Shearer at al [51] discusses a number of design details including the generation and handling of the internal voltages developed in the generators. Crawford and Damerow [52] discuss a class of these generators where detonating the armature explosive at both ends essentially cuts the generator burn time in half. The stator is thus symmetric about the mid length of the generator, where the output to the load is located. This technique significantly reduces the adverse effects of skin-loss and conductor displacement, both of which increase with time. Morin and Vedel [53] discuss a generator where the turn pitch and width are varied continuously, to accommodate the increased current during generator operation. Noteworthy, also, is the completeness of the analysis describing the generator performance. Pavlovskii and his coworkers [54–56] discuss many generator design features. Among these is the use of a concrete overcast to support the stator. Increased current carrying capacity as generation proceeded was accomplished by paralleling (usually called *bifurcating*) the conductors, often followed by one or more additional bifurcations and thus ending up near the generator output with many parallel conductors to carry the current. Each such bifurcation increases the pitch of the windings. A family of generators is described that ranges from low to very high output and provisions are described that allow coupling these together in such fashion that the output of a smaller generator supplies the input energy to a larger generator. This process in which one generator, usually smaller, supplies the initial energy to a larger output generator is called boosting. With its large possible gains, boosting is one of the major uses of helical generators. Generators are sometimes operated in series or parallel. The Pavlovskii team operated four large generators in parallel, which delivered the very high energy of 60 MJ to a load. For an excellent more recent discussion of helical generators, the paper of Novac et al [57] may be consulted. Here, actual detailed construction techniques are discussed, which are not commonly given.

Sometimes special care is taken in the stator design to minimize voltages, for example the internal generator drive voltage, IdL/dt. As noted by Fowler et al [58], by equating this expression to a constant voltage, $-V$, and using some model to express the current as a function of the inductance, the inductance can then be determined as a function of time (or distance along the stator as determined from the explosive detonation velocity) such that the voltage equals (does not exceed) $-V$. The models contain the load inductance, and thus the stator winding design is best suited for loads in the vicinity of that used in the model. Chernyshev et al [59] have rather faithfully reproduced such a calculated inductance, in a generator requiring 15 sections, each section having a specified number of turns, wire diameter, and pitch.

Mention has been made earlier that component displacement goes as the square of the time. It is important that unwanted component displacement does not occur during initial generator loading. The Los Alamos Mark IX helical generator, designed by Fowler et al. [60], was designed to deliver up to 35 MA. It was wound with #00 copper wire (0.365" D) starting with 5 parallel wires at the generator input end and, through 3 successive bifurcations, ended with 40 parallel turns at the generator output. The generator delivered 7–10 MJ into various loads when powered initially with 400–450 kJ from a 600 kJ (20 kV) capacitor bank module. To increase the output, it was decided to load the generator to about 900 kJ by using two modules. When the modules were connected in parallel, the additional loading time and increased current resulted in sufficient internal motion of the generator turns that some were apparently shorted together. This led to considerably reduced generator performance. Caird [61] then connected the two modules in series. This led to the same initial loading current, but in only half the time. The generator easily accepted this loading and performed well, delivering 18 MJ to the load at some 25 MA.

When used to power various loads, some type of power conditioning is usually called for. Often, an opening switch, fuse, or transformer is required. These are discussed in Sec. 4. Some of these applications will be mentioned in Sec. 5, in which these power conditioning techniques are used. In some cases, the conditioning may only require a closing switch; perhaps the simplest form of conditioning. An example of this is the Birdseed power package discussed later in Sec. 5.1.

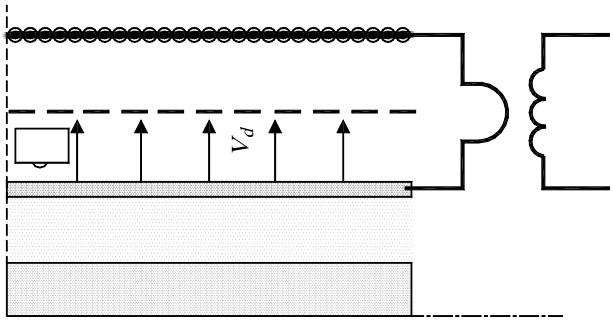

Fig. 7. Simultaneous helical FCG with axial initiation shown Powering a transformer primary coil. (See Ref. 10 for more details).

Finally, we mention the Simultaneous Helical Generator developed at Los Alamos [62–64]. It is similar to that shown in Fig. 7, where the armature explosive is detonated simultaneously on axis. In this case, the generator burn time is governed only by the time it takes the armature to contact the windings.

Thus, the generator inductance is wiped out in a short time, leading to high internal impedance. As noted in the references cited, flux diffusion losses can be large. The generator gains are therefore relatively small, but the device has since been shown to power loads at much higher voltages near burnout than does the conventional helical generator.

2.2. Plate Generators

These generators, so named because their conductor plates are driven by explosive simultaneously detonated over the plate area, are presently the fastest operating devices available for powering external loads. Figure 8 shows such a generator where both the top and bottom plates are overlaid with explosive. Initial flux is supplied to the generator and load by passing current through the input slot. The explosives are simultaneously initiated over the surfaces to close the input slot at or near peak flux in the system. Generator burnout occurs when the two plates collide at the generator center. Typical parameters, which can vary widely depending upon the application, might be: top and bottom plates made from 1/8-inch-thick 6061 aluminum that are 5-inch wide and 20-inch long and initially separated by five inches. The explosive charge is PBX 9501 and is 2-inches thick. Closure time for these conditions is somewhat over 14 μs and the plates collide with a relative speed of about 10 mm/μs.

The initial inductance of the generator is given by Eq. (16), with neglect of an edge effect correction. With the dimensions cited above, the correction factor is approximately 0.5, but approaches unity near the plate collision or generator burnout time. In these generators, it is customary to rate them by squares; that is, the length of the generator divided by the width. There are about four squares in the generator pictured in Fig. 8. Aside from the edge correction, from Eq. (16) the inductance per square is then, **with x_0 in meters**

$$L_{\text{per square}} = 1.257 \cdot 10^{-6} x_0 \text{ Henrys/square.}$$

Near burnout, the generator internal impedance is relatively large. With v approaching 10^4 m/s, $|dL/dt| > 0.01$ Ω per square. Generators of this class have been used in many applications, particularly those requiring short pulses at high current, voltage, and power levels. Near burnout, they can deliver multimegampere currents at terawatt power levels to low-inductance loads with pulse half-widths of less than a microsecond. They are easily adaptable to variations that may be required. Plate widths can be controlled to allow for current-carrying capacity, while lengths and separations can also be controlled to vary initial generator inductance and burn time. Caird et al. [65,66] have discussed this generator class in detail

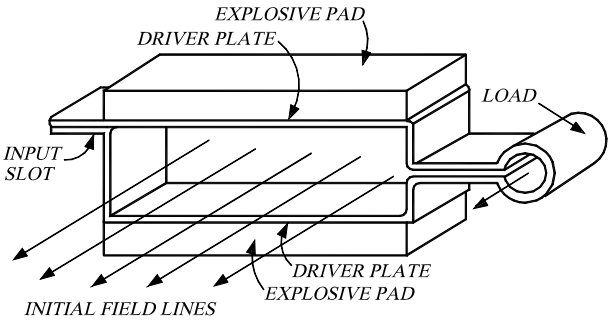

(a)

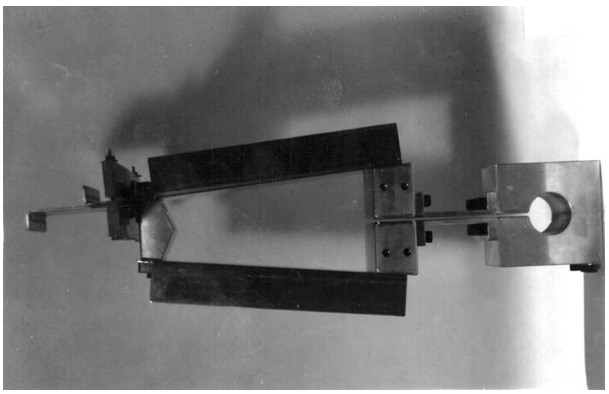

(b)

Fig. 8. (a) Sketch of plate generator with cylindrical load coil and (b) photo of trapezoidal plate generator.

and give more realistic models for its performance. They also consider the case where the two driven plates are not parallel, giving rise to the "trapezoidal" plate generator shown in Fig. 8b. This construction results in a different output pulse shape, which may be more suitable for some applications.

Applications of this generator, where significant power conditioning is required, are discussed in Sections 4 and 5.3. However, we mention here one application where only a closing switch offered sufficient power conditioning. Freeman et al [45] have successfully powered a Dense Plasma Focus (DPF) with plate generators, obtaining yields of 3 x 10^{11} DD neutrons. The only power conditioning required was a closing switch that switched the DPF into the circuit 3 to 4 μs before generator burnout.

2.3. Strip Generators

The strip generator, so named because its active elements consist of arbitrarily long strips of copper and explosive, is shown schematically in Fig. 9. Its most useful characteristic is its capacity to carry relatively high currents (up to megampere peak values) for long times (of millisecond order). Initial inductances vary considerably with the particular dimensions selected but are typically in the low-microhenry range. Although one of the earliest generator types developed, some detailed construction

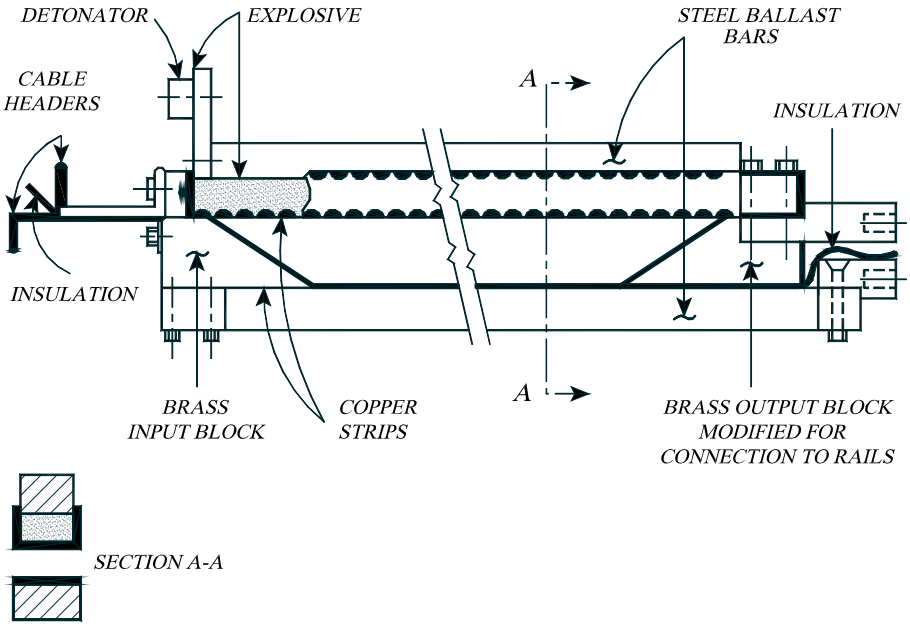

Fig. 9. Sketch of strip generator. The ballast bars help resist generator expansion from magnetic forces.

features have been furnished only recently after it proved to be a useful power source for railguns [67,68]. The generator consists of long parallel strips of copper, one of which is overlaid with explosive sheets, together with input and output blocks for capacitor bank cable input leads and for connection to the load, respectively. The long edges of the upper copper strip are bent up to add structural rigidity. The strip then assumes the form of a shallow U-shaped channel as noted by the sectional sketch in Fig. 9. For one of the commonly used generators, the copper strips are about 57 mm wide, 1.6 mm thick and 2.45 m long and are separated by 51 mm. Two layers of DuPont C-8 Detasheet explosive, 45-mm wide, are placed over the upper copper strip. To minimize expansion of generator components from magnetic forces, steel ballast bars, 51 mm wide and 12.7 to 25.4 mm thick, are laid on top of the Detasheet explosive and directly under the bottom copper strip. The input and output wedges are cut from 51 mm square brass bar stock and then drilled and tapped individually to accommodate cable input header attachments and to make output connections to the various loads tested. In some applications, where larger currents were required, the cross-section dimensions were doubled, except for the copper strip, explosive and ballast bar thicknesses, which remained the same.

Initial flux is supplied to the generators by a capacitor bank located at the firing site. The detonator is fired shortly before the maximum current is delivered to the generator and load. The resultant detonation of the explosive strip closes the current input slot, thus trapping the magnetic flux. As detonation proceeds, the top plate is driven into the bottom plate, thereby pushing the flux into the load.

This class of generators is by far the cheapest to fabricate and we have used it widely when the output pulse is suitable. Its parameters may easily be changed: the strip length can be varied to change the output pulse length; the plate width and thickness may be varied to suit current demands; the plate separation can be varied to alter the generator inductance; and the plate width can be varied along its length to give added flexibility in controlling the output pulse shape. By using relatively simple load input header adjustments, two or more of these generators have been fired simultaneously into a load, connected in parallel for greater current-carrying capacity or connected in series for greater gain.

A related class of generators, often called "bellows" generators, was described by Herlach et al [69] and by Bichenkov [70]. In the bellows generator, the explosive strip is sandwiched between two conducting strips, both of which are driven outward towards stationary return conductors. Thus, the strip generator described here has the appearance of half of a bellows generator. The bellows generator clearly makes more efficient use of the explosive and it should be easier to ballast the outer conductors. We have found that they perform very well, especially for shorter lengths. In general, however, they are more expensive and it is not as easy to vary their dimensions.

2.4. Cylindrical Implosion System

Several views of a cylindrical implosion system are shown schematically in Fig. 10. Two of the sketches show the system before detonation. The initial assembly consists of a thin-walled cylinder centered within an explosive ring charge to which

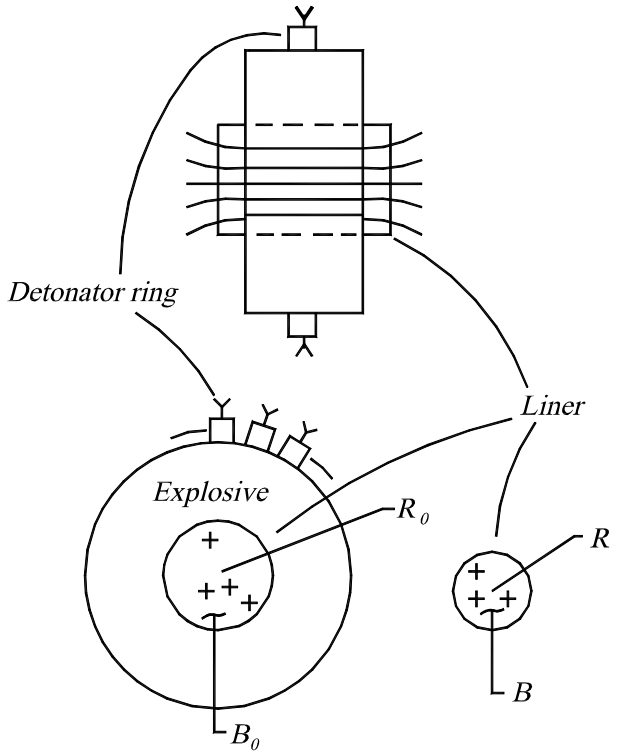

Fig. 10. Initial views of a cylindrical implosion system and a view during implosion (lower right).

is attached a ring of high-quality detonators. The thin-walled metal cylinder, usually called a liner, plays the role of the generator armature. An initial flux is induced within the liner, in most cases by passing current through coils external to the system. Detonation of the charge is timed to correspond to peak flux in the liner. The third sketch shows the position of the liner at a later stage in the implosion.

This class of generators is of historical interest because it was the first generator discussed experimentally in the literature [13]. The systems were developed for use in imploding liner plasma compression experiments [71].

If the liner of Fig. 10 was perfectly conducting then, from flux conservation, the magnetic field would increase inversely as the square of the radius: $\phi = B_0 R_0^2 = BR^2$. The magnetic pressure exerted on the liner would therefore increase inversely as the fourth power of the radius. Hoyt and Kazek (see [13]) made a number of hydrodynamic calculations with perfect flux compression. They showed that the magnetic pressures got large enough to stop the inward motion and drive the liner outward. This minimum radius is now called the "turn around" radius. The magnetic field attains its maximum value at this radius. In Ref. 13, magnetic fields in excess of 10 MG were reported. The time resolved data suggested the existence of a turn-around radius, but not conclusively. Somewhat later, Bescancon et al. [72] carried out an extensive study of these high-field systems that remains definitive. More recently, Pavlovskii and his coworkers [73,74] have developed very reproducible systems, known as MC-1 generators, and have used them in a number of high-field investigations. In the early 1990's, relations between Los Alamos scientists and their counterparts at Arzamas-16, the Russian laboratory similar to Los Alamos, had progressed to the stage where plans were made for joint experiments. Several MC-1 generators (for which Los Alamos had to furnish all the explosive components) were purchased for use in a set of high-field solid-state studies, together with some Los Alamos high field systems. An overview of that shot series, notable in that it was the first time such joint experiments were conducted in a security area at Los Alamos, are given by Fowler and Freeman [75]. The success of that series led to later ultra-high magnetic field shot series in which scientists from several different countries and universities were invited to participate. A summary of the results of the second shot series, called Dirac II, is given by Clark [76]. The collaboration between these two laboratories is quite extensive as will be noted in Section 2.6. Boyko et al [77] have recently produced record fields, up to 2800 T, extending the techniques used by the Pavlovskii team.

Since the publication of the original work, there have been many studies devoted to the diffusion of magnetic fields into the liner. A number of these calculations are given in [1]. In particular, the calculations reported by Kidder (see [1]) were advanced for the time and contain points that are still pertinent. In modeling the experiments of [13], his conclusions were that the effects of field diffusion in the liner did not affect the peak field maxima appreciably, but that they occurred at a somewhat smaller radius than that predicted with the assumption of perfect liner conductivity.

2.5. Coaxial Generators

The upper sketch of Fig. 11 shows a coaxial generator and load coil. Generators of this type are upon occasion also called "cylindrical generators". The basic generator components include the stator, or outer cylinder, and the armature, the explosive-loaded inner cylinder. The load coil pictured is annular or doughnut-shaped. Initial current is supplied by a capacitor bank, or commonly by another generator, through the annular input slot at the left. Arrows show that the current flows along the outside cylinder, through the load coil, and back through the armature. Magnetic field lines B, indicated by circles and crosses, are circular or tangential. They encircle the armature and are restricted essentially to the annular space between the stator and armature and to the load coil.

Detonation of the armature explosive is again timed to close the input current slot at such time that maximum current or flux is in the system. As

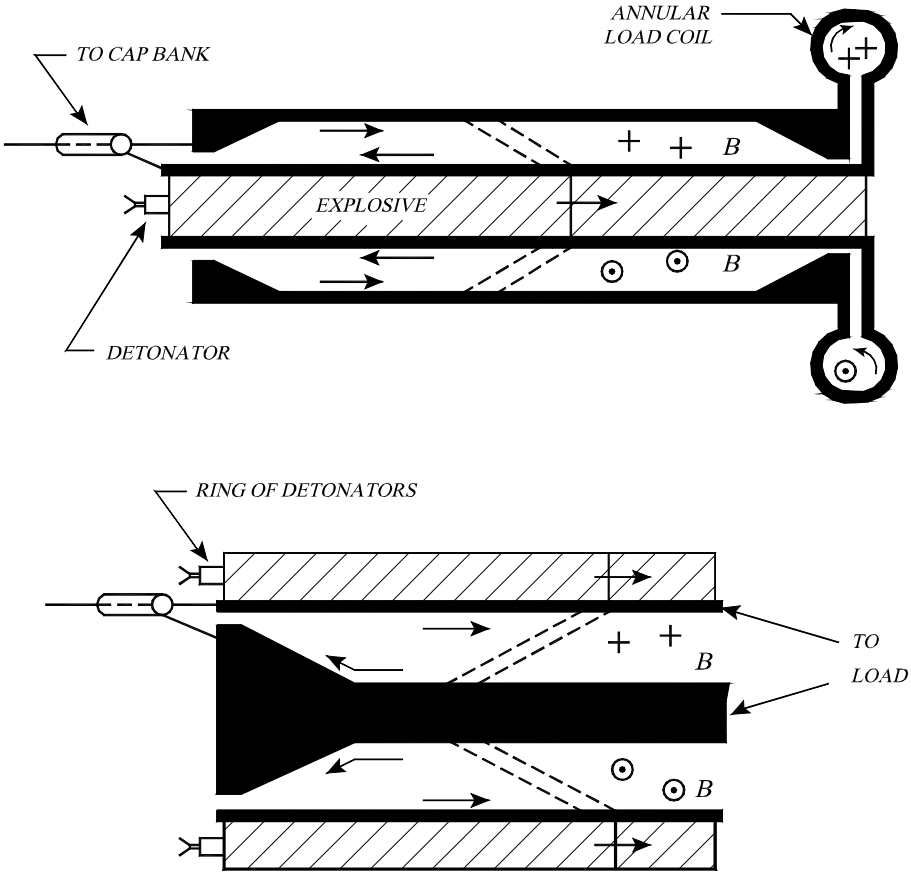

Fig. 11. Sketches of coaxial or cylindrical generates powering an annular load (shown only in the upper view). Most often, the explosive and armature are inside the stator as in the upper sketch. Upon occasion, the armature and explosive are outside the stator, as in the lower sketch.

the detonation proceeds, the armature expands in a conical front, which moves with detonation velocity. Again, the manner in which flux is compressed is clear.

The lower sketch of Fig. 11 shows a variant of this class of generators. Here the central cylinder plays the role of stator, while the outer cylinder becomes the armature.

These generators are of low impedance, but are extremely rugged, can carry very large currents, and are quite efficient in conserving flux. They are frequently built as an extension of a helical generator, whose armature has been extended in length to power the coaxial section. It is common to find that this stage of such generators accounts for much of their overall gain. In some cases, the stators have been especially contoured to approximately match the armature expansion angle so that closure in this last section of the generator is almost simultaneous near burnout, to increase its effective impedance [78]. In another variant, the armature explosive was detonated simultaneously, on axis, to increase the impedance. Performance details of two generators of this type are given in [79]. A photograph of one generator [79a] is given in Fig. 12 (foreground). The initial current of some 6 MA was supplied by a "booster" generator (the LANL Mark IX), which can be seen attached to the coaxial generator (foreground) by a number of parallel coaxial cables. The inside diameter of the stator at generator output was about 22 inches. This gave a circumference of about 175 cm to carry the output current, which was sufficient for the maximum calculated current of 175 MA. The maximum current delivered to a low-inductance load (a few nH) was $\sim$ 160 MA. The Los Alamos "Ranchero" generator [79b] has both an aluminum stator and armature. The stator has a diameter of 12". It has been tested to currents exceeding 50 MA and should be capable of generating some 90 MA into low inductance loads. It has been designed to be cost effective and to allow for series or parallel staging of more than one generator.

As noted earlier, generators with such coaxial outputs can carry large currents in the typical operational time scales on the order of a MA per cm width. The disk generators, described in the next section, also deliver final currents in a coaxial way and thus, also, can carry currents of this magnitude. As noted below, one class of these generators has an output diameter of a meter and can deliver nearly 300 MA to low inductance loads.

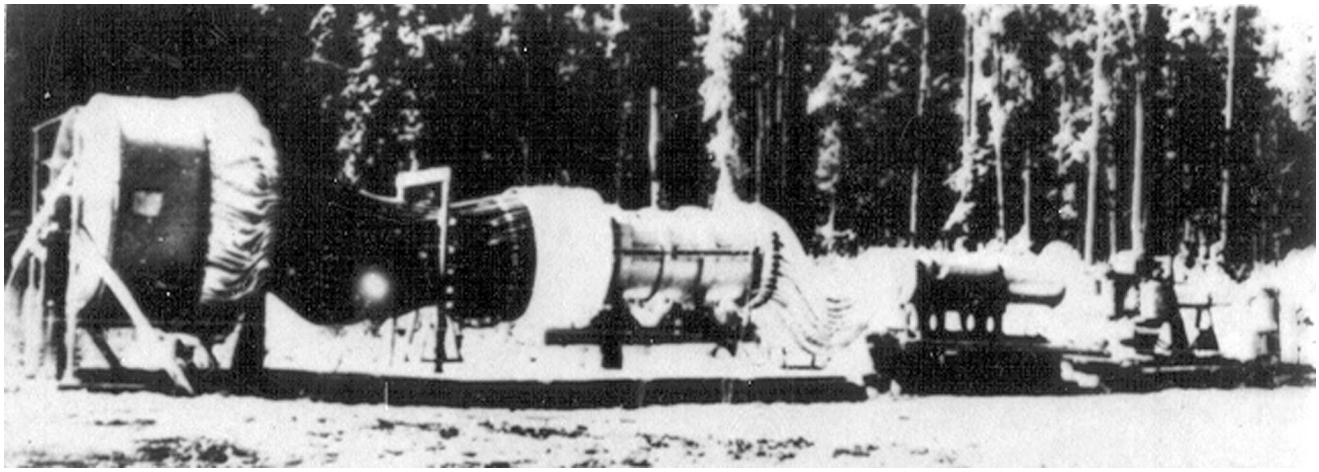

(a)

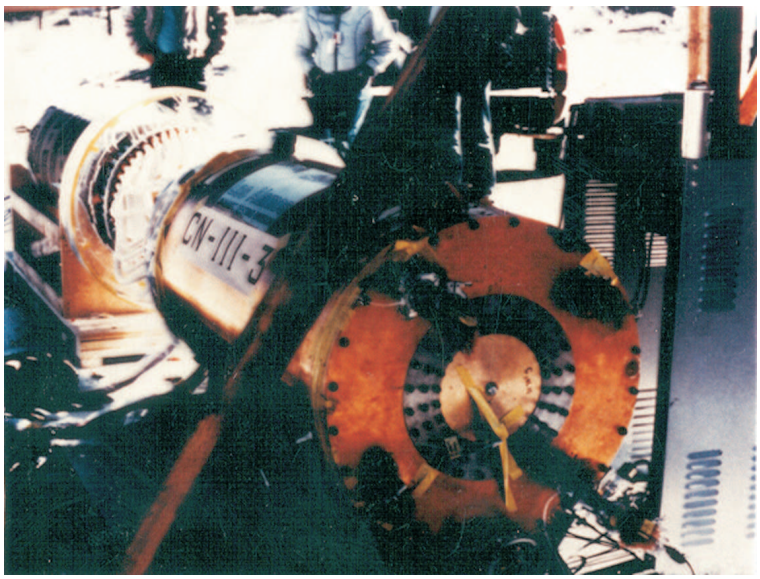

(b)

Fig. 12. Top, series of increasingly large helical generators boosting the final out coaxial generator. Bottom, coaxial generator with helical generator boster.

2.6. Disk Generators

Figure 13a shows the radial cross-section of a "disk" generator developed by Chernyshev and his coworkers [80]. The entire device is a figure of revolution about the centerline. As can be seen, the device is of modular construction, two, of which, are shown in the sketch. Solid lines show the current carrying disks and the explosive components are shown crosshatched. Magnetic field lines are azimuthal, as in the coaxial generator discussed above, and the flux is mainly confined by the generator cavity regions that are ultimately compressed by the explosive. When peak magnetic flux is attained, from a capacitor bank discharge for example, the current input opening is closed, such as by firing a ring of detonators. About the same time, the main charges are detonated, driving the cavity plates together as the detonation front progresses radially outward. Flux is ultimately transferred to the toroidal load coil through the outer coaxial transmission line. The geometric arrangement is quite favorable for generating large currents since, as generator action proceeds and currents increase, so does the cross-section of the conductors. Similarly, there is an increase in the amount of explosive with radius. This makes for more efficient use of the explosive, since current, power, and energy delivered by the generator increase towards burnout. Demidov et al. [81] described a three-module generator, with outer conductor diameter of 1 meter, which delivered a current of over 250 MA into a 3 nH load or about 97 MJ of energy. The initial current was 13.7 MA and, thus, the current multiplication factor was 18.7. The explosive to electric energy conversion efficiency was stated to be 14 % giving an estimated explosive weight of order 100 kg. The generator burn time was about

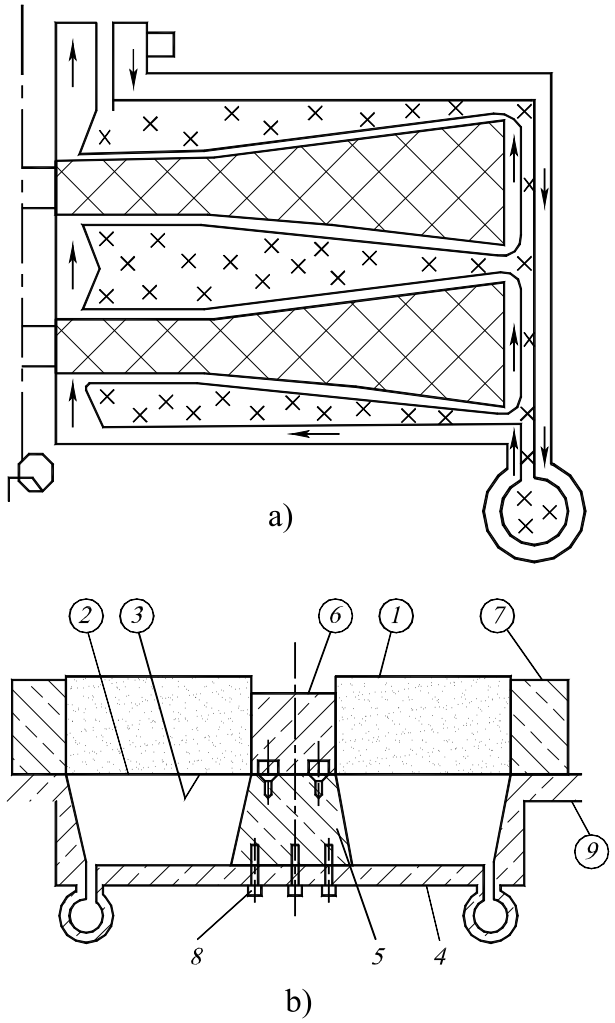

Fig. 13. Dish generator (a) and post generator (b). In (a) the complete generator is a figure of revolution about center line. The explosive, shown cross-hatched, is initiated near the cylindrical axis. Two explosive stages are shown, but many stages can be assembled is series. In (b), the explosive is simultaneously initiated over the top annular surface. These systems can be made very fast, but lack the current-carrying capacity that type (a) has.

60 μs and a peak dI/dt value of $2.2 \cdot 10^{13}$ amp/s was obtained. Lindemuth et al [82] describe an experiment done jointly by people from Los Alamos National Laboratory and VNIIEF at Sarov, Russia, describe an experiment in which a large disk generator was used to implode a cylindrical aluminum alloy liner that weighed about 1 kg. The liner was magnetically accelerated radially inward to a velocity of about 6.5 km/s with an estimated kinetic energy of more than 20 MJ. The disk generator had 5 modules with outer diameter of 1 meter. A helical generator supplied the initial loading.

Figure 13b shows a "simultaneous" disk or post generator described by Fowler, Hoeberling, and Marsh [83]. Current is injected radially, generating azimuthal magnetic field lines encircling the central post. The explosive ring is detonated simultaneously over its top surface. The angles of the glide cylinders and the central post, together with the support post and ring were selected such that the top or driver plate remained approximately parallel to the bottom plate. With about 4.5 kg of explosive and initial current of 1.08 MA, a final current of 30.8 MA was achieved, with a current gain ratio of 28.5. The generator was designed for short burn time, with a consequent large dI/dt value of $3 \cdot 10^{13}$ amp/s. As noted in the reference, tests with this generator showed a definite improvement in performance when the driver plate was accelerated in a nearly shockless manner. This comparison was made by firing the system, first with the explosive charge in direct contact with the driver plate, and then with the explosive standing off the plate. This resulted in a nearly shockless acceleration of the plate, and better performance.

It was mentioned earlier that generators were often given names by their developers to emphasize some aspect of their construction. The name of the generator just described was given as "disk" before the authors were aware of the generators, previously described, developed by Chernyshev et al, and also called disk generators. Needless to say, the developers of the last described generator have deferred to the high-performing Chernyshev generators, and now refer to their generator as a "post" generator.

2.7. Loop Generators

A generator intermediate to that of the high-speed helical generator that can generate currents in the range 5–20 MA and the coaxial and disk generators that have generated currents in the range 60–300 MA is the "loop" generator (Fig. 14). The stator of this generator is a single wide loop with two cuts. One cut serves as the input for the seed current and the second as the output. These generators are simple in design and relative low cost to produce. Their characteristics include relatively high volume energy densities (200–250 MJ/m^3) and surface current densities (0.70–0.80 MA/cm). They can operate with a wide range of loads with inductances ranging from a few nH to some tens of nH. They are very convenient devices for doing experiments, since they can be easily filled with high explosives at any time, because the HE charging process is an independent process. It is also convenient to connect these generators in series or in parallel.

The loop generator armature consists of an outer wide loop with two cuts and an inner cylinder filled with high explosives. A capacitor bank or another booster generator provides the initial current supplied to the outer loop, or stator. The explosive charge is initiated along its axis simultaneously using a detonator chain. When the explosive is detonated, the

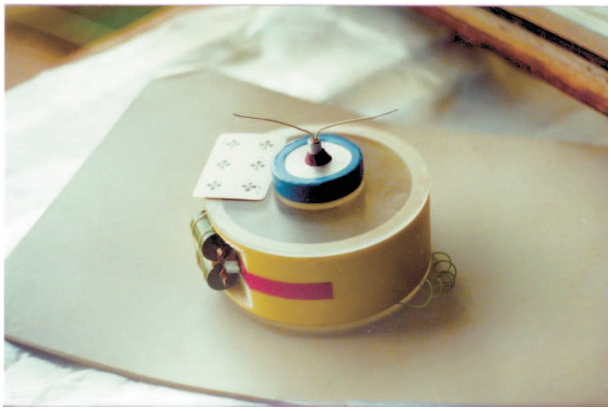

(a)

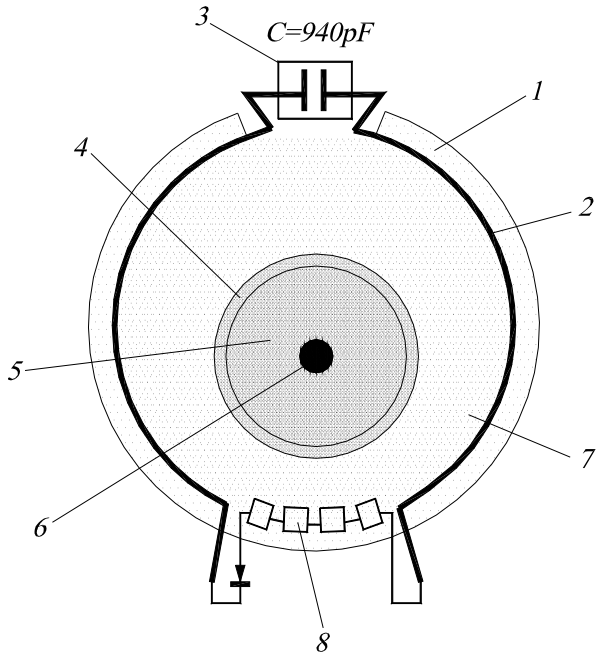

(b)

Fig. 14. a) Photograph and (b) sketch of small loop FCG (courtesy of Dr. A.B. Prishchepenko). 1– Body of Dielectric, 2 – Electrodes, 2 – Capacitor, 4 – Aluminum Tube, 5 – Explosive Charge, 6 – Detonator, 7 – Gap Between Electrodes Filled with sulfur Hexafluoride, 8 – Ferroelectric Elements.

inner cylinder expands and closes the input terminals at the moment the seed current reaches peak value. The cylinder continues to expand, compresses the magnetic field, and forces the field into the load. Compression of the magnetic field by every portion of the cylinder ensures optimal generation of current density. These generators have a relative low current gain of 7 to 10 and an e-fold time of about 9 to 12 μs. Loop generators were first described by Lukasik [84]. These generators were small and were designed to make large magnetic fields in very small volumes. In their best experiments they achieved a field multiplication of 26 resulting in a magnetic field of 133 T.

Later experiments with much larger generators and loads were conducted by Vasyukov [85]. He tested a single loop generator with a loop diameter of 30 cm and a width of 60 cm that had an inductance of 87 nH. This generator produced 50 MA, 10 MJ, and 30 to 35 kV in an 8 nH load. He then connected three of these generators in series to a 30 nH load. The total inductance of the three generators was 260 nH. This system generated 46 MA of current, 30 MJ of energy, and 4 TW of power. Higher currents could have been generated by connecting the generators in parallel or by increasing the width of the generators. The characteristics of these generators are discussed in some detail by Altgilbers et al [10].

3. Losses and Efficiencies

Generator efficiency is usually defined as the ratio of magnetic energy produced by the explosive to that of the energy content of the explosive. In most cases, efficiency is not a factor much considered. In fact, as noted earlier, in most cases the energy content of the explosive is considered so large that it is not considered as a limitation on generator performance. It is therefore treated, as a virtually inexhaustible source of energy available to meet the energy needs required from flux conservation. Nevertheless, there are situations where higher efficiency is desired. These arise when overall system weight is at a premium, when danger of fragment or blast damage to nearby components must be minimized, or to reduce the size and weight of containment vessels in which shots are fired. Efficiencies are more dependent on the load characteristics and on various losses that can occur during generator operation, which we discuss first.

Generator losses are generally categorized as those that are related to magnetic diffusion and those arising from mechanical effects.

3.1. Diffusion Related Losses

Magnetic fields diffuse into the generator conductors and the associated flux is generally non-recoverable. The basic principles of diffusion are well known. For simple geometries, the major uncertainty lies in the value of the electrical conductivity. Some of the complexities may be seen by considering Fig. 2. The explosive drives the top plate, but not the bottom plate. If the explosive is in direct contact with the upper plate, then a shock wave is generated in the plate with a corresponding temperature rise. Thus, there is a decrease in electrical conductivity from this effect over and above that caused by current heating, such as occurs also in the bottom plate. The situation is even more complicated since the top plate is subjected to various waves, both shock and release,

during its motion. This leads to corresponding spatial and temporal variations of both temperature and pressure throughout the plate thickness. However, much of the average temperature increase arises from the first shock through the plate, mitigated by the subsequent release at the free surface. The severity of the first shock may be greatly reduced by standing off the explosive from the plate or by interposing low-density foam between explosive and plate. This is frequently done, but sometimes other circumstances prohibit it.

In spite of these complexities, it is usually possible to qualitatively account for the flux losses by diffusion theory if the geometries are relatively simple and the current densities are not too large. It is found empirically; however, that in some situations that the losses became anomalously large when the magnetic fields exceed certain values for long enough times. Bichenkov and Lobanov [86] noted the onset of high losses in a strip generator (copper strips) when the magnetic fields approached about 400 kG, while Fowler et al. [12] observed a similar onset in brass coils when the fields exceeded 500 kG. It is possible that these effects arise partly from crack formation in some of the conductors [83] since a magnetic field of 500 kG has a magnetic pressure of about 10 kbars, which is above the elastic limit of brass.

In most situations, generator conductors are thick compared to skin depths developed during their time of operation. The flux loss by diffusion thus resides in the conductors and can be approximately calculated from skin depth estimates, provided the magnetic fields do not get too high [87,88].

There are, however, situations where skin depths are not small compared to the conductor thickness. These cases arise when relatively thin conductors carry currents for long times. In this case, additional flux is lost by radiation from the outer conductor surface. This situation was discussed by Fowler [89,90].

3.2. Mechanical Related Losses

Major losses generally occur by flux trapping and unwanted component motion arising from magnetic pressure.

Flux trapping or *pocketing* occurs when part of the magnetic flux is inadvertently isolated from the generator and load. This can happen in a number of ways.

3.2.1. Mechanical Tolerances

If the plates on the plate generator of Fig. 8 were thicker on the input side than on the load or output side, plate closure would occur earlier on the load output side, leaving trapped flux between the lagging plates on the input side. Similarly, in the helical generator of Fig. 6, eccentricity of the armature or variations in the armature wall thickness could cause premature contact of a downstream stator turn. This would result in loss of the flux between this turn and unshorted upstream turns. Chernyshev and his coworkers [91] examined the consequences of armature eccentricity in considerable detail.

3.2.2. Moving Contact Effects

With the exception of the cylindrical implosion systems, all of the generators described here require moving metallic contacts to carry the current during generator operation. These contacts sometimes are rough or bumpy and, in any case, frequently have some conducting metal spray running ahead of the major hard contact. It is difficult to quantify the resulting flux loss for lengthy contact regions, as in the strip generator of Fig. 9, where the strip lengths might be as long as 3 m. It is thought that this may be a significant loss. Bichenkov and Lobanov [86] and Knoepfel [9] address this point.

3.2.3. Explosive Produced Jets

These arise in a number of ways and if the jets arise from explosive-metal interactions, they are usually conductive enough to form an alternate, flux-trapping current path. Imperfections in either the explosive or metal, in the armature of a helical generator, for example, can lead to jets that will short to a stator turn before the armature makes major contact and, thus, lead to a flux loss. Metallic jets can also be produced at sliding contacts, such as the moving plates of the generator shown in Fig. 8 with the side glide blocks. Since these jets move ahead of the plates, it is clear that they would produce a short circuit in front of the load output slot before generator action had ceased. These jets caused us considerable trouble in the earlier development stages of the plate generators. Guided in part by the classic study on jets by Walsh et al. [92] and later work by Caird [93], we eventually solved this problem by careful selection of the angle between glide planes and moving plates and by proper location of the explosive.

3.2.4. Undesired Component Motion

Unwanted motion of metallic components can lead to reduced performance (Fig. 15), since the motion increases the inductance of the system. Two examples of this effect are shown on Fig 15. Here, flash x-ray photography revealed massive motion of the metal conductors connecting a strip generator power source to a railgun. The motions, of course, can arise when other power sources are used, but they are especially serious for flux compression generators since the maximum theoretical energy gains are rigorously controlled by circuit inductances.

3.3. Efficiencies

The efficiency of conversion of explosive to

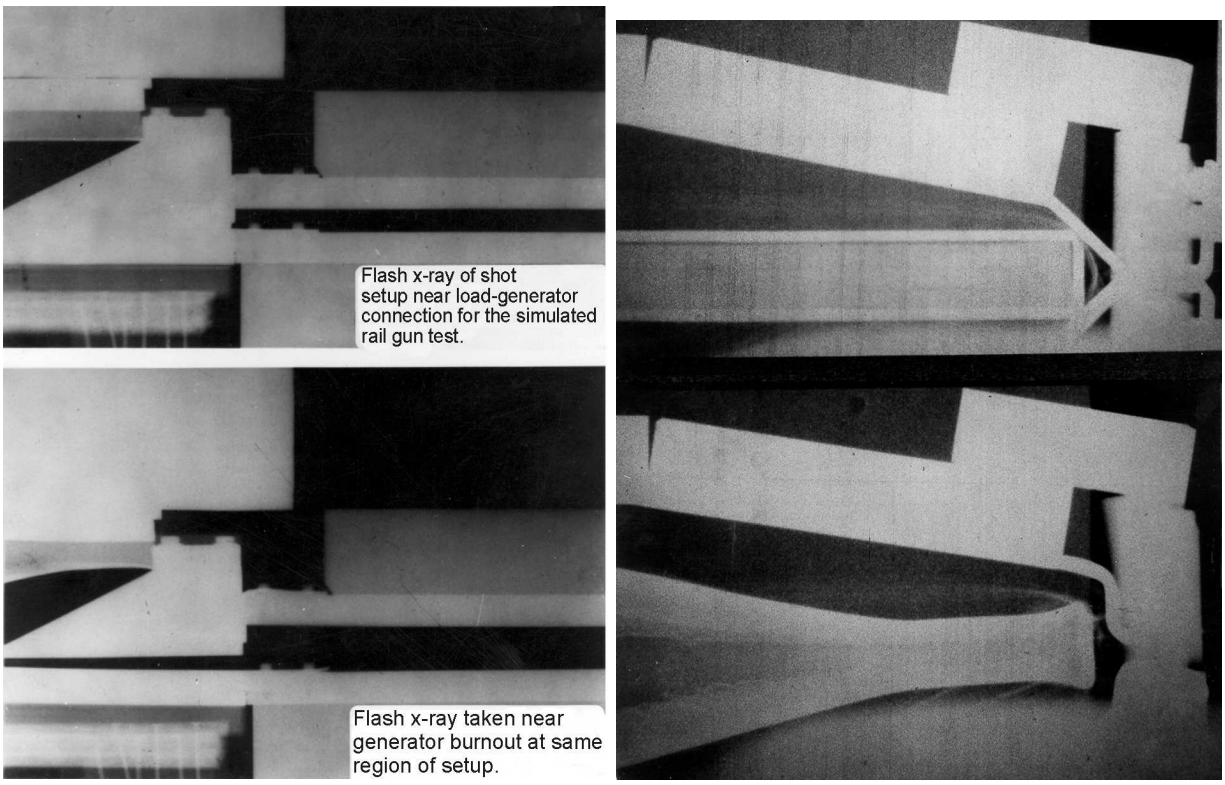

(a) (b)

Fig. 15. Undesirable motion caused by magnetic forces. Upper Views show different assemblies before firing. Lower views show displacement and distortion of metal components near generator burnout caused by magnetic forces.

electromagnetic energy is limited by a number of factors including the particular characteristics required by the load and special requirements of the explosive.

As an example of the load influence, consider Eq. (14). Even if the generator system is lossless, e.g. both l and R are negligible; the maximum energy that can be delivered to a load L_1 is $E_1 = E_0(L_0+L_1)/L$. It is clear that if L_1 is comparable to the initial generator inductance L_0, the final load energy would at most double the initial energy.

The disposition of the explosive is also significant. Often, more explosive than ideally required is needed for practical reasons. For example, in the cylindrical implosion system of Fig. 10, there are practical limits on how closely spaced the detonators may be mounted. The wall thickness of the explosive ring must be large compared to the detonator spacing; otherwise, perturbations from the detonation points will affect the subsequent liner motion.

Generators in which the explosive is confined by the armature are normally more efficient. In the helical generator of Fig. 6, the loop generator of Fig. 14, and the upper coaxial generator of Fig. 11, the explosives are confined by the armatures and do maximum work against them. These systems may be compared to the generators shown in Figs. 8–10 and the lower view of Fig. 11. Here the explosives are unconfined on one surface, and only a portion of the explosive energy is used to drive the armatures. Under some conditions, part of the lost energy can be recovered by "tamping" the explosive; that is, by putting some heavy ballasting material such as steel plates over the explosive. The resulting gains are, however, not very large.

Efficiencies are not often reported. Under some circumstances, relatively high values have been obtained. In all cases, generator and load inductances have been chosen to give relatively large ratios and the explosives have been armature confined. Bichenkov and Lobanov [86] reports efficiencies of 12–14 % using a bellows-type strip generator. Morin and Videl [53] report a 13 % efficiency using a helical generator followed by an in-line coaxial generator. Pavlovskii et al. [55] reports efficiencies of 20 % with helical-coaxial generators, under specialized conditions. A word of caution is in order, however, in rating generator efficiencies. Usually, the useful energy delivered to a load L_1 is defined as $0.5L_1I^2$. However, the total generator electrical output is the integral of the power delivered. This latter value is frequently as much as 50 % larger than the load energy, since the generator must supply energy for resistive losses, flux trapped in conductor skins, and expansion of metal components. Degnan et al. [94], for example, described a helical generator that delivered 10 MJ of energy to an

inductance load, but the integrated power (i.e. energy) delivered by the generator was 15 MJ. Pavlovskii and his coworkers [55] have cited similar data.

Frequently, efficiencies can be increased but at an increase in cost. For example, in the cylindrical implosion system of Fig. 11, the charge wall thickness can be reduced in some cases, if more detonators are used. However, high-quality detonators, which are required for such systems, are expensive. In another study, Fowler [95] doubled the efficiency of a helical generator by boring out half of the armature explosive and reducing the armature wall thickness somewhat. However, the additional explosive machining nearly doubled the explosive cost.

In summary, in certain applications, efficiencies can be relatively good. Usually, existing efficiencies can be increased but often at increased cost. In most cases, improved efficiency is not particularly important but several exceptions were listed earlier. Generally speaking, the major criteria are whether significant weight and volume reductions can be made by using generator power sources and in some cases when no other reasonable power source can supply the load power requirements

4. Power Conditioning

Many of the power handling and conditioning techniques used in nonexplosive pulsed power systems have been adapted to explosive pulsed power conditioning. Among these are opening and closing switches, transformers, and exploding wire or foil fuses.

4.1. Switches

Switches, either closing or opening, and often both, are normally required in power conditioning. General treatments of the subject are available in several references, such as the books *Opening Switches* [96] and *High Power Switching* [97], which contain comprehensive reviews of the subject.

4.1.1. Closing Switches

Most closing switches used at Los Alamos are activated by detonators including those that switch in the capacitor banks that normally supply the initial flux. The configuration usually employed consists of an insulator, such as polyethylene, Mylar, polypropylene, captan, etc., sandwiched tightly between two metal plates. One of the plates is connected to an active circuit and the other plate is connected to the circuit to be switched in. Detonators are mounted on one of the plates over small holes drilled through the plate. After initiation, the detonators produce small jets that tear up the insulation thus allowing current flow into this plate and the rest of the circuit. This type of switch has proved to be quite reliable. Premature switch breakdown during capacitor bank charge-up is usually as disastrous as failure of the switch to close. If the switch fails to close, the timing sequence of the usual shot is such that the generator explosives are detonated anyway. If the switch breaks down prematurely, often the explosive is not detonated, but the magnetic forces produced by the early current flow will frequently tear up the generator system and, often worse, may break up the explosive, scattering undetonated pieces over the firing table.

Another type of closing switch used occasionally depends upon the two plates discussed above to short to each other when the voltage difference across the plates reaches a certain preset value. As normally used here, the insulation used between the plates has been selected to break down at a certain voltage. Once that voltage level has been reached, the insulation breaks down, thus letting current flow through the plates and the part of the circuit that has now been switched in.

4.1.2. Opening Switches

Two kinds of opening switches, when required, have been used in most Los Alamos FCG experiments. They are electrical exploding wires, or fuses, and what are termed explosively formed fuses (EFFs).

Fuses: The study and use of fuses has been around for a long time. Generally speaking, they are used to open a circuit branch, or to become so resistive that current flow in the circuit branch is greatly reduced and shunted to another branch of the circuit. Generally, as the fuse resistance increases, so does the voltage, IR, across the fuse. In the work discussed here, fuses are then generally designed to not only open one circuit branch, but to also put a high voltage across the new circuit being shunted or switched into the system. Much information on the history, behavior and applications of fuses can be found in the four collections of papers edited by Chace and Moore [98] under the titles "Exploding Wires" and spanning the years from 1959 to 1968.

When used with FCGs, fuses are usually in the form of metal foils or a number of parallel wires. The fuses are usually "tamped" to inhibit expansion of the fuse material. Foils, for example, are often placed between heavily clamped plates and wires are frequently embedded in materials like quartz sand. If expansion is unlimited, the expansion kinetic energy can dwarf the internal energy at certain stages of the fuse heating. To calculate the performance of a well tamped fuse as a circuit element, the fuse length, l, in the direction of current flow, and cross-sectional area, A, of the foil or wires must be given, as well as the specific resistivity, $\rho(E)$, and material density, D, often taken as functions of specific electrical energy, E, deposited in the fuse. Figure 16, modeled roughly after the data of DiMarco and Burkhardt [99], gives a plot of resistivity vs. specific energy for well-tamped copper foils of various dimensions. The lower curve

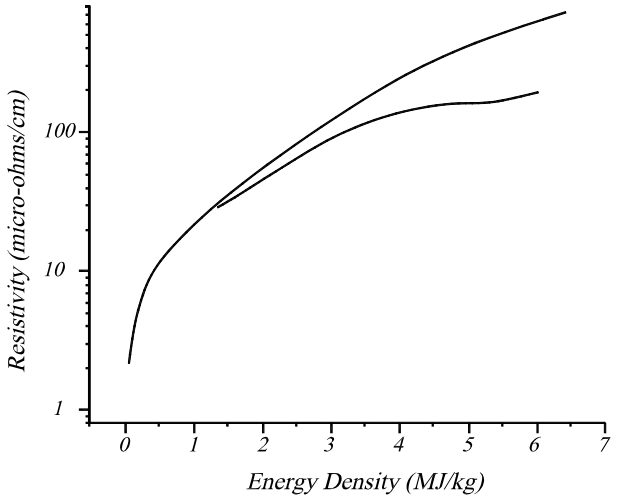

Fig. 16. Resistivity vs. specific energe for copper (after [99]).

was for very thin, short foils. Up to the onset of vaporization, which occurs when the specific energy is about 1.3 MJ/kg, the fuse specific resistivity is largely independent of dimensions. Except for very thin foils, the specific resitivity up to 3–4 MJ/kg, is still reasonably good, with a data spread within 15–30 %. This data is consistent with that taken for wires. At higher energy densities, above 5 MJ/kg, there is more scatter in the data. Proper accounting for all the factors affecting fuse behavior would be a formidable task indeed. Lindemuth et al [100] have, however, developed a code that accounts for many factors not normally treated in fuse calculations and that shows favorable comparisons of calculated and experimental results for various FCG-fuse experiments. We have found, however, that in many cases using the simple equation for resistivity, given below, yields results not too different from those obtained with more sophisticated codes. The equation used, Eq. (29a), is a rough fit to the DiMarco-Burkhardt data (upper curve of Fig. 16)

$$\rho(E) = 1.7 + 20\mathrm{xE} + 2.0\mathrm{xE}^2, \quad \mu\mathrm{ohm-cm}, \quad (29a)$$

$$E = \int I^2 R dt/M, \quad \text{joules/kg}, \quad (29b)$$

$$R = l\rho(E)/A, \quad (29c)$$

$$M = lAD(E). \quad (29d)$$

The above relations are solved iteratively with the generator circuit equations. For heavily tamped fuses, the D and A are taken as constant. For untamped fuses, a big uncertainty generally lies in estimating the density from which the area, A, is obtained and, indeed, suggests that there are wide variation of the physical properties throughout the fuse volume. The general complexity of the subject is illustrated by Webb et al [101].

The term "Action", used in fuse technology, is frequently encountered:

$$\text{Action} = \int I^2 dt. \quad (29e)$$

Tucker and Neilson [102], for example, found a better correlation of some properties with action than with specific energy. In particular, fuse designs have sometimes been based upon action integrals rather than on specific energies. This integral also appears in the analysis of magnetically accelerated plates.

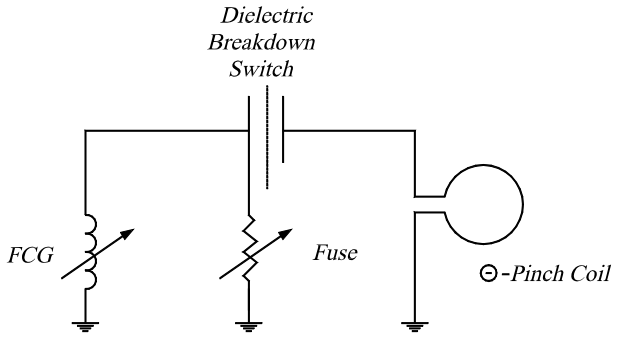

Fig. 17. FCG powered Θ-pinch with fuse and dielectric breakdown switch.

Figure 17 is a sketch of an early application of fuses employed in an FCG powered experiment reported by Damerow et al [103]. The demands on the fuse were to deliver a predetermined voltage across a Θ-pinch coil a few microseconds before generator burnout. The thickness of the dielectric material between the two switch plates was chosen to breakdown at a desired voltage. Laboratory tests confirmed that breakdown voltages could be controlled to within 5–10 % of the pre-selected voltage, as indeed they did on the subsequent successful shot series. Quite recently, a Russian team has employed the same technique in FCG-powered Vircator experiments, as noted in Sec. 5.3. As a final comment, before using a fuse in an expensive shot, it goes without saying, that considerable pre-testing should have been done

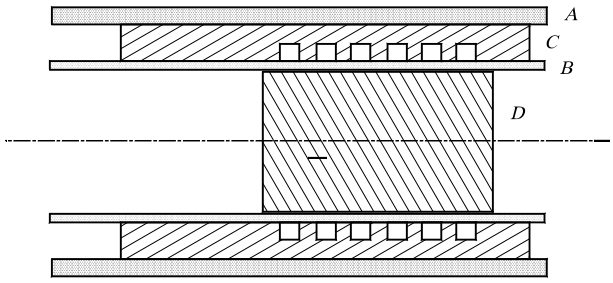

Fig. 18. Explosively Formed Fuse: A – outer conductor, B – inner conductor, C – grooved Teflon insulator, D – explosive initiated simultaneously on axis.

EEFs: Figure 18 shows the basic elements of an *Explosively Formed Fuse*. The inner metallic cylinder,

one of the current carrying conductors, is driven radially outward at the appropriate time by the central explosive charge. The circular grooves in the Teflon insulator act in such fashion as to nearly cut the conductor. These switches are sometimes referred to as "cutter" switches, but as Goforth and Marsh [104] noted from various 2-D hydro calculations, the actual action is one of greatly thinning the portions of the conductors in the grooves, in essence making much of the conductor into a thin foil, as in a foil fuse. In a later paper, Goforth et al [105] were able to switch a current of about 20 MA into a load in a time of 2 μs. Chernyshev et al [106] had earlier used a planar version of this switch. In these papers, various closing switch systems are described that switch in the second circuit branch.

4.2. Transformer Coupling

Large impedance loads, not capable of being powered effectively by direct connection to a generator, can be effectively energized by transformer coupling to the generator.

4.2.1. Powering a Large Inductance

Equation (14) shows that the maximum energy (at generator burnout) that can be delivered by a generator of initial inductance L_0 to a series connected load L_1 in the absence of circuit resistance and source or loss inductance is

$$E = E_0(L_0 + L_1)/L_1. \tag{30}$$

Thus, a generator could, even in the ideal case, at most deliver twice the initial circuit energy into a load whose inductance equaled or exceeded that of the initial generator inductance.

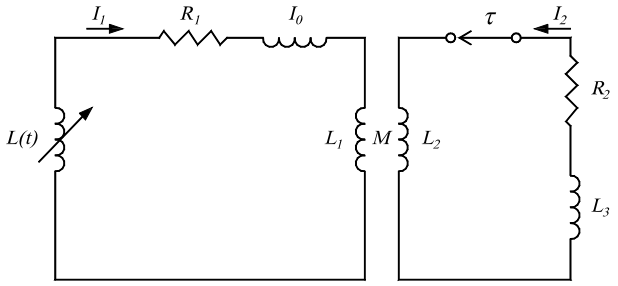

Fig. 19. Circuit showing how FCGs power larger impedance loads, L_3, R_2, through an impedance matching transformer.

The situation is different, however, if we connect the load to the secondary coil of a transformer coupled to its primary coil that is powered by the generator, as shown in Fig. 19. In this figure, the primary circuit contains the generator $L(t)$, a resistance R, a source or loss inductance l_0, and the inductance L_1 that serves as the transformer primary. The secondary circuit contains the transformer secondary L_2, a resistance R_2, and the inductance L_3, which is the load to be energized. Provisions are made to close the secondary circuit at a later time τ through the switch shown in the figure. The currents I_1 and I_2 flow through the two circuits. The primary and secondary circuits are mutually coupled with an inductance, M, which can also be expressed in terms of a coupling coefficient k,

$$M = k\sqrt{L_1 L_2}. \tag{31}$$

For purposes of illustration, both resistances are set equal to zero. This allows algebraic solutions for the currents from simple flux conservation laws. Up to switch time τ, the current flows only in the primary and the primary current, I_1 is determined from

$$(L(t) + l_0 + L_1)I_1 = (L_0 + l_0 + L_1)I_0 = \Phi_0 \cdot t \le \tau. \tag{32}$$

At switch time, the current $I_1(\tau)$ is given by

$$I_1(\tau) = \Phi_0/(L(\tau) + l_0 + L_1) \tag{33}$$

and the flux in the secondary circuit, Φ_2, is

$$\Phi_2 = MI_1(\tau). \tag{34}$$

After switch time, with Eqs. (32) and (34), the conservation of flux yields the following circuit equations

$$(L(\tau) + l_0 + L_1)I_1 + MI_2 = \Phi_0, \tag{35a}$$

$$MI_1 + (L_2 + L_3)I_2 = \Phi_2 = M\Phi_0/(L(\tau) + l_0 + L_1), \tag{35b}$$

At generator burnout, $L(t) = 0$, so that the above equations yield

$$I_2(burnout) = \frac{-ML(\tau)\Phi_0}{(L(\tau) + l_0 + L_1)[(L_2 + L_3)(l_0 + L_1) - M^2]}. \tag{36}$$

As will be seen also in later examples, choosing optimum values for the transformer inductances can increase I_2 at burnout. This will, of course, increase the energy delivered to the given load, L_3. As an example, with other parameters fixed and with the use of Eq. (36), the current I_2 at burnout, Eq. (36), is optimized by proper choice of the transformer secondary inductance

$$L_2(\text{optimum}) = \frac{L_3}{\left(1 - k^2\dfrac{L_1}{L_1 + l_0}\right)} \cong L_3/(1 - K^3), \tag{37}$$

where the effective coupling coefficient K is defined through

$$K^2 = k^2 L_1/(L_1 + l_0).$$

From Eqs (36) and (37) the burnout current ratio for optimum secondary inductance becomes

$$\frac{I_2(burnout)}{I_0} = \frac{-K}{2\sqrt{1-K^2}} \times \frac{L_0+l_0+L_1}{L(\tau)+l_0+L_1} \cdot \frac{L(\tau)}{\sqrt{L_3(l_0+L_1)}} \quad (37.7)$$

and the corresponding load energy at burnout becomes

$$\frac{1}{2}L_3 I_2^2(\text{optimum}) = \frac{E_0}{4} \cdot \frac{L_0+l_0+L_1}{l_0+L_1} \times \left(\frac{L(\tau)}{L(\tau)+l_0+L_1}\right)^2 \cdot \frac{K^2}{1-K^2}. \quad (38)$$

Here, E_0 is the initial circuit energy, $0.5(L_0 + l_0 + L_1)I_0^2$.

As an example, we calculate the energy gain ratio, $0.5L_3I_2^2/E_0$, for an inductive load $L_0 = 10$ μH. Other parameters are: $L(0) = 10$ μH, $L_1 = 0.1$ μH, $l_0 = 0.05$ μH, $k = 0.85$, and secondary switching is delayed until $L_\tau = 2$ μH. The parameter $K^2 = k^2L_1/(L_1 + l_0) = 0.4817$ and from Eq. (37), the secondary inductance should be

$$L_2(\text{optimum}) = 10.0/(1 - 0.4817) = 19.29\ \mu\text{H}$$

and, from Eqs. (37.7) and (38), the current and energy ratios are

$$\frac{1}{2}L_3I_2^2/E_0 = 13.60 \text{ and } I_2/I_0 = 3.719.$$

This example illustrates several points.

- The gain of 13.60 is respectable from a generator whose initial inductance is no larger than that of the load. It will be recalled that a maximum gain of two could be realized by directly powering the load.
- When the secondary is not optimized, the gain is reduced, but only slightly for L_2 values even substantially greater than that for the optimum energy. On the other hand, the gain drops off rather quickly for L_2 values much less than the optimum value.
- When the secondary is not optimized, the gains are reduced, but only slightly for values of L_2 greater than that for the optimum current.
- The factor $K^2/(1 - K^2)$ in the energy gain equation varies from 4.26 for $K = 0.9$ to 0.56 for $K = 0.6$. This shows the importance of high coupling coefficients, k, and minimizing the source inductance, l_0. If l_0 had been zero in the numerical example given above, the gain ratio would be 38.1. It is clear that for given k and l_0, K^2 improves with an increase in the primary inductance L_1. However, this decreases the value of the other energy gain factors.
- The factor $[L(\tau)/(L(\tau) + l_0 + L_1)]^2$ changes relatively slowly until $L(\tau)$ drops to a few times the residual inductance, l_0+L_1. The difference in gain from switching in the secondary quite late, $L(\tau) = 1$ μH. and quite early, $L(\tau) = 9$ μH, results in a gain decrease of only 22 %. This result is important in power conditioning, when load power times must be much shorter than the basic generator burn time.
- Multiplication of Eq. (36) by L_3 gives the flux in load L_3 at burnout. Using the optimum value of $L_2 = 19.29$ μH and the corresponding value of $M = 0.85 \cdot \sqrt{(0.1)(19.29)}$ μH, the ratio of flux in L_3 to ϕ_0, the initial circuit flux is -7.15. This flux increase in L_3 over the initial circuit flux is usually called *flux multiplication*. At first thought, this seems almost a contradiction in terms since the flux in a perfectly conducting circuit cannot increase. The answer lies, of course, in that the large negative fluxes in the secondary inductors, L_2I_2 and L_3I_2, are almost balanced by the large positive mutual inductive flux, MI_1, in the secondary circuit.

4.2.2. Powering Large Resistances

In some cases, the loads to be energized are mainly resistive and include such devices as flash lamps, some diodes, and laser cavities. As noted in Eq. (11), the load resistance must be substantially less than the average generator impedance to be powered directly in an effective way. With rare exceptions, this limits load resistances to less than an ohm. However, with proper selection of the transformer inductances of Fig. 19, resistive loads placed in the secondary circuit can be efficiently energized. The coupled circuit equations for Fig. 19 cannot, in general, be solved analytically in tractable form. Consequently, the equations have been numerically solved, in a fairly general way. The primary circuit consists of the generator, $L(t)$, a source or loss inductance, l_0, the primary transformer inductance, L_1, and a resistance term R_1. The secondary circuit contains the transformer secondary L_2, load resistance R_2, provisions for a load inductance L_3, and a closing switch at time τ. The mutual transformer inductance is M. It is usually expressed in terms of a coupling coefficient $k = M/(L_1L_2)^{1/2}$.

The generator inductance is written explicitly as

$$L(t) = L_0[1 + A(t/T_1) + B(t/T_1)^2 + C(t/T_1)^3, \quad (39)$$

where L_0 is the initial generator inductance and T_1 is the generator burnout time. A, B, and C may be selected somewhat arbitrarily, provided that $L(t)$ decreases monotonically to zero as $t \to T_1$. Equation (39) is general enough to represent fairly well

the inductance behavior of a plate generator. If we set $A = 1$, $B = C = 0$, Eq. (39) reduces to Eq. (15), which we have used to approximately represent the plate generator. However, for most of the examples given below, we have used the following:

$$\begin{aligned} &L_0 = 10\ \mu\text{H}, \quad T_1 = 100\ \mu\text{s}, \\ &A = -0.75, \quad B = -1.5, \quad C = 1.25. \end{aligned} \tag{40}$$

These values result in $L(T_1) = 0$, $dL(T_1)/dt = 0$ and give a flex point in the inductance at $t = 0.2T_1$. This behavior is qualitatively characteristic of many helical generators. The primary resistance R_1 may be a fixed resistance or it may also include a fuse. When fuses are used here, they are considered to be of copper, and their performance to be governed by Eqs. (29a–29d). The fuse input parameters consist, then, only of the fuse length and cross-sectional area. Most of the examples to follow do not incorporate the fuse. It is effectively removed from the circuit by giving it a ridiculously large cross-sectional area — say 0.5 m^2. For later examples, where it is used, it is somewhat surprising how well it yields results in reasonably good agreement with calculations employing more sophisticated models such as those developed by Lindemuth et al. [100].

As a first example, we consider energizing a 20 Ω load directly by the generator. The primary resistance R_1 becomes the load of 20 Ω. The source inductance is $l_0 = 0.1$ μH and the initial current is $I_0 = 200,000$ amperes. L_1 is taken as zero and the secondary circuit is suppressed by setting $k = 0$. The initial inductive energy in the system is

$$E_0 = 0.1LI_0^2 = 0.4 \cdot [10.1] \cdot 10^{-6} \cdot [2 \cdot 10^5] = 202 \text{ kJ}.$$

Upon solving the circuit equation, it is found that only 202.8 kJ are delivered to the 20 Ω load and almost all of it is in a time of only 2–3 μs. If the circuit inductance L_c did not change, the initial inductive energy would transfer to the resistive load as follows

$$E_R(t) = 0.5L_cI_0^2(1 - e^{-2Rt/L_c}).$$

With an initial inductance of 10.1 μH and resistance of 20 Ω, 99.9 % of the initial energy would be delivered to R in less than 2 μs. In this time, according to Eq. (39), the generator inductance has decreased only about 1 %, but there is almost no flux left in the generator to compress. In total, the generator managed to deliver only an additional 800 J to the original inductive energy of 202 kJ, hardly an impressive performance!

Energizing Through a Transformer: We will now consider powering the same 20 Ω resistor through a transformer. In this case, R_2 of Fig. 19 is the 20 Ω load. We first solve a standard problem and then investigate the effects of varying some of the parameters.

The upper curve of Fig. 20 shows the energy deposited in the 20 Ω load as a function of time.

Table 2. Standard Problem.

Primary Circuit	
Generator Equations	(1.39) and (1.40)
Primary Inductance	$L_1 = 0.50$ μH
Source or Loss Inductance	$L_0 = 0.1$ μH
Resistance	$R_1 = 0.005$ Ω
Initial Current	$I(0) = 200$ kA
Secondary Circuit	
Secondary Inductance	$L_2 = 800$ μH
Secondary Loss Inductance	$L_3 = 0.50$ μH
Load Resistance	$R_2 = 20$ Ω
Initial Current	$I_2(0) = 0$
Switch Time	$TS = 0$
Fuse	No
Coupling Constant	
$k = M/(L_1L_2)^{1/2} = 0.90$	

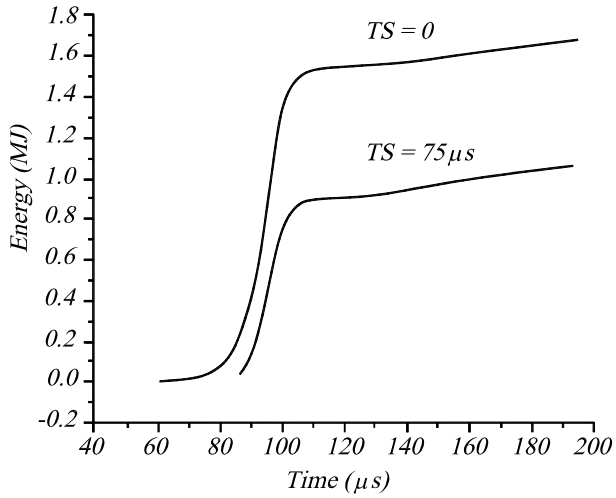

Fig. 20. Energe delivered to a 20 Ω load vs. time: upper curve for the standard problem, Table II; lower curve same except the secondary circuit is switched in at 75 μs.

At generator burnout, 100 μs, 1.26 MJ have been deposited. At generator burnout, the primary current exceeds 4 MA and there is a considerable amount of inductive energy stored in the circuits. This results in an additional energy transfer to the load beyond generator burnout as the currents decay. In this case, the final energy delivered to the load reaches 1.77 MJ. Ninety eight percent of this final load energy is delivered in less than 300 μs or somewhat less than 200 μs after burnout. In general, however, it would be difficult to keep the explosive from blowing the circuit apart for such a long time. However, as seen from Fig. 20, over 1.5 MJ is delivered to the load in 110 μs,

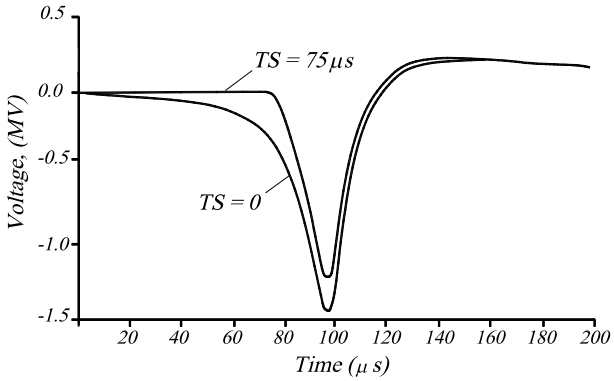

Fig. 21. Voltage developed across 20 Ω load vs. time, for the standard problem ($TS = 0$) and for standard problem except the secondary circuit is switched in at $TS = 75$ μs.

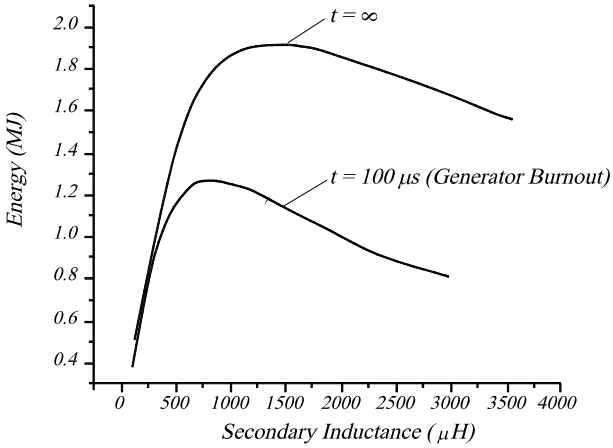

Fig. 22. Variation of energy delivered to a 20 Ω load as a function of transformer secondary inductance. All other circuit parametters are those given for the standard problem in Table II. The lower curve gives the energy delivered up to the time of generator burnout, $t = 100$ μs; the upper curve gives the total energy delivered, $t = \infty$.

or only 10 μs beyond burnout making it relatively easy to protect the rest of the circuit. The lower curve shows the effect of switching in the secondary circuit 75 μs after the start of generator action. The curves in Fig. 21 show the voltage developed across the 20 Ω load for switch times of 0 and 75 μs after generator start. In the former case, it reaches a peak of nearly – 1.5 MV a little before generator burnout and, although reduced, still exceeds – 1 MV for the latter case.

We consider, now, how variations of some of the parameters influence the energy delivered to the load at generator burnout and the final energy.

Primary Source Inductance: With a reduction of the source inductance from 0.1 μH to 0.05 μH, the energy at burnout increases from 1.26 MJ to 1.69 MJ and the final energy increases from 1.77 MJ to 2.28 MJ. Good generator design calls for minimizing primary source inductances, particularly when transformers are used.

Primary resistance: If the primary resistance in the standard problem is reduced from 0.005 Ω to 0.002 Ω, the energy at burnout increases from 1.26 MJ to 1.76 MJ and the total energy from 1.77 MJ to 2.57 MJ. On the other hand an increase of the resistance to 0.008 Ω decreases these energies to 0.91 MJ and 1.25 MJ, respectively. Coaxial cables are often used to connect generator outputs to the load. Since the cable braids are frequently thin compared to skin depths, they may be characterized by a resistance and an inductance per unit length. If the cables are not too long, a sufficient number may be paralleled to keep the resistive losses manageable. Most of the other metallic conductors in a generator circuit are relatively thick compared to skin depths. Losses in those elements should be treated as source inductance losses, although these inductances vary with time [89].

Coupling coefficient: If the coupling coefficient is reduced from 0.9 to 0.8, the load energy at burnout is reduced from 1.26 MJ to 0.75 MJ and the total energy from 1.77 MJ to 1.16 MJ. A number of transformers for generator applications have been constructed with $k = O.9$. However, it is rare to find expendable transformers with k exceeding 0.85 that withstands megavolt potentials. Some of these transformers will be discussed later.

Variation of transformer inductance: As with energizing inductances, there are optimum values of the primary and secondary inductances for maximum energy delivery to resistive loads.

Figure 22 shows how the energy delivered to the 20 Ω load varies with the secondary inductance, assuming that the other circuit parameters remain at the values prescribed for the standard problem. The lower curve gives the energy delivered up to the time of generator burnout, while the upper curve gives the final energy. As seen, a secondary inductance of about 800 μH delivers a maximum energy of 1.26 MJ at generator burnout, while an inductance of about 1500 μH delivers the maximum total energy to the load. These curves are typical in that they show a relatively rapid rise in energy delivered to the load with increasing inductance up to the optimum value, with a rather gradual fall-off in delivered energy for inductances beyond the optimum. A similar behavior is observed for variations in the primary inductance. Optimization of both primary and secondary inductances occurs when $L_1 = 0.35$ μH and $L_2 = 685$ μH. Energy of 1.29 MJ is delivered to the 20 Ω load at generator burnout. In this particular example, which has a rather wide range in both L_1 (0.2 to 0.7 μH) and L_2 (500–2000 μH), the generator still delivers load energies no less than 75 % of the

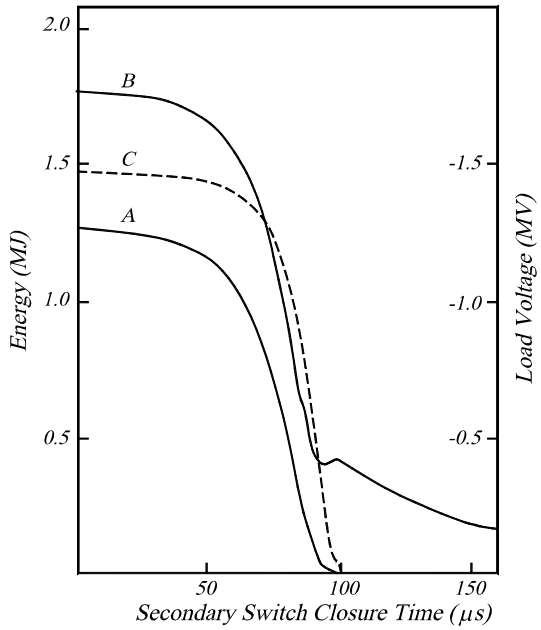

Fig. 23. Variation of load parameters vs. secondary circuit switch time. All other circuit parameters are those for the standard problem in Table II. Curve A gives the energy delivered to the 20 Ω load at generaror burnout, $T = 100$ μs. Curve B gives the total energy delivered to the load, $t = \infty$, while curve C gives the peak voltage developed across the 20 Ω load.

optimum value.

Variation of Secondary Switch Closure: In some applications, it is undesirable to have the load in the circuit during the entire generator burn time. For the typical generator, with its rising current pulse, the load energy and voltage are not degraded seriously, even when the secondary circuit is not switched in until late in the generator run. The curves in Figs. 20 and 21 marked $TS = 75$ μs show the time evolution of energy delivered to and voltage across the load when the load is switched in at 75 μs. As noted in these figures, the energy delivered at generator burnout is still over 0.7 MJ while the peak voltage remains high, (-1.2 MV). The rise times are of course, also shorter. Figure 23 shows how some of these quantities vary with switch closure time. Curve A gives the energy delivered to the load at generator burnout, curve B shows the total energy delivered to the load, and curve C gives peak voltage developed across the load. As noted, these values drop off very little for switch times as late as 50 μs. Even for switch times as late as 80 μs, over half a megajoule is delivered to the load at generator burnout and the peak voltage developed still exceeds a megavolt. The small ripple in the total final energy near burnout might be an artifact owing to the simple energy algorithm used in the code. However, the general circuit behavior is quite complicated, so this behavior cannot be ruled out. In any event, it is not evident that any advantages occur from switching in the load after burnout in the present situation.

Load size: As noted in Fig. 22, secondary inductances of hundreds of microhenrys are required to power the 20 Ω load effectively. This is not too surprising, in that it might be expected that RT_1/L should be of order unity, where L is some weighted inductance of the transformer. With $R = 20$ Ω and $T_1 = l00$ μs, L might be expected to be in the millihenry range. As inferred from Fig. 22, secondary currents must approach 75 kA in order to develop voltages of nearly 1.5 MV across the 20 Ω load. It would be very difficult to build secondary inductances in the millihenry range of a reasonable size that would carry this current and retain a large coupling coefficient. On the other hand, we would expect smaller secondary inductances if the load resistance was smaller. For example, if the load resistance was reduced to 2 Ω in the standard problem, the inductances are 80 μH for maximum energy delivered at burnout (1.24 MJ) and about 160 μH for maximum total energy (1.92 MJ). These energies are about the same as those delivered to the 20 Ω load, but the secondary inductances are much more reasonable. However, it should be noted that peak voltages across the load are less than 0.5 MV or less than a third of those developed across the 20 Ω load.

Generator Burn Time: If the burn time of the generator is reduced, it might be expected that the optimum transformer inductance would be correspondingly reduced. As an example, if the burn time T of the standard problem were reduced to 20 us, the optimum secondary inductances are about 170 μH to deliver a maximum energy at burnout of 1.95 MJ to the 20-Ω load and somewhat over 600 μH to deliver maximum total energy of about 4 MJ. These values are to be compared to 800 μH and 1,600 μH for the standard problem where $T_1 = 100$ μs. Peak voltages across the load, that occur a few microseconds before burnout, exceed 4 MV in these calculations. The large voltages developed would be expected since the generator inductance is wiped out in one-fifth of the time. The larger energies have a more complicated explanation. The shorter operation time has two effects. The energy deposited in the load is reduced because the currents flow for shorter times. However, for the same reason, the resistance in the primary circuit has less time to attenuate the primary current. Coupled with the faster rate of change, the increased secondary currents more than offset the effect of having less time for the load to accumulate energy.

For an experimental example, we quote the results of a shot described by Erickson et al. [107], in which a plate generator powered a resistive load through a transformer. As noted, the plate generator had an initial inductance of 174 nH and a burn time of 7.7 μs. The primary inductance was 27.3 nH and the secondary inductance was 19 μH. The load was

an encapsulated solution of copper sulfate having a resistance of 25.5 Ω. The primary-secondary coupling coefficient, which was measured, was 0.76. Estimates of the loss terms were: primary source inductance, 7 nH; primary resistance, 1.3 mΩ; and secondary stray inductance, 400 nH. With an initial current of 900 kA, and, therefore, an initial inductive energy of about 84 kJ, the following results were obtained:

Peak voltage across load:	1.08 MV
Load energy at burnout:	23 kJ
Total load energy:	40 kJ

The computer simulation used the approximate expression Eq. (15) for the plate generator. The coefficients for Eq. (39) thus became:

$$L_0 = 0.174\ \mu\text{H},$$
$$T_1 = 7.7\ \mu\text{H},$$
$$A = -1, \qquad B = C = 0,$$

with the loss terms and transformer parameters cited above. The values predicted by the code are:

Peak voltage across load:	1.24 MV.
Load energy at burnout:	32 kJ.
Total load energy:	48 kJ.

The agreement between calculated and measured values is reasonable in view of the following: the plate generator model is overly simplistic as noted earlier [65,66]. The primary load coil was switched into the circuit at the start of generator burn. Before this time, current was carried by a 'ballast" load, without which the circuit would be incomplete. This load remained in the circuit during the complete shot. However, as seen from Eq. (29), where L_τ is essentially L_0, the peak primary current (I_2 as used in the equation) is not affected much by the presence of the parallel ballast load.

The voltage pulse rose to its peak (at about generator burnout) rapidly and also dropped rapidly after peaking, with a pulse half width of 1.2 μs. Both the voltage pulse shape and energy delivered to the load were quite satisfactory for the proposed use.

However, the total energy of 40 kJ delivered to the load was less than the initial inductive energy in the system. The causes for this arise from the presence of relatively high loss terms and rather poor coupling of the primary and secondary of the transformer. A comparison of the same problem with no primary resistance, the primary source inductance reduced to 1 nH, and the coupling coefficient increased to 0.9 yielded a peak voltage greater than 3 MV, an energy of about 140 kJ at generator burnout, and a total energy nearly 180 kJ. These results point out again, the importance of minimizing the loss terms and increasing the coupling, in particular for energy sources that work on the principle of flux conservation.

Fuses in Primary Circuit with Transformer: With a properly dimensioned fuse in the primary circuit, the primary current drops rapidly as the fuse resistance increases. This leads to a large negative value of the primary dI/dt, with a corresponding positive voltage developed in the secondary circuit. This technique, particularly when using FCG drivers, was first proposed by Reinovsky et al [108]. Good fuse design calls for maintaining the fuse resistance low until generator burnout is approached, so the basic generator current gain is not reduced too much before fuse action. In some respects, this behavior makes the interesting part of the generator action, at least for transformer purposes, occur in much shorter time. Thus, much smaller inductances are required to efficiently power the load than are required without the fuse.

We consider the problem again, but now incorporate the fuse in the primary circuit, see (Eq. (40). The fuse has heretofore been suppressed by giving it a ridiculously large cross-sectional area that has forced its resistance to remain very low. There are many parameters to be juggled to find optimum transformer values. However, Reinovsky, Lindemuth, and Vorthman [109] have developed a model, based, in part, on the work of Lindemuth et al [100] that allows assignment of the fuse parameters and secondary inductance for optimum performance. In the present example, with a primary inductance of 0.5 μH and load resistance of 20 Ω, near optimum values are: fuse-length 1.75 m, fuse cross-sectioned area 2.5 x 10^{-5} m^2, and secondary inductance 45 μH.

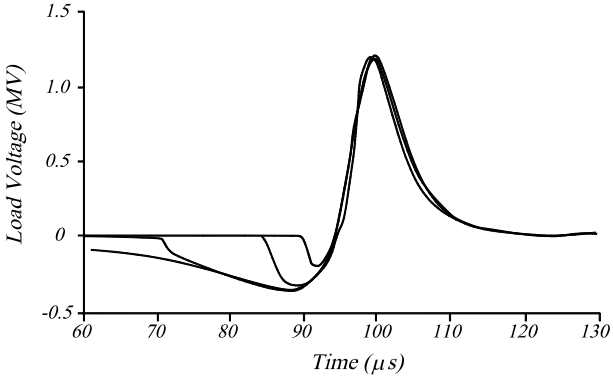

Fig. 24. Voltages developed across 20 Ω load with a fuse in the primary Circuit. As noted in the text, a much lower inductance secondary may be used. In this case, the optimum value is L_2 = 45 μH. The four curves correspond to secondary switch times of 0, 70, 85, and 90 μs. The negative voltage pulse disappears entirely for switch times exceeding 94 μs.

As noted earlier, as the fuse resistance suddenly increases, the primary dI/dt becomes negative with a resultant positive voltage induced in the secondary circuit. However, before the fuse resistance changes

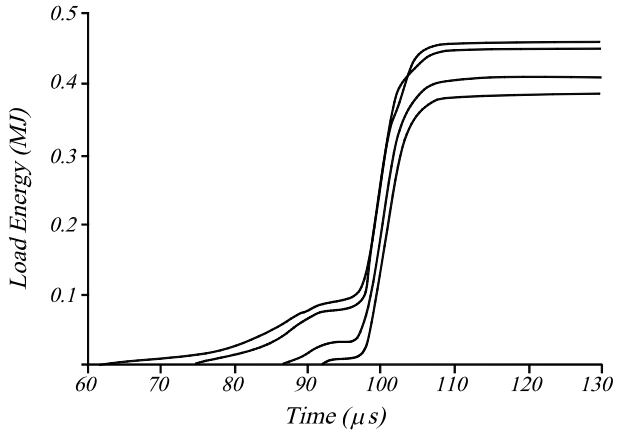

Fig. 25. Energies delivered to a 20 Ω load corresponding to the conditions displayed in Fig. 24. It may be noted that the total energy delivered does not diminish much even when the secondary circuit is switched into the circuit as late as 90 μs.

substantially, the primary dI/dt is positive and the normal negative voltage is induced in the secondary. In many cases this earlier negative part of the secondary voltage pulse is undesirable. However, it may be eliminated without too much loss by delayed switching in the secondary circuit. Figure 24 shows the secondary voltage across the 20-Ω load for several different secondary closing switch times. As the switch time is more delayed, the negative voltage peak continually diminishes. At a switch time of about 94 μs, it disappears altogether. Peak positive voltages exceed 1.2 MV for switch times as late as 98 μs. The curves for load energy vs. time, Fig. 25, show a flex point at the time of peak negative voltage, reflecting the contribution of this part of the voltage pulse. This behavior, of course, disappears for switch times after 94 μs. The energy delivered from the rising part of the voltage pulse (obtained by subtracting the energy at the flex point from the total energy delivered) is surprisingly independent of the switch time (up to 98 μs) and equals about 370 kJ.

Advantages to this approach are: large inductance gains and longer burn times may be used with reasonable sized secondary inductances. Calculations indicate that these systems can operate effectively with somewhat lower coupling coefficients. Problems can arise, however, from development of large primary voltages, lack of holding close tolerances on the fuses, and difficulties in controlling secondary switch times. Reinovsky, Lindermuth, and Vorthman [109] have obtained secondary voltages exceeding a megavolt across high resistance loads using this technique.

4.3. Transformers

Most of the primary coils in generator-powered transformer systems consist of a single-turn hollow cylinder machined from a solid block or fabricated by bending a plate to the required diameter. In either case, the coils are powered directly through an axial input slot through the cylinder walls. Sometimes the primary coil is switched into the circuit at a later time, while ballast loads carry the generator current before switching. Some other primary coils will be described below.

For primary coils of this kind, the secondary coil usually consists of a cylindrical dielectric core, over wound with enough conducting turns to produce the required secondary inductance. The secondary coil is then placed within the cylindrical primary coil. The secondary turns are usually wound in the form of a single layer helix or as tape-wound coils. Normally, the lengths of both primary and secondary coils are about the same. For either kind of coil, the coupling coefficient goes approximately as the square of the ratio of the primary coil radius divided by the mean radius of the secondary coil. These radii must include the current skin depths, which will reduce the coefficient from those calculated from the mechanical radii. For very high voltages, more insulation between primary and secondary will also reduce the coupling.

4.3.1. Helical-wound coils

These coils are often used when the secondary voltages are not too high. In this case, it is possible to get very high coupling coefficients. Khristoforov et al. [110] reported on a number of experiments where various inductive and resistive loads (up to 1.3 Ω) were successfully powered using transformers of this kind. Coupling coefficients were very high — 0.94 ± 0.02. Energy gains approaching 10 (final load energy to initial generator energy) were achieved in some experiments. For resistive loads, the energy at generator burnout was frequently about half the final energy. Load voltage maxima were generally low (typically in the vicinity of 10 kV) except for the larger resistive loads where 170 kV was reported for one experiment. The generator employed was a long strip generator, with burn time of about 300 μs. In an earlier report, Christiansen, Garn, and Fowler [111] reported similar results, but employed a helical generator with effective burn time of $\sim$ 100 μs. The coupling coefficient was reduced to about 0.8 to reduce the voltage in key parts of the secondary circuit. Fowler et al. [112] studied the performance of transformers of this kind in very high magnetic fields. Several different wire materials and dielectric substrates were used. Even for copper wire, transformer integrity was maintained in external magnetic fields as high as 160 T. However, the $\mathbf{j} \times \mathbf{B}$ forces on the wires drove them radially inward into the dielectric substrates, thus, further reducing the already rather low initial coupling coefficients. Loads of various kinds were powered, including resistances

from 0.4 to 40 Ω, inductances from about 10–40 μH, and in one case a 7.15 μF capacitor. Generally, the energies delivered were quite small. Only when the external fields were 40 T or less did the delivered energies approach those initially in the generator.

Reinovsky et al. [113] have worked with a class of helical generators where the primary coil is simply an extension of the stator windings. Sometimes more than one turn is used for the primary. The secondary coil consists of a helical coil wound closely over the primary coil. Bichenkov, Prokopiev, and Trubachev [114] report on similar experiments where the secondary winding covers not only the primary coil but the generator stator winding as well. That part of the secondary winding over the active part of the stator is wiped out by the expanding armature along with the stator. By reversing the winding direction of the primary turns, they obtained coupling coefficients of opposite signs on the two regions of the secondary coil. An analysis of the resulting equations shows that inductive loads may be powered more effectively than by the more conventional methods described above. Some experimental data cited support these calculations.

4.3.2. Tape-wound coils

Tape wound secondary coils were used by Erickson et al. [107] in the megavolt systems mentioned earlier. These coils were wound from thin copper sheets around a dielectric mandrel much like a roll of aluminum foil, but with insulation between the turns. Their construction draws heavily on the techniques described by Martin, Champney, and Hammer [115]. In the present case, the turns were loosely wound, resulting in a rather low coupling coefficient of 0.76. In the most successful configuration, the outermost turn of the secondary coil was attached to one end of the single-turn primary coil. Thus, the high-voltage side of the secondary appeared on the inner turn, farthest away, and therefore, most insulated from the primary. With plate generators serving as the power supply, megavolt potentials were obtained across resistive loads of 25.5 Ω. These results were considered particularly gratifying in that the entire secondary package was contained in a 4-in. diameter primary coil. In an effort to improve the coupling coefficients, Freeman et al [116] have developed larger diameter coils with more closely packed turns. Coupling coefficients have been obtained in the range 0.90±0.02. To date, with plate generator power sources, near open circuit voltages in excess of 600 kV have been obtained. Transformers designed for higher voltages have suffered mainly from creep breakdown. Further work is in progress to solve this problem. To date turn-to-turn breakdowns have not occurred, which is encouraging. Figure 26 shows a (a) photograph and (b) drawing of a tape wound transformer developed by the Institute of Electromagnetic Research in Kharkov, Ukraine.

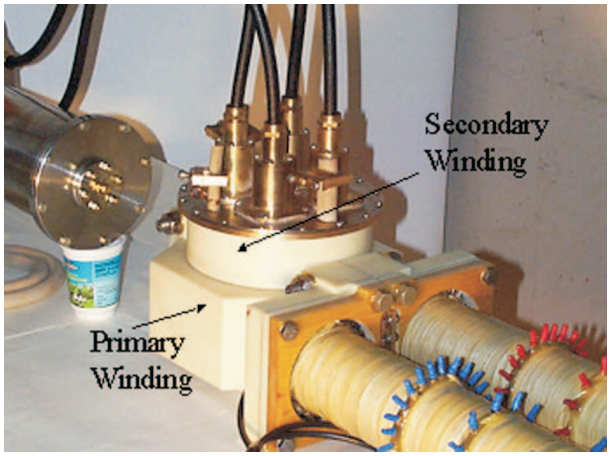

(a)

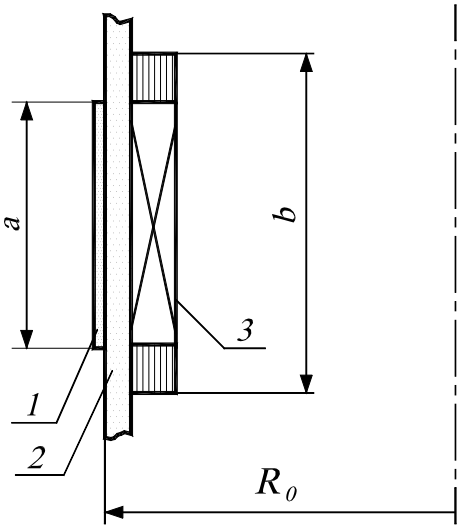

(b)

Fig. 26. a) Photograph and (b) sketch of tape wound impulse Transformer: 1 – Primary Winding, 2 – Insulating Layer, and 3 – Secondary Winding. (Courtesy of the Institute of Electromagnetic Research, Kharkov, Ukraine).

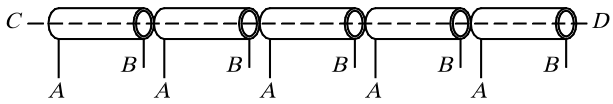

Fig. 27. Sketch showing construction of coaxial cable transformer.

4.3.3. Coaxial cable transformers

Figure 27 shows the construction of a coaxial cable transformer. The outer braid is broken into N segments A-B, where N is the number of turns required for the secondary. The ends A are attached together and serve as one of the primary coil input

leads. Ends B are attached together and serve as the other primary input lead. Thus all segments A-B are in parallel. The center core CD serves as the secondary. Clearly, the pulse generated across CD tends to be N times the primary pulse. The Authors do not know the origin of this technique, but they have been used at the Los Alamos National Laboratory for at least 40 years. Coupling coefficients for these transformers can be quite high. Values exceeding 0.97 at 500 kHz were measured at Los Alamos using very low inductance coaxial cable (22 nH/ft) [117]. Clearly, however, high voltage limits are set by the breakdown strength of the coaxial cable. These transformers have been brought to a high state of development by Pavlovskii et al. [118]. A number of transformer configurations are described by these authors, as well as, their use in powering various loads.

4.4. Generator Flux Sources (Seed Sources)

In this section, we will first consider sources that provide the initial flux to a generator system. This will be followed by a brief discussion in which one generator supplies the initial flux to a second generator. Capacitor banks are normally used to supply initial flux. Most often the banks are series connected to the generator and the initial flux is generated by the current flowing through the generator. In this case, care must be taken not to exceed the structural strength limits of the generator, since the accompanying magnetic forces tend to move the generator components according to Eq. (26). As noted by this equation, component motion may be reduced by decreasing the time T required to generate the required flux, increasing the effective mass of the conductors, or otherwise inhibiting their motion. A highly effective way to inhibit stator coil motion in helical generators has been developed by Pavlovskii et al. [55]. They overcast the stators with a layer of concrete. We have found that this not only supports the coil turns well, but seems to reduce shrapnel range from the ensuing explosion. For the plate generators of Sec. 2.2, the aluminum plates are light, yet the current loading density is high. The initial weight of the explosive serves as additional tamping. Without this additional weight, the plates would separate substantially during the initial loading time.

Reduction in loading time can be accomplished by using higher voltage banks of equivalent energy. Fowler and Caird [119] describe a generator designed for an initial loading of 600–700 kJ, normally obtained from two modules of a capacitor bank connected in parallel. By hooking the two modules in series, the time scale for transfer of energy was cut in half. Under these conditions the generator encountered no difficulty in accepting energies in excess of a megajoule. Finally, we know that in the typical sine wave discharge from a capacitor bank into a generator, very little flux is added to the generator in the last 10–20 % of the quarter period, yet much of the integral of the square of the current evolves here. It is, therefore, more or less standard practice to start generator action sometime before peak currents would be developed. Not only are generator component motions substantially reduced, but so, also, are heating effects in the conductors. As a general rule, most generators are designed so that injected current loading times are short, seldom exceeding a millisecond and usually much less. This, unfortunately, mainly eliminates use of the power grids or batteries as a source of direct injection current. Vorthman et al. [120] describe a battery powered source, but it ultimately charges a capacitor which actually loads the generator.

Flux may also be injected in some generators by application of external fields. In a few cases, permanent magnets have been used. Generally speaking, however, such systems become very massive and expensive if more than a few joules of magnetic energy are required by the generators. However, pulsed fields generated in external coils can be effective flux sources. This is particularly true when initial axial magnetic fields are required by the generator, such as in helical generators or in cylindrical implosion systems [121]. In most cases, (but see [122]), the time constants of the external coils are too short to penetrate the generator conductors. Thus, the generators must remain open-circuited during the loading. The advantages of this technique are that there are no net translational forces on the generator components during loading. There is, of course, field diffusion into the conductors, with consequent heating, and there are net compressive forces on the conductors. Under normal circumstances these effects are not a serious problem. A disadvantage of these systems is that some generators do not allow good coupling to external coils. For example, it is difficult to get a coupling coefficient as high as 0.5 between a suitable external coil and a plate generator.

The type of generator used to power a load is, of course, selected on the basis of being best able to deliver the pulse required by the load. For various reasons, the initial energy requirements for such generators may not be readily accessible from prime energy sources such as capacitor banks. In this case, the required energy may be supplied by another generator, sometimes called a "booster" generator. The use of one generator to energize another is also called "staging". Even a cursory inspection of the literature will reveal many examples of boosting or staging. One of the most common examples is to use a helical generator to power a series connected coaxial generator. Frequently, the armature for the helical generator is simply extended into the coaxial generator. In general, booster generators are series connected to power low inductance generators such

as plate and coaxial generators.

The situation is different for boosting large generators such as most helical generators. These generators are usually boosted in one of the following two ways. In the first method, the booster generator first delivers energy to a low inductance load. In one method, this load serves as the primary of a transformer. The secondary of the transformer is then selected to deliver energy most effectively to the generator to be boosted. This generator is essentially a fixed inductive load before detonation of the armature explosive. Equations (30) to (38) contain the idealized results governing this process. Pavlovskii and his coworkers [118] discuss several staged systems, some of them employing two or more boosting stages, where energy gain ratios (final output electrical energy divided by initial electrical energy) are many thousands. The transformers normally employed are made from coaxial cable, as described earlier. In the second method, the booster generator again delivers energy to a low inductance load. But in this case the second generator fits inside the booster load, and thus obtains its flux inductively from the booster generator. This method has been variously described also by the terms "flux capture", "dynamic transformer", or "flux trap". There has been some discussion as to which of the methods is more effective. Cnare, Kaye, and Cowan [123] perhaps lean toward the transformer coupling method, but point out advantages and disadvantages of both methods, while Chernyshev et al. [124] argue in favor of the flux trapping method. The arguments supporting these positions are mainly analytical. There are, however, practical considerations that may be the determining factors. The very large coupling coefficients obtainable with coaxial cable transformers are certainly beneficial, but secondary voltages must be maintained below the cable breakdown limits. The flux trap systems are usually simple to construct, but often require awkward topologies. Examples of the physical layouts employed may be seen in Fig. 8, [118] for a transformer coupled system and in Fig. 3, [123] for a flux trap system.

Over the years, permanent magnets, piezoelectric (or ferroelectric) gvenerators (PEGs), and ferromagnetic generators (FMGs) have been considered potential candidates as seed sources for FCGs and some limited experiments were conducted. Recent advances have made these seed sources viable, especially with current interest in micro FCGs. Boydston et al [125], Prishchepenko et al [126], and Littrell et al [127] have used permanent magnets to seed FCGs with some success. Freeman and his colleagues built and tested the Texas A&M (TAMU) Mark I generators, which were 2.54 cm long and had stator inner diameters of 2.54 cm. The armatures had an outer diameter of 1.27 cm and a wall thickness of 0.889 mm. All of these units had stators that contained 16 turns of a single length of 12 gage magnet wire with a center tapped load connection. The armatures with glide planes were machined from single pieces of 1100 aluminum. The explosive loads extended 1.27 cm beyond the inside attachment of the glide planes on both ends. Two Reynolds RP-501 detonators were used to simultaneously initiate $\sim$ 9.8 g of C-4 explosive. The Nd-Fe-B ring magnets had inner bores of 1.27 cm and outer diameters of 3.175 cm. The residual flux of these magnets was about 12 kGauss at the pole face. Using less than 10 g of C-4, they have generated in excess of 1 kA of current. They have subsequently built and tested other variants of these permanent magnet FCGs, as well as those seeded with a capacitor bank.

Both Diehl in Germany and Texas Tech have developed PEGs as potential seed sources. Texas Tech and the Agency for Defense Development in South Korea have also developed FMGs (Fig. 28) as a seed source [128]. In the summer of 2002, they successfully used a FMG to drive a small FCG. The FMG had two end detonators and contained $Nd_2Fe_{14}B$ having an outside diameter of 2.54 cm and length of 3.8 cm. Using 1 g of C-4, they were able to provide a seed current of 3.1 kA in a 16 μs pulse. In separate tests, Texas Tech has generated currents on the order of 6.5 kA.

5. Applications

Flux compression generators have been used to power several different systems including detonator arrays, high power microwave sources, such as the Vircator and MILO, direct drive wideband RF devices, high power lasers, plasma focus machines, plasma guns, X-ray sources, particle accelerators, electromagnetic launchers, and in very high magnetic field research. We will not discuss all these applications, but rather will pick three examples: Project Birdseed, railguns, and microwaves. These topics have been chosen partly to illustrate the versatility of FCGs, but also to acquaint the reader, through the text and references, with additional people working with FCGs.

5.1. Project Birdseed

The objective of Project Birdseed [44] was to inject 150–200 kJ of fast neon plasma into the ionosphere (at an altitude of $\sim$ 200 km). The plasma should have sustained a substantial fraction of its mass with velocity greater than 5 cm/μs. The plasma was created by using a Marshall Plasma Gun powered by a FCG that used a high energy density capacitor bank as the seed source (Fig. 29). The system was launched aboard a Sandia Strype rocket which had a payload of $\sim$ 220 kg. Two successful tests were conducted in 1970 and one in 1971.

Two generators were used in the test: the LANL

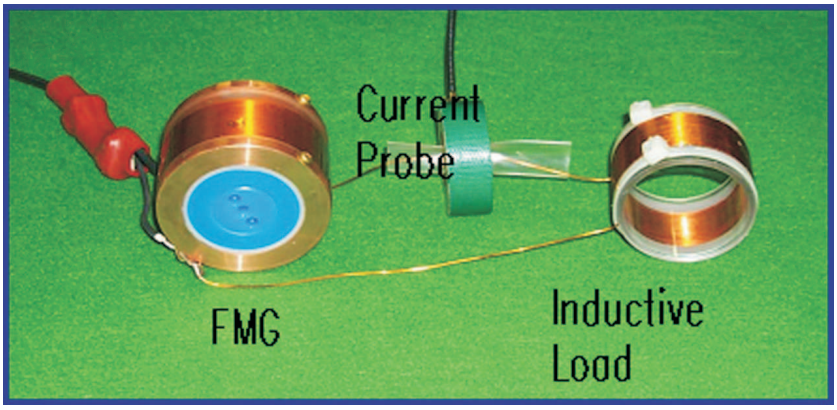

(a)

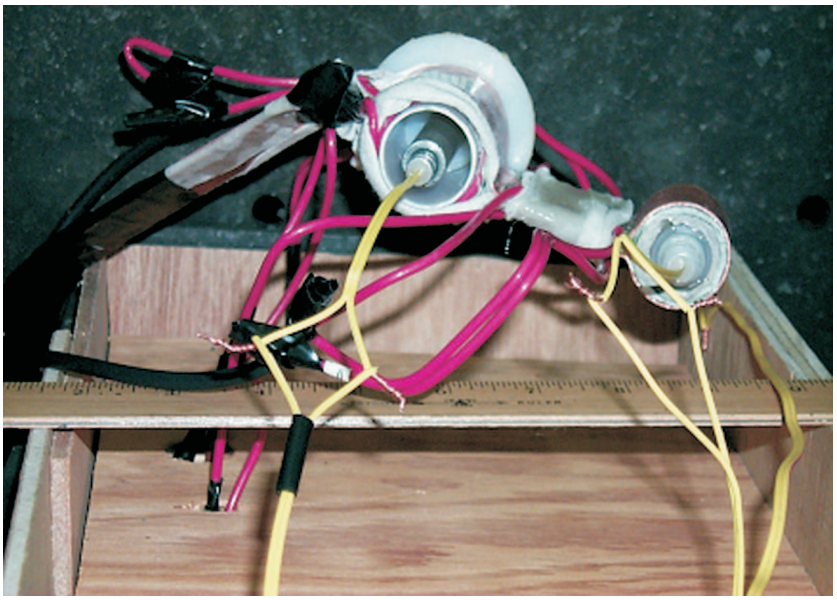

(b)

Fig. 28. (a) ADD and (B) TTU ferromagnetic generator seed sources. The TTU FMG (on the right) is being used to seed an FCG.

Mark V and the Sandia Model 169. The Mark V was used as a booster to drive the Model 169 generator. The Mark V was an end fired helical generator with one detonator and the Model 169 was an end fired helical generator with detonators at each end. A total of 21 Mark V generator shots were fired in the entire program. The first three shots were tests of a LANL fabricated Mark V generator, which became the prototype for the production version built by the Bendix Corporation that were used in the remainder of the tests.

It was initially thought that in order to get the required inductance in the feed generator system, that it would be necessary to use two feed generators. However, a series of case motion shots revealed that a bigger than expected expansion ratio of the generator armature could be tolerated. This enabled LANL to use a bigger diameter generator coil that resulted in sufficient feed inductance. When the Mark V was mated with the Model 169, it was found that the Model 169 could withstand the 80 kV generated by the Mark V. A ballast load was used to get the rise times and the voltage across the gun breech required by the gun. Two switches, actuated with detonators, were used to connect the capacitor bank to the Mark V and the generator set to the plasma gun.

There was some concern as to whether or not the capacitor banks would survive the four minute trip from launch to ionosphere without breaking down electrically. However, it was determined that all three shots were successful.

5.2. Railguns

Work has continued over the past 7 centuries to accelerate macro-sized projectiles to increasingly higher velocities [129]. Higher speeds mean longer ranges and shorter flight times. At present the muzzle velocities of current projectile launchers is

(a)

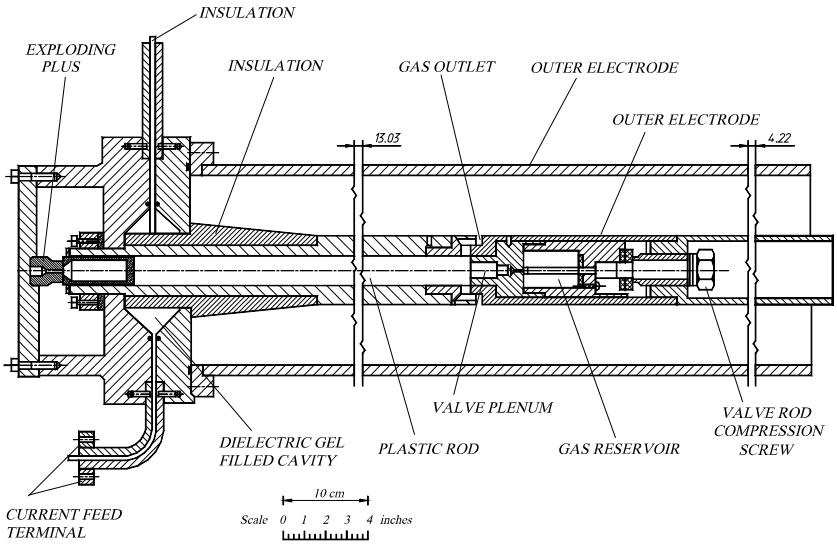

(b)

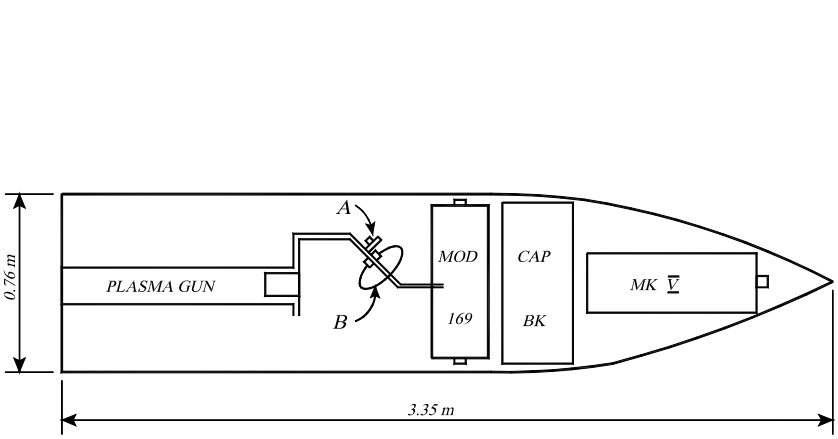

(c)

(d)

Fig. 29. Project Birdseed: (a) two stage FCG into a dummy load, (b) plasma gun, (c) sketch of system in rocket and (d) check out before launch.

Fig. 30. Strip generator powered railgun at Ancho Canyon firing site (LANL).

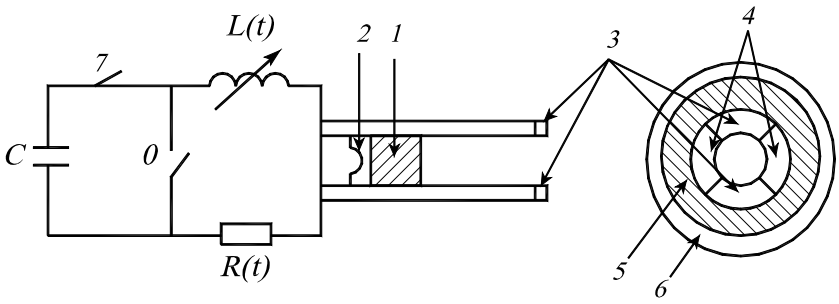

Fig. 31. FCG Driven railgun scheme proposed by Shvetsov et al. [132].

limited to 1.5 km/s, which are determined by the properties of the propelling gases. Higher velocities have been achieved by two stage light gas guns and electromagnetic launchers (railguns). In light gas guns, hydrogen gas is compressed and heated in the second stage by a propellant driven piston in the first stage. By this means, velocities exceeding 8 km/s have been achieved. In railguns, electromagnetic forces generated by an electrical power supply are used to launch the projectile. The first point to note about railgun power supplies is that they must be capable of generating very high electrical currents; that is, megaamps and higher. The second is that they must generate high powers, which means that high voltages are required as well. A number of different power supplies have been used to drive railguns including capacitor banks with inductors to slow down the pulse, homopolar generators combined with energy compression inductors, batteries, and flux compression generators. Attention is focused on the latter of these power supplies.

Peterson and Fowler [130] first proposed using FCGs to power railguns. Soon after this proposal, a series of experiments were undertaken at the Los Alamos Ancho Canyon Flux Compression Facility in collaboration with colleagues from Lawrence Livermore National Laboratory. Some of the results obtained are given by Hawke et al [131]. Reliable velocities on the order of 6 km/s were obtained for gram-sized projectiles. Some higher velocities were reported, but these are uncertain either because the data were not complete or because the projectiles fragmented upon leaving the railguns. Figure 30 shows an assembly on the firing table. The railgun is at the upper right while the strip generator (see Fig. 9) is at the lower left. Cables from the capacitor bank that supplied the initial flux may be seen connected to the generator input.

Spvetsov et al. [132] conducted a study in which they compared how effective three different FCGs (cylindrical, helical, and plate) were in powering railguns. Assuming the FCG driven railgun scheme presented in Fig. 31, they estimated the lower bounds of the generator's dL/dt required to achieve projectile velocities of 5 and 10 km/s. Further assuming that the detonation velocity is 7.6 km/s, the railgun channel inductance per unit length is 0.25 μH/m, and the circuit resistance is 2 mW, the generator inductance per unit length must be 0.42 μH/m to achieve a projectile velocity of 5 km/s. Using the same detonation velocity and railgun channel inductance and a circuit resistance of 3 mΩ, the generator inductance per unit length must be 0.7 μH/m.

Using these methods, the authors looked at whether or not three different generators could be used to drive railguns. The first generator was the cylindrical generator. Assuming that the ratio between the radii of the outer and inner conductors is 2, the generator inductance per unit length was calculated to be 0.14 μH/m, which is too small to provide the conditions for accelerating the projectile to 5 km/s. The second generator was a helical generator. Assuming that the ratio between the diameters of the helical coil and the inner conductor is 2 and that the width of the winding is equal to the diameter of the inner conductor, the generator inductance per unit length was calculated to be 12 μH/m, which is more than sufficient to accelerate the projectile to 10 km/s. However, they found that to design a generator with the proper inductance, it is necessary to decrease the width of the winding, thus complicating the generator. The third generator was the strip generator. Assuming that the width of the conductors is equal to the distance between them, the generator inductance per unit length was calculated to be 0.6 μH/m. The strip generator is adequate to accelerate projectiles to speeds $\geq$ 5 km/s.

LANL conducted a series of experiments called HIMASS [133] in which they used a Mark 10 multi-wire helical FCG to drive a railgun. Both solid and plasma armatures were eventually used to accelerate masses ranging in size form 0.6 to 1.0 kg. Since the operation time of the FCG is too short to serve as the direct power supply for the railgun, an intermediate inductive storage coil was used. The Mark 10 stator was composed of a copper wire winding wound on a 252 mm diameter mandrel. The three section winding pattern consisted of 15 turns of four parallel wires over a length of 558 mm, 7 turns of eight parallel wires over a length of 515 mm, and 3.4 turns of sixteen parallel wires over a length of 510 mm. The stator was overcast with a 100 mm thick layer of concrete. The armature was annealed copper with an outside diameter of 127 mm and a thickness of 5.1 mm. The explosive charge consisted of 32 kg of Composition B, which was initiated by a small plane wave lens. The initial inductance of the Mark 10 was 24 μH. The inductive load consisted of parallel copper plates, each 2.35 m long, 25.4 mm thick, and 305 mm wide and separated by a distance of 152 mm. The inductance of the load was 1 μH. The railgun had a bore diameter of 105 mm and a length of about 1.5 m. The seed capacitor bank delivered 180–190 kA to the FCG, which in turn delivered 2.6 and 3.0 MA to the inductive store. In two of the shots, 103 mm diameter lexan projectiles weighing approximately 0.6 kg achieved velocities of 1.2 and 1.4 km/s, using a plasma armature. In the third shot, a solid metal armature, partly to reduce flux losses, was used to accelerate a projectile to a velocity on the order of 1 km/s. The armature and projectile had a total mass of 1.053 kg.

5.3. Microwaves

Beginning in 1994, A.B. Prishchepenko and his colleagues [134] published a series of papers on using very small or "micro" FCGs, as well as explosive driven piezoelectric and ferromagnetic generators, to drive radiating elements to generate radio frequency waves. These are "direct drive" devices in that the FCG drives the antenna directly through a power conditioning circuit. FCGs have also been used to drive microwave sources such as virtual cathode oscillators (Vircators) and magnetically insulated linear oscillators (MILOs), which are referred to as "electron drive" devices, since the energy from the power supply is first converted into electron kinetic energy, which is then converted into microwaves. Several laboratories are now working to develop both direct drive and electron drive systems based on FCGs.

B.M. Novac and I.R. Smith [135] at Loughborough University examined the technical issues associated with the development of compact energy sources based on FCGs to drive high power microwave sources. Taking the MILO, which requires a very fast rising 500 kV power supply that supplies a constant voltage for hundreds of nanoseconds and which has a resistance of some ohms, as an example, they examined several schemes for developing an autonomous compact power source based on FCGs. Unlike others who have considered using plasma opening switches (POS) and/or high voltage transformers (HVT) to provide fast rising, long duration high voltage pulses to high impedance loads, they also considered two additional power conditioning units: the explosively formed fuse (EFF) and a fast pulse helical FCG (F-H-FCG). By combining these additional power-conditioning units with the two impedance matching units they identified four different power systems that are depicted in Fig. 32. The results of their analysis indicate that System I in Fig. 32 is the most robust solution for this problem, since it utilizes already proven techniques and since the design is straightforward. They estimated that

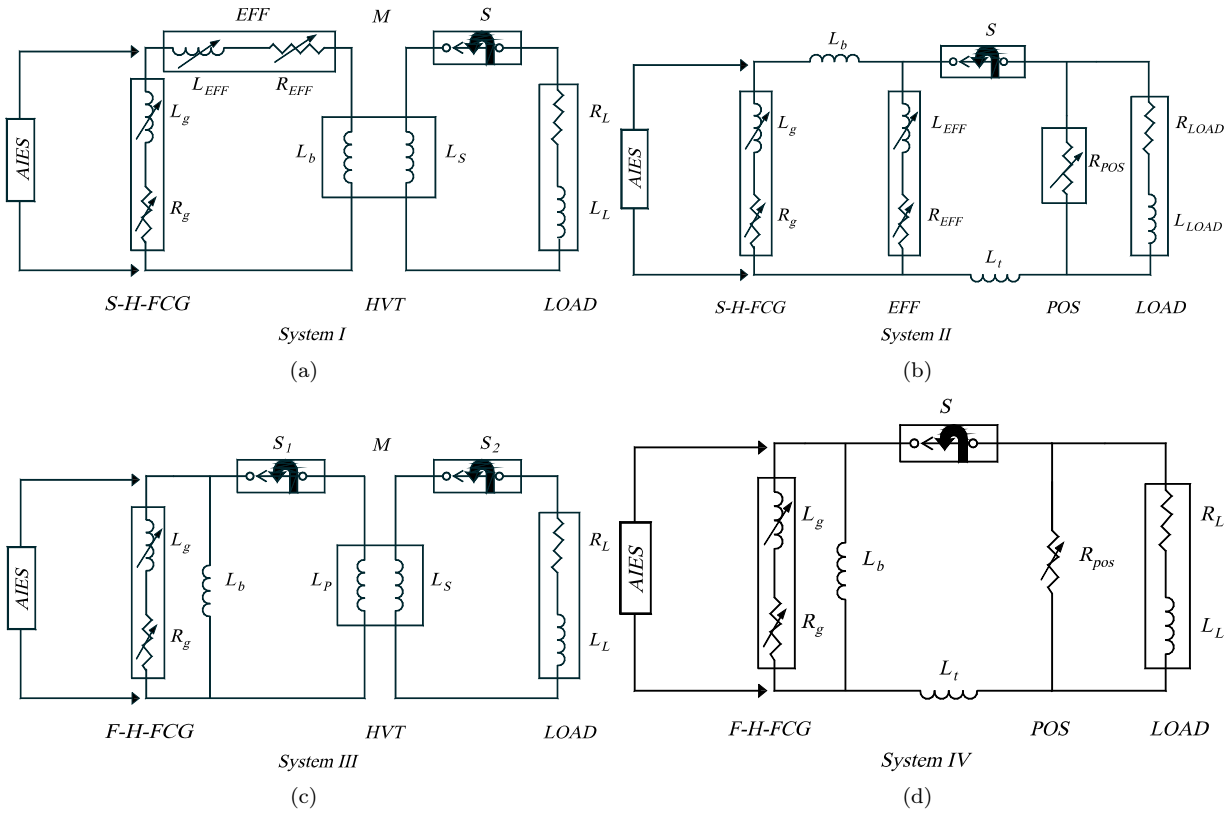

Fig. 32. Four different schemes proposed by Loughborough University for driving RF sources [10].

the overall system weight will be less than 200 kg in a volume less than 1.5 m^3. However, they do point out that System IV could potentially generate much higher voltages with extremely short rise times and be lighter and more compact provided a vacuum version of the F-H-FCG capable of handling internal voltages of hundreds of kilovolts and a long conduction time POS can be developed.

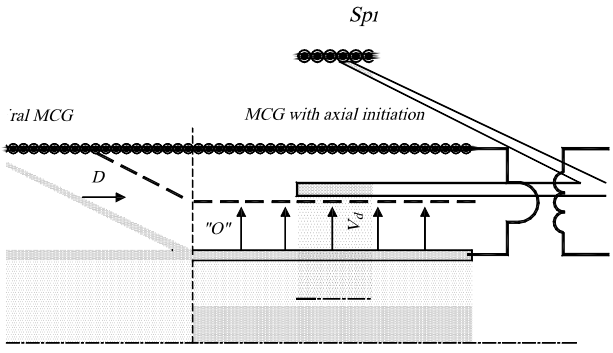

Fig. 33. Four different schemes proposed by Loughborough University for driving RF sources [10].

Mintsev and his colleagues [136] at the Institute of High Temperatures in Russia have developed a pulsed high voltage power supply based on a fast helical generator, electrically exploding wire opening switch (EEOS), and transformer to drive relativistic electron beam (REB) accelerators and vircators. The FCG is a two stage device, with the first stage being a standard end fired helical FCG and the second stage a simultaneous helical generator (Fig. 33). This system is capable of generating 450 kV pulses with a risetime less than 540 ns and pulse length of 200 ns. The maximum output power is 80 GW and the pulse energy is approximately 20 kJ. Experimental data as well as numerical simulations indicate that this power system should be able to drive a vircator that is capable of generating microwave power levels on the order of 1 GW and energy levels on the order of 100 J [137]. Fortov et al [138] describe a system employing a fuse and voltage breakdown switch (See Fig. 17) that powered a Vircator. Microwave radiation was generated.

In the mid 1980s, B.L. Freeman et al [139] at LANL used a fast plate generator to drive a vircator. The plate generator was selected because it has the fastest rate of voltage change and because of its demonstrated reliability. The generator was connected through an air-core transformer to achieve impedance matching to the diode of the vircator and to increase the output voltage of the power supply to meet the requirements of the vircator. One key to making this system work was the proper selection of the cathode geometry, which turned out to be a 13 cm cup shaped cathode. In the experiments, radiation was detected in the L-, S-, and X-bands of the spectrum.

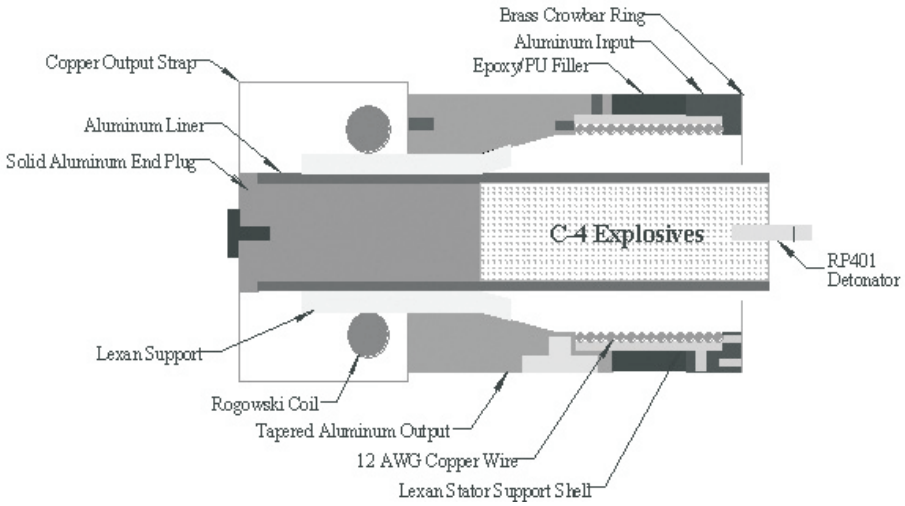

(a)

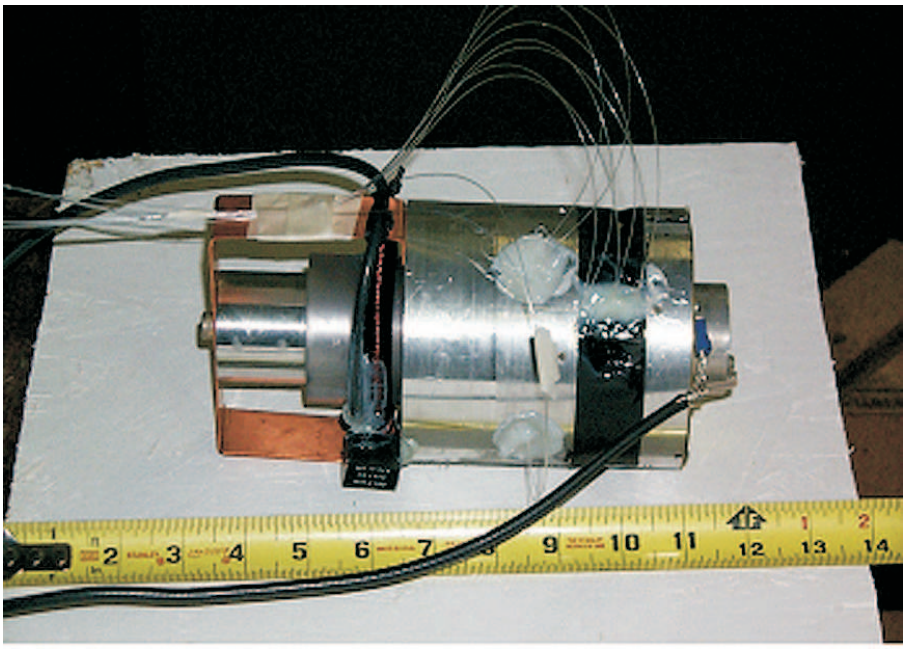

(b)

Fig. 34. Texas Tech Standard FCG (Courtesy of Dr. A. Neuber, Texas Tech University.

6. Recent FCG Activities

In recent years, there have been renewed activities at several government and industrial laboratories and at several universities to understand the various physical processes that affect the operation of FCGs, to understand their limitations, and to develop new applications. In addition, there has been work to develop and benchmark computer codes to model FCGs. Of particular importance is the Multidisciplinary University Research Initiative (MURI) Program at Texas Tech University, the work on micro-FCGs at Texas A&M University, the code and application development at Eglin Air Force Base, and code development and experimental work at Loughborough University. Each of these programs will be briefly discussed following detailed consultation with people directly involved in them. There are ongoing efforts at government, industrial, and university laboratories in France, Germany, and other countries, but due to the lack of specific information this discussion will be very limited.

6.1. Universities

If the most recent activities, probably the most systematic effort is that of the five year MURI Program entitled "Explosive-Driven Power Generation for Directed-Energy Munitions", which included Texas Tech, Texas A&M, University of Texas Austin, and

University of Missouri in Rolla in the US and Loughborough University in the UK. The stated objectives of this program [140] were to:

- Gain improved understanding of the basic phenomena involved in the dynamic Magnetic Flux Compression Generator processes. This information is needed in order to improve the generator efficiency.
- Develop methods for efficient conversion of the typically 10's s, low voltage (10's kV), high current (MA) output from the FCGs into forms more suitable for directed energy systems (e.g. 600 kV, 100 kA, 1 ms pulses (possibly repetitive)).

In order to make these determinations, Texas Tech developed their "standard" FCG. This generator, shown in Fig. 34, has 32 turns of insulated 12-AWG copper wire, initially wound on a 64-mm diameter mandrel. The input plane is a 45 mm inner diameter slotted brass disc, called a *crowbar ring*, with 0.02 mm thickness. The load side of the generator has a 14 degree tapered output plane, which reduces the inner diameter from 64 mm to 51 mm. The liner (38.1 mm OD, 3 mm wall thickness) and stator are at this point separated by a 6 mm wall Lexan cylinder.

Some of the lessons learned, as reported relative to their standard FCG, not all of which pertain to larger FCGs, were:

- Good contact must be maintained between the crowbar and the generator input.
- For small seed currents, the maximum output current is linearly proportional to the seed current. For seed currents $>$ 1 kA, they are no longer linearly proportional. When the seed current $>$ 0.5 MA, additional losses such as premature helix wire deformation and material melting occur.
- An investigation of the metallurgical properties of the liner [141] revealed that:
  - The evolution of the grain structure begins with grain elongation along the axial direction without appreciable changes in the transverse direction.
  - During expansion, severe grain elongation was observed in the circumferential direction with minimal change in the axial direction.
  - Axial cracks form during expansion.
  - Changes in the grain structure can be attributed to rapid plastic deformation.
- An investigation of the expansion characteristics of the liner revealed that:
  - The first few turns of the stator do not make contact with the armature due to "end effects".
  - Loss of compression efficiency during detonation run-up may be due to the formation of large axial ripples on the surface of the armature.
  - The expansion angle decreases with increasing wall thickness-to-radius ratio.
  - The length of the "end effect" increases with increasing wall thickness-to-radius ratio.
  - The impact velocity between the armature and the stator decreases with increasing wall thickness-to-radius ratio.
  - The contact velocity is initially greater than the detonation velocity and gradually approaches the detonation velocity due to the "end effects".

Fig. 35. Texas A&M 25 mm diameter FCG (Courtesy of Dr. B.L. Freeman, Texas A&M University.)

Texas A&M University [142] is investigating micro-FCGs. These are FCGs having an overall diameter of around 25 mm (Fig. 35). Texas A&M fired their first micro-FCG in the summer of 2001, and Texas Tech conducted similar tests a few months later. Texas A&M has experimented with several different designs including the Mark I, discussed earlier in Sect 4.4, which used permanent magnets to create the seed fields and two end detonators, and a series of other generators seeded by capacitors with either tapered or straight stators. Some of the findings that have come out of the Texas A&M efforts are: to replace the aluminum glide planes with either brass or copper because the aluminum armature colliding with the aluminum glide plane is very likely to "tent peg" material over on the glide plane, leading to armature separation with associated significant flux losses; to use larger gage magnet wire since the flux losses in the smaller units do not presently enable higher gains; and to preferentially use tapered stators

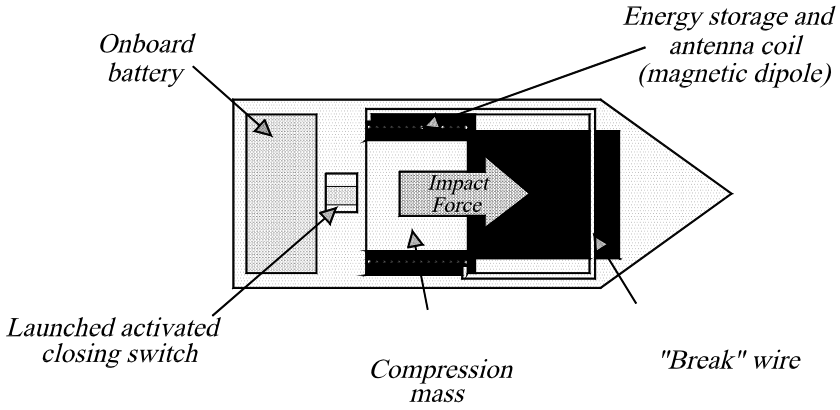

Fig. 36. Impact driven FCG (Courtesy of Dr. G. Engel, University of Missouri in Columbia).

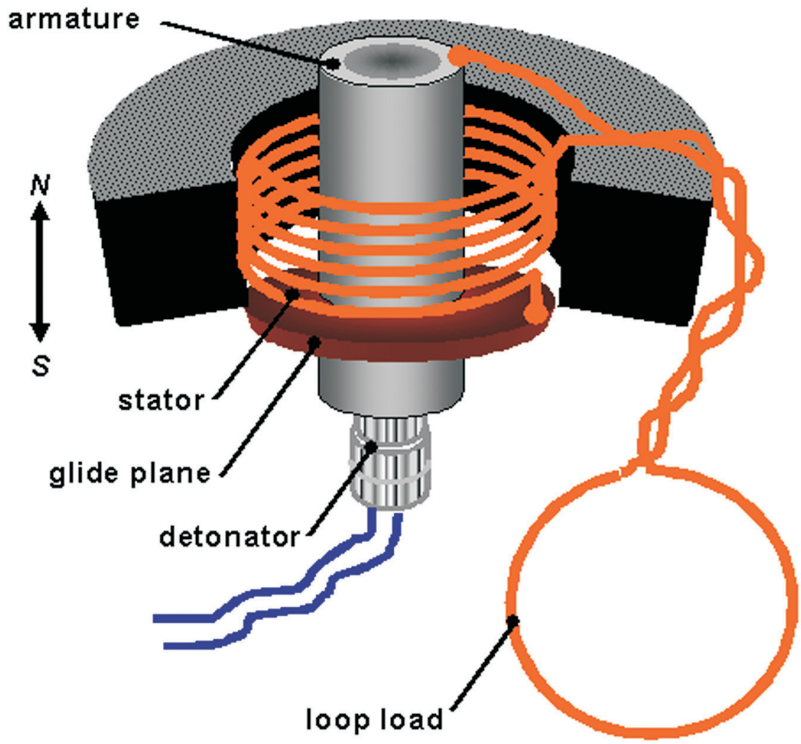

Fig. 37. Test configuration for a small FCG with a simple load (Courtesy of Dr. D. Littrell, Engin Air Force Base).

for faster performance by the generators without appreciable degradation in overall gain. The A&M effort will return to the double initiation systems when the application requires the faster closures, but a significant issue with this form of initiation is that the ring jet from the collision of the two detonation fronts must be avoided. This is easily addressed, so the option for the effective doubling of generator speed is quite viable.

In order to compare the output efficiency of micro versus larger FCGs, a "figure of merit" [12,140] is used, which is defined through

$$G_I = \frac{I}{I_0} = \left(\frac{L_0}{L}\right)^{\beta},$$

where G_I is the current gain, I_0 and L_0 are the initial current and inductance respectively, I and L are the current and inductance at some time t, and β (or α in [12]) is the figure of merit. β is one only for perfect flux compression. For the FCG to deliver more than the initial energy to the load, β must exceed 0.5. For larger generators, β values usually range from 0.75 to 0.90. Texas Tech has concluded that it will be difficult for small generators to achieve $\beta > 0.6$, which limits their applicability as power sources [143]. In addition, they have shown that the current and energy gains generally decrease as the size of the generator decreases.

In addition to being a member of the Texas Tech MURI team, Loughborough University has developed

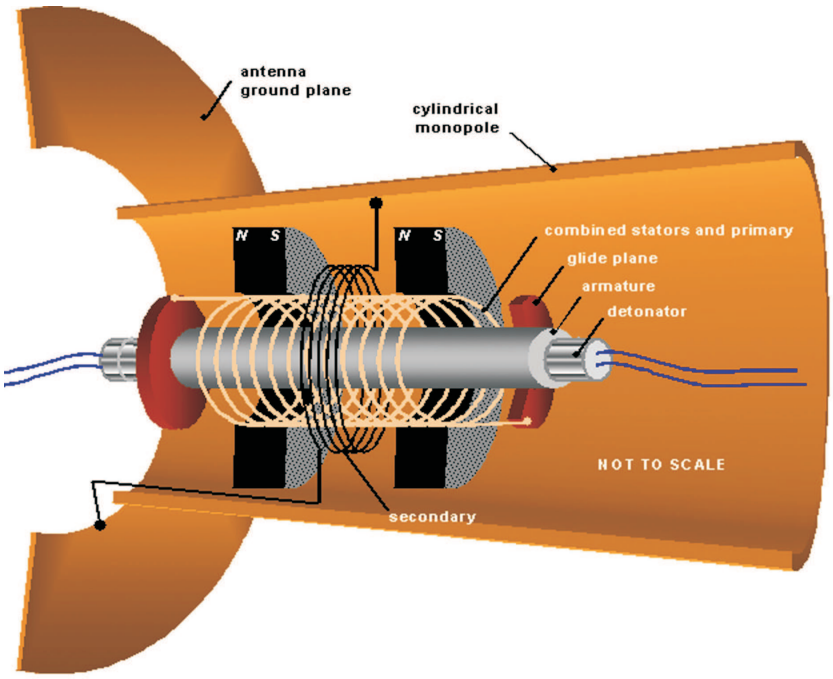

Fig. 38. Conceptual drawing of the dual-ended generator with integral antenna (courtesy of Dr. D. Littrell, Eglin Air Force Base).

and tested a helical generator called FLEXY I [144]. This generator was used to validate 2D circuit [145] and 3D MHD [146] codes that they had also developed. They have also done considerable work on foil switches and a circuit for converting single high power pulse into multiple pulses. While this last activity was done using a capacitor bank as the pulse source, the real objective is to use an FCG as the source.

The University of Missouri in Columbia has designed and demonstrated 30 mm flux compressor and piezoelectric compressor pulsed power supplies Fig. 36 [147]. Both compressors convert the kinetic energy of an impact event into electrical pulses. Explosively driven compressors are certainly possible, but the University does not have local facilities to perform this type of research. Piezoelectric based supplies have produced 30 kW peak power pulses. The FCG based supplies have demonstrated 10 kW peak power pulses. The University selected a PZT based generator for miniaturization and is presently developing optimization theory and pulse conditioning techniques. They have PZT compressor designs that produce multiple pulses, but have not yet constructed and tested them. They have developed integrated antenna structures for both FCG and PZT pulse generators that are approximately 15 % efficient at 100's of MHz

6.2. U.S. Government and Industrial Laboratories

In addition to LANL, other U.S. government and industrial laboratories have developed and/or utilized FCGs including Sandia National Laboratory, Lawrence-Livermore National Laboratory, Air Force Research Laboratory at Kirtland, SAIC, and others. These efforts are well documented in the proceedings of the Megagauss Conferences and of the IEEE Pulsed Power Conferences. The most recent activities have been those of the Air Force Research Laboratory at Eglin.

Eglin is working on miniature permanent magnet FCGs for pulsed telemetry [127]. They used off-the-shelf magnets to provide the seed field for a series of small helical FCGs. Given that the dimensions of the available toroidal magnets fixed the magnet-bore size, the remaining FCG components were designed to conform to them. Figure 37 shows the general configuration of simple load tests; the tests were directed at optimizing FCG power output with stator design. Note that the magnetization is axial, producing a field direction in the bore that matches the field from the stator. Several stators wound with differing wire gauges were fabricated; different winding mandrels were used to ensure that the outside dimension of each of the stators was a good fit to the magnet bore. The measured FCG outputs (current and voltage) were compared with the predictions of their code called FCGMAX, which is a physics-based circuit model of the performance of a variety

of FCG types. The simulation data substantially over predicts the observed currents, but variation of the output with stator winding gauge evidently agrees with experiment, with lower outputs predicted and observed with the largest and smallest wire gauges.

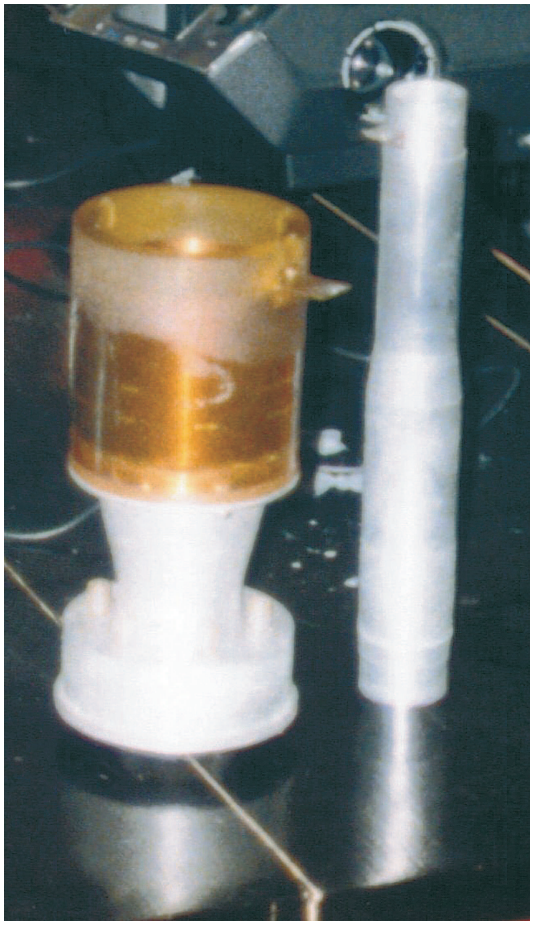

Fig. 39. Helical FCG developed by the Southwest Institute of Fluid Physics, Mianyang, China.

The results of these initial tests led to the development of a dual-ended generator design. First, with small generators it is difficult to reduce stray inductance below the levels of a load inductance when a reasonable distance separates the generator and load. Second, since voltage is a critical output parameter, it seemed obvious that detonating an armature from both ends would provide a much larger time rate of change of inductance for any given stator design. The success of the single magnet design suggested that one might simply replicate the single magnet design and add it to the original with a small gap between the two stator windings where the generator's load would be inserted into the connecting conductor. It addition, it seemed ideal to have the load be in the form of a transformer consisting of a loosely wound primary helix completely covered by a tightly wound secondary winding that drives the antenna (Fig. 38). This geometry presents some unique factors when modeling the generator, such as the fact that the armature expands within the load transformer and the fact that both the primary and the secondary windings are immersed in the DC magnetic field of the two permanent magnets. At this time, this later version of the pulsed telemetry system is still under development.

6.3. Non U.S. Government and Industrial Laboratories

In this section, a brief summary of current FCG programs at specific laboratories outside the U.S. will be presented. We will not cover the extensive programs in Russia or the UK, since their programs are quite broad, well documented in the various journals and proceedings, and have been addressed some what in this paper. Most of these efforts are small, but focused programs, although larger scale joint programs done jointly with Los Alamos and Russian scientists occur frequently.

China: China has been developing, building, and testing FCGs since 1967 [148]. Most of their effort appears to have been focused on helical generators (Fig. 39). In their latest paper, Sun et al [149] from the Institute of Fluid Physics describe a multi-branched helical FCG having a length of 600 mm, diameter of 120 mm, and mass of 10 kg that can deliver 512 kA of current and 47.2 kJ of energy to a 360 nH inductive load. Other papers can be found in the Megagauss proceedings [5–7].

France: In France, the Centre d'Etudes de Gramat has worked a number of years on FCGs and has published on pulse-shaping schemes for using FCGs to do high pressure and isentropic compression in materials and to drive X-ray sources [150].

Germany: In Germany, two companies are building and testing FCGs: Diehl and Rhinemetall-Wm. Diehl has done considerable work modeling helical generators driving a HPM and UWB sources, as reported by Staines [151], and has investigated both experimentally and theoretically the Russian Explosive Magnetic Generator of Frequency, which is a helical FCG with a capacitive load. Rhinemetall has built and tested helical FCGs with capacitive and inductive loads [152].

South Africa: The Atomic Energy Corporation of South Africa [153] has conducted research on FCGs since 1992. Initial efforts focused on a double ended initiated system, but more recently single end initiation has been considered.

South Korea: In South Korea, the Agency for Defense Development has worked a number of years on helical FCGs. More recently they have cascaded FCGs, Fig. 40, in series [154] and in parallel [155]. Using a capacitor bank as the seed source, they serially connected two FCGs, each with an initial

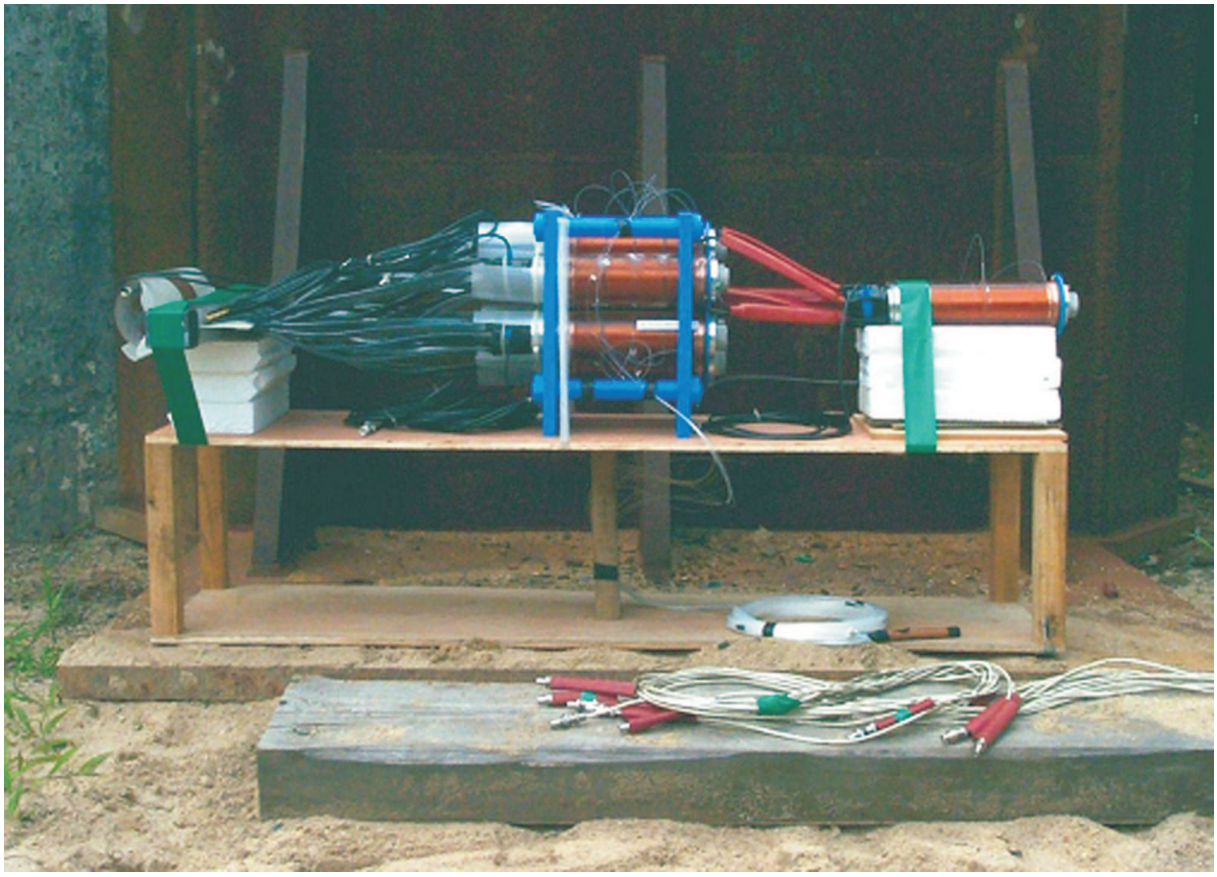

Fig. 40. Serially and Parallel connected FCG's developed by the Agency for Defense Development, Taejon, South Korea [155,156].

inductance of about 45 μH, to drive a 136 nH load. They also used a capacitor bank to seed a single FCG, which was then used to seed four FCGs. They found that the energy multiplication was dependent on the ratio of the initial inductance to that of the load inductance and that the output voltage across the load increased as the number of FCGs increased. They also used a capacitor bank to seed two FCGs in parallel and a capacitor bank to seed a single FCG that seeded four FCGs in parallel. They found that the load voltage was almost constant regardless of the number of FCGs in parallel provided the initial current and load inductance were kept the same and that differences in the activation time between FCGs connected in parallel caused severe distortions of the dI/dt waveform due to the different load inductance felt by each FCG. Reduction in output energy caused by a 1 μs jitter was as high as 12 % for two FCGs in parallel.

The Agency for Defense Development has also investigated two versions of the FMG as a seed source for FCGs [156]. The first version is a cylindrical design with the HE charge placed next to the magnet and the second version is an annular design with the HE placed inside a hollowed out magnet. The found the annular design to be more efficient.

Sweden: At FOI in Sweden, the focus has been on helical FCGs for compact HPM applications [157].

Ukraine: The Institute of Electromagnetic Research has developed a two stage FCG [158], the first stage of which is a end-fired helical generator and the second stage of which is a simultaneous helical generator. Flux trapping is used to capture the flux from the first stage into the second stage. The generator produces 150 kV and 44 GW of electrical power. In order to produce higher voltages, they use a tape wound transformer (Fig. 26) and an exploding wire switch. The primary winding of the transformer is a copper ring. The secondary winding is a reeled thin foil of the same width as the primary and is placed inside the ring. Insulation between the turns consists of several layers of plastic film and capacitor paper impregnated under vacuum by a liquid insulator. The internal coil of the secondary winding is intended to sustain high voltages. The external coils have smaller potential and shield the high-voltage end from the grounded primary winding that reduces the effect of the total voltage. Such a design is based on the well documented technology used to make paper-film capacitors and permits one to obtain high discharge gradients (up to 2 MV/cm and greater). The transformer steps the voltage up to

450 kV.

7. Computer Codes

Due to general interest in applying FCGs to solve certain technological problems, several computer codes have been developed through the years. They include the following:

- LANL developed a general circuit analysis code, called SCAT95 with provisions for several types of FCGs [159].
- CAGEN is a commercially available code for helical FCGs [160].
- TTU developed a circuit analysis code for helical FCGs with an empirically adjustable factor to account for losses [161].
- SAIC developed FCGSCA, which is a circuit analysis code for helical FCGs [162].
- Tracy developed for the U.S. Army Space and Missile Defense Command, a circuit analysis code for helical FCGs with an empirically adjustable factor [163].
- Loughborough developed 2D circuit and 3 D MHD codes for helical FCGs [164]. Loughborough University has also developed a fast code to model helical FCGs with multi-sectioned stator windings that can each have a different (but constant) pitch and where the number of turns in each section can be chosen arbitrarily [165].
- The Nuclear Energy Corporation of South Africa has developed a circuit analysis code for helical FCGs [166].

These codes vary in complexity from the very simple Tracy code written in Basic to the more complicated MHD codes developed at Loughborough University. All of the codes have been benchmarked against specific generators. For example, SCAT95 was benchmarked with the Mark IX, the TTU code with the TTU standard generator, and the SAIC and Tracy codes with several generators including the Mark IX and FLEXY I.

8. Summary

In Summary, the authors have attempted to summarize the knowledge they have gained from years of experience in designing, building, testing, and applying FCGs at Los Alamos. It was felt that this was needed due to the recent establishment of FCG programs in several countries, some of which have had no experience in working with this technology. The authors regret that time did not permit addressing two very important subjects, particularly, more recent work:-the efforts to produce significant D-T fusion, and the study of high magnetic field solid state properties It is probably safe to say that the impetus for the original FCG work ,both at Los Alamos and in Russia, came from the fusion attempts. Work in this area continues in Russia, much of it jointly with Los Alamos. A recent paper by Chernyshev et al [167] contains references to past work in this program. A considerable amount of high magnetic field solid-state research has been reported in the journal "Physica" and in the Megagauss Conference Proceedings [1–8]. An interesting new application of FCGs to generate very high pressures, isentropically, has been reported by Tasker et al [168]. As with any technology, we continue to learn how to improve and apply FCGs as exemplified by the 5 year MURI effort at Texas Tech University and to fully understand the various physical and chemical processes that occur during FCG operation. In addition, there are also ongoing efforts at Texas A&M and Loughborough University to further understand the limitations and uses of FCGs.

References

[1] Proceedings of the Conference on Megagauss Magnetic Field Generation by Explosives and Related Topics, Eds. H. Knoepfel and P. Herlach, Euratom, Brussels (1966).

[2] Megagauss Physics and Technology, Ed. P. Turchi, Plenum Press, New York and London (1980).

[3] Ultrahigh Magnetic Fields, Physics, Techniques, and Applications, Eds. V. M. Titov and G. A. Shvetsov, Nauka, Moscow (1984).

[4] Megagauss Technology and pulsed Power Applications, Eds. C. M. Fowler, R. S. Caird, and D. J. Erickson, Plenum Press, New York and London (1987).

[5] Megagauss Fields and Pulsed Power Systems, Eds. V. M. Titov and G. A. Shvetsov, Nova Science Publishers, Inc., New York (1990).

[6] Megagauss Magnetic Field Generation and Pulsed Power Applications, Eds. M. Cowan and R.B. Spielman, Nova Science Pub., New York (1994).

[7] Megagauss and Megampere Pulse Technology and Applications, Eds V. K. Chernyshev, V. D. Selemir and L. N. Plyashvevich, Sarov, VNIIEF, (1997).

[8] Proceedings of the Eight Megagauss Conference, in publication.

[9] Knoepfel H., Pulsed High Magnetic Fields – Amsterdam and London: North-Holland Publishing Company. – 1970.

[10] Altgilbers L.L., Brown M.D.J. , Grishnaev I., Novac B., Smith I.R., Tkach Ya. and Tkach Yu. Magnetocumulative Generators – New York: Springer-Verlag. – 2000.

[11] Herlach F. Megagauss Magnetic Fields // Prog. in Phys. X, part 1. – 1968. – P. 341–417.

[12] Fowler C.M., Caird R.S. and Garn W.B. An Introduction to Explosive Magnetic Flux Compression Generators // Los Alamos National Laboratory Report, LA-5890-MS. – I975.

[13] Fowler C.M., Garn W.B. and Caird R.S. Production of Very High Magnetic Fields by Implosion // J. Appl. Phys. – 1960. – V. 31. – P. 588–594.

[14] J.A. Stratton, Electromagnetic Theory, McGraw-Hill Book Company, Inc., New York and London (1941). This book, written more than a half century ago, remains one of the classic treatments of the subject. The electromagnetic stress and strain energy tensors occur frequently in the text, but are carefully indexed. Rationalized MKS units are used throughout.

[15] Dobraty B.M. and Crawford P.C. LLNL Explosive Handbook, Properties of Chemical Explosives and Explosive Simulates // (January 31, 1985), report UCRL-52997, Change 2 (from National Technical Information Service, U.S. Department of Commerce, 5285 Post Royal Road, Springfield, VA 22161).

[16] LASL Explosive Property Data, Eds., T.R. Gibbs and A. Popolato, University of California Press, Berkeley, Los Angeles, London (1980).

[17] Fickett W. and Davis W.C. Detonation, – Los Angeles, London: University of California Press, Berkeley. – 1979.

[18] Cooper P.W. Explosives Engineering – New York: VCH Publishers, Inc. – 1996.

[19] Mader C.L. Numerical Modeling of Explosives and Propellants, 2nd Ed., – CRC Press. – 1998.

[20] Detonator Fabrication (see Ref. 18, Chapters 22 - 25).

[21] Steinberg D.H. and Wade J.P. Axial Detonation for Simultaneous Ignition of Multiple HE Points Ref. 4, – P. 471–978.

[22] Fowler C.M., Caird R.S., Garn W.B. and Thomson D.B. Flux Concentration by Implosion, Ch. 25 in High Magnetic Fields, Eds. Kolm H., Lax B., Bitter F., and Mills R. – New York and London: MIT Press and John Wiley and Sons, Inc.

[23] Herlach F., Knoepfel H. and Luppi R. Magnetic Field and Current Amplification with Non-Cylindrical Explosive Systems Ref. 1 (Fig. 4, p. 294).

[24] See Ref. 13.

[25] Chapman B.L. Development of Magnetic Field Compression Techniques for Metallic Particle Acceleration, see Fig. 13, p. 125, Ref. 1.

[26] Meyers W.H. Application of Slapper Detonation Technology to the Design of Special Detonation Systems // presented at the 12th Symposium on "Explosives and Pyrotechnics", San Diego, CA, Man 13-15 1987 (available as Los Alamos Report LA-UR-87-391).

[27] Jones M.S., Jr. and McKinnon C.N., Jr., "Explosive Driven Linear MHD Generators", Ref. I, – P. 349–356.

[28] E.P. Velikhov, Yu.M. Volkov, V.S. Golubev, N.V. Lobanov, F.G. Rutberg, and A.A. Yakushev, "Plasma MHD Generator for Modeling Energy Conversion in Pulsed Thermonuclear Reactors", translated from Atomnaya Energiya, Vol. 39, No. 6, pp. 387-391, December 1975.

[29] D.W. Baum and W.L. Shimmin, "Explosive Plasma Source Experiment" Ref. 2, pp. 77-88.

[30] S.P. Gill, 'Directed Energy Power Source Could Generate EW Technology Revolution,' Defense Electronics, April 1984, pp. 116-118.

[31] W.F. Weldon, H.H. Woodson and M.D. Driga "Compensated Pulsed Alternator", U/S. Patent 4,200,831.

[32] E.P. Velikhov, A.A. Vedenov, A.D. Bogdanets, V.S. Golubev, E.G. Kasharskii, A.A. Kiselev, F.G. Rutberg, and V.V. Chernukha, "Generation of Megagauss Magnetic Fields Using a Liner Compressed by High-Pressure Gas", Sov. Phys. Tech. Phys., Vol. 18, No. 2, pp. 274-279 (1973).

[33] R. Hahn, "Study and Experimentation with a High-Energy Pulsed Electric Generator Using a Gaseous Explosive", thesis for the Doctor of Science Degree, University of Paris-Sud, Centre d'Orsay, April 1975.

[34] E.C. Cnare, "Magnetic Flux Compression by Magnetically Imploded Metallic Foils", J. Appl. Phys., 37, No. 10, pp. 3812-3816 (1966).

[35] N. Miura, Y. Matsuda, K. Uchida, S. Ikada, T. Ikaida, Ts Sekitani, T. Osada and F. Herlach "Generation and Application of Megagauss Fields at the Kashiwa Megagauss Lboratory" to be published in the Proceedings of the Ninth Megagauss Conference, July 7-14, 2002, Moscow-St. Petersburg.

[36] P.J. Turchi, A.L. Copper, R.D. Ford, D.J. Jenkins, R.L. Burton, "Review of the NRL Liner Implosion Program", Ref. 2, pp. 375-386.

[37] A.E. Robson, The Linear Concept in Unconventional Approaches to Fusion, Eds. B. Brunelli and G.G. Leotta, Plenum Publishing Corporation (1982).

[38] J.G. Linhart, "Plasma and Megagauss Fields", Ref. 1, pp. 387-396.

[39] F.S. Felber, F.J. Wessel, N.G. Wild, H.U. Rahman, A. Fisher, C.M. Fowler, M.A. Liberman, and A.L. Velckovich, "Magnetic Flux Compression by Plasmas: Experiments on a Gas-Puff Z-Pinch", Ref. 4, pp. 117-124.

[40] C.M. Fowler, R.S. Caird, R.S. Hawke, and T.J. Burgess, "Future Pulsed Magnetic Field Applications in Dynamic High Pressure Research", in High-Pressure Science and Technology, Eds., K. D. Timmerhaus and M. S. Barber, Plenum Press, New York and London, Vol. 2, pp. 992 (1979).

[41] P. Williams, "An Introduction to Magnetic Flux Compression Guns", in Proceedings of the International Symposium on Intense Dynamic Loading and its Effects, Chengdu, China, June 9-13, 1992, Eds. K. Yang, Q. Wu, and Y. Wang, Sichuan University Press, Chengdu, China, pp. 232-235 (1992).

[42] R.A. Marshall "A Reusable Inverse Railgun Magnetic Flux Compression Generator to Suit the Earth-to-Space Rail Launcher" IEEE Trans Mag. 20, 223 (1984).

[43] J.D. Powell and K.A. Jamison "Analysis of an Inverse Railgun Power Source" IEEE Transmag, Vol. Mag-22, No. 6, pp 1669-1674 (1986).

[44] C.M. Fowler, D.B. Thomson, W.B. Garn, and R.S. Caird, LASL "Group M-6 Summary Report: The Birdseed Program", Los Alamos National Laboratory Report, LA-5141-MS (January, 1973).

[45] B.L. Freeman, R.S. Caird, D.J. Erickson, C.M. Fowler, W.B. Garn, H.W. Kruse, J.C. King, D.E. Bartram, and P.J. Kruse, "Plasma Focus Experiments Powered by Explosive Generators," Ref. 3, pp. 136-144.

[46] Ref 12, pp. 25-27.

[47] C.M. Fowler, R.S. Caird, W.B. Garn and D.B. Thowson "The Los Alamos Flux Compression Program from its Origin", Ref 1, pp. 7-8.

[48] Pulsed High Magnetic Fields, H. Knoepfel, North-Holland Publishing Company, Amsterdam and London, pp. 49-54 (1970), Figs. 3.2 and 3.3, and Eq. (3.32).

[49] Ref 12, pp. 4-11.

[50] D.B. Cummings and M.J. Morley "Electrical Pulses from Helical and Coaxial Generators" Ref 1, pp 451-470.

[51] J.W. Shearer, F.P. Abraham, C.M. Aplin, B.P. Benham, J.E. Faulkner, F.C. Ford, M.M. Hill, C.A. McDonald, W.H. Stephens, D.J. Steinberg, and J.R. Wilson, "Explosive-Driven Magnetic-Field Compression Generators", J. Appl. Phys. 39, No. 4, pp. 2102-2116 (1968).

[52] J.C. Crawford and R.A Damerow, "Explosively Driven High-Energy Generators", J. Appl. Phys., 39, No. 11, pp. 5224-5231 (1968).

[53] M. Jacques Morin and J. Vedel, "Generateurs de Courants Intenses par Conversion d'Energie Explosive en Energie Electrique", C. R. Acad. Sc. Paris, t. 272, Ser B, pp. 1-4 (1971).

[54] A.I. Pavlovskii, R.Z. Lyudaev, V.A. Zolotov, A.S. Seryoghin, A.S. Yuryzhev, M.M. Kharlamov, V.Ye. Gurin, G.M. Spirov, and B.S. Makaev, "Magnetic Cumulation Generator Parameters and Means to Improve Them", Ref. 2, pp. 557 - 583.

[55] A.I. Pavlovskii, R.Z. Lyudaev, L.L. Sel'Chenkov, A.S. Seryoghin, V.A. Zolotov, A.S. Duryzhev, D.I. Zenkov, V.Ye. Gurin, A.S. Boriskin, and V.F. Basmanov, "A Multiwire Helical Magnetic Cumulation Generator", Ref. 2, pp. 585-593.

[56] A.I. Pavlovskii, R.Z. Lyudaev, A.S. Kravchenko, V.A. Vasyukov, L.N. Pljashkevich, A.M. Shuvalov, A.S. Russkov, V.Ye. Gurin, B.A. Boyko, "Formation and Transmission of Magnetic Cumulation Generators Electromagnetic Energy Pulses", Ref.2, pp. 595-609.

[57] B.M. Novac, I.R. Smith, H.R. Stewardson, P. Senior, V.V. Vadher and M.C. Enache "Design, construction and testing of explosive-driven helical generators" J. Phys D-Appl Phys. 28, pp 807-823 (1995).

[58] Ref 12, pp 27-30

[59] V.K. Chernyshev, E.J. Zharinov, V.A. Demidov and S.A. Kazakov "High-Inductance Explosive Magnetic Generators with High Energy Multiplication, Ref. 2, pp 641-649 (See Table I).

[60] C.M. Fowler, R.S. Caird, B.L. Freeman and J.B. VanMarter, "Performance of the Mark IX Helical Flux Compression Generator," M-6 Technical Note No. 5, Los Alamos National Laboratory Report, (December, 1983).

[61] R.S. Caird "Characterization of the Mark IX Generator" M-6 Technical Note, No. 17, Los Alamos National Laboratory Report: LA-UR 87-4211 (1987).

[62] R.S. Caird and C.M. Fowler, "Conceptual Design for a Short-Pulse Explosive-Driven Generator," Ref. 4, pp. 425-431.

[63] C.M. Fowler, R.S. Caird, B.L. Freeman, and S.P. Marsh, "Design of the Mark 101 Magnetic Flux Compression Generator," Ref. 4, pp. 433-439.

[64] B.L. Freeman, C.M. Fowler, J.C. King, A.R. Martinez, J.B. VanMarter, L.R. Veeser, and J.E. Vorthman, "Testing of the Mark 101 Magnetic Flux Compression Generator," Ref. 4, pp. 441-445.

[65] R.S. Caird, C.M. Fowler, D.J. Erickson, B.L. Freeman, and W.B. Garn, "A Survey of Recent Work on Explosive-Driven Magnetic Flux Compression Generators", Energy Storage, Compression and Switching, Vol. 2, Eds. V. Nardi, H. Sahlin and W. H. Bostick, pp. 1-18, Plenum Press, New York and London (1983).

[66] R.S. Caird, D.J. Erickson, C.M. Fowler, B.L. Freeman, and J. H. Goforth, "A Circuit Model for the Explosive Driven Plate Generator", Ref. 3, pp. 246-253.

[67] C.M. Fowler, R.S. Caird, D.J. Erickson, B.L. Freeman, and J.C. King, "Explosive Flux Compression Generators for Rail Gun Power Sources", IEEE Trans. Mag., Vol. 18, No. l, pp. 64-67 (January, 1982).

[68] C.M. Fowler, D.R. Peterson, J.F. Kerrisk, R.S. Caird, B.L. Freeman, and J.H. Goforth, "Flux-Compression Strip Generators", Ref. 3, pp. 282-291.

[69] F. Herlach, H. Knoepfel, and R. Luppi, "Magnetic Field and Current Amplification with Non-Cylindrical Explosive Systems", Ref.1, pp 287-304 (See Figs. 3 and 4 and related text).

[70] E.I. Bichenkov, "Explosive Generators", Sov. Phys. Doklady, Vol. 12, pp. 567-569 (1967).

[71] Atomic energy Research in the Life and Physical Science, (report of the U.S. Atomic Energy commission, available from he Superintendent of Documents, U.S. Government printing Office, Washington DC), p. 104 (1960).

[72] J.E. Besancon, J. Morin, and J.M. Vedel, "Production de champ magnetique intense par implosion de tubes en cuivre non fendus," C. R. Acad. Sc Paris, t. 271, Ser. B, pp. 397-399 (August, 1970).

[73] A.I. Pavlovskii, N.P. Kolokolchikov, O.M. Tatsenko, A.I. Bykov, M.I. Dolotenko, and A.A. Karpikov, "Reproducible Generation of Multimegagauss Magnetic Fields", Ref. 2, pp.627 - 439.

[74] A.I. Pavlovskii, A.I. Bykov, M.I. Dolotenko, A.A. Karpikov, N.P. Kolokolchikov, V. 1. Mamyshev, and 0. M. Tatsenko, "Limiting Value of Reproducible Magnetic Field in Cascade Generator MC-I.", Ref. 4, pp. 37-54.

[75] C.M. Fowler and B.L. Freeman. "The Los Alamos-Arzamas-16 High Magnetic Field Shot Series, Ancho Canyon Site, 1993", Los Alamos National Laboratory report: LA-UR-94-2802.

[76] R.G. Clark, "Dirac Series: Results and Challenges" to be published in the Proceedings of the Eighth Megagauss Conference.

[77] B.A. Boyko, A.I. Bykov, M.I. Dolotenko, N.P. Kolokol'chikov, I.M. Markevtsev, O.M. Tatsenko and A.M. Shuvalov "Generation of magnetic Fields above 2000 T with the cascade Magneto-Cumulative Generator MC-1" to be published in the Proceedings of the Eighth Megagauss Conference.

[78] S. Felber, R.S. Caird, C.M. Fowler, D.J. Erickson, B.L. Freeman, and J.H. Goforth, "Design of a 20 -MJ Coaxial Generator", Ref. 3, pp.321-329.

[79] (a) M.G. Sheppard, B.L. Freeman, R.L. Bowers, J.H. Brownell, C.M. Fowler, J.N. Fritz, A.E. Greene, S.P. Marsh, T.A. Oliphant, D.L. Tubbs, and D.L. Weiss, "Design, Testing, and Modeling of a High-Gain Magnetic Flux-Compression Generator", Ref. 4, pp. 479-488.

(b) J.H. Goforth, W.T. Atchison, C.M. Fowler, R.E. Keinigs, H. Oona, D.G. Tasker, D.B. Reisman, P.T. Springer and R.C. Cauble, "Design of High Explosive Pulsed Power Systems for 20Mb Isentropic Compression Experiments" to be published in the Proceedings of the MG IX Conference.

[80] V.K. Chernyshev, B.E. Grinevich, V.V. Vahrushev, and V.I. Mamyshev, "Scaling

Image of 90 MJ Explosive Magnetic Generators", Ref. 5, pp.347-350.

[81] V.A. Demidov, A.I. Kraev, V.I. Mamyshev, A.A. Petrukhin, V.P. Pogorelov, V.K. Chernyshev, V.A. Shevtsev, and V.I. Shpagin, "Three-Module Disk Explosive Magnetic Generator", Ref. 5, pp. 351-354.

[82] I.R. Lindemuth, C.A. Ekdahl, C.M. Fowler, R.E. Reinovsky, S.M. Younger, V.K. Chernyshev, V.N. Mokhov and A.I. Pavlovskii "US/Russian Collaboration in High Energy Density Physics Using High Explosive Pulsed Power: Ultrahigh Current Experiments, Ultrahigh Magnetic Fields Applications and Progress Toward Controlled Thermonuclear Fusion" IEEE Trans Plasma Sci. 21, No 6,1997, pp 1357-1372.

[83] C.M. Fowler, R.F. Hoeberling, and S.P. Marsh, "Disk Generator with Nearly Shockless Accelerated Driver Plate," Ref. 5, pp. 337-345.

[84] S.J. Lukasik, G.W. Zepko and R.I. Jameson "Magnetic Flux Compression in an Expanding Geometry", Ref 1, pp. 397-419.

[85] V.A. Vasyukov, "Explosive Magnetic Generators of a Loop Type Operating within a Middle Range of Fast Current Pulses (15-45 MA)", in Ref. 7, pp. 292-293.

[86] E.I. Bichenkov and V.A. Lobanov, "Limiting Currents and Losses in Unshaped Flat and Coaxial Magnetic Compression Generators," Fizika Goreniya Vzryva, Vol. 16, No. 5, pp. 46-47 (1980).

[87] Knoepfel, "Very High Electromagnetic Density Research at Frascati up to the Seventies and Beyond", Ref. 4, pp. 7-18. (See Figs. 5 and 6).

[88] B.L. Freeman and D.G. Rickel, Los Alamos National Laboratory, private Communication. They have satisfactorily explained flux losses in simultaneous helical generators using reasonable skin-depth calculations.

[89] C.M. Fowler, "Losses in Magnetic Flux compression Generators, Part 1, Linear Diffusion", Los Alamos National Laboratory, Report LA-9956, Part 1, p. 12 (1984).

[90] C.M. Fowler, "Losses in Magnetic Flux Compression Generators, Part 2, Radiation Losses", Los Alamos National Laboratory Report, LA-9956-MS, Part 2, pp. 11-12 and 39-40 (1988).

[91] V.K. Chernyshev, E.I. Zharinov, S.A. Kazakoo, V.K. Busin, V.E. Vaneev and M.I. Korotkov, "Magnetic Flux Cutoffs in Helical Explosive Magnetic Generators", Ref. 4, pp. 455-469.

[92] J.M. Walsh, R.G. Shreffler, and F.J. Willig, "Limiting Conditions for Jet Formation in High Velocity Collisions", J. Appl. Phys., Vol. 24, No. 3, (1953) pp. 349-359.

[93] R.S. Caird, Los Alamos National Laboratory, private communication.

[94] J.H. Degnan, W.L. Baker, C.M. Fowler , R.S. Caird, D.J. Erickson, and B.L. Freeman, "Test of 10 Megajoule Electrical Output Magneto-Cumulative Generator", Ref. 3, pp. 352-358.

[95] C.M. Fowler, Los Alamos National Laboratory, private communications.

[96] Opening Switches, eds. A. Guenther, M. Kristiansen, and T. Martin, Plenum-Press, New York and London (1987). This book is the first of the ongoing series, "Advances in Pulsed Power Technology", edited overall by A. Guenther and M. Kristiansen.

[97] I. Vitkovitsky, High Power Switching, Van Nostrand Reinhold Company, New York (1987).

[98] 98. W.G. Chace and H.K. Moore, eds., Exploding Wires, Vol. 1 (1959), Vol. 2 (!962), Vol. 3 (1964), and Vol. 4 (1968), Plenum Press, New York.

[99] J.N. DiMarco and L.C. Burkhardt, "Characteristics of a Magnetic Energy Storage System Using Exploding Foils", J. Appl. Phys., 41 (9), pp. 3894-3899 (1970).

[100] I.R. Lindemuth, J.H. Brownell, A.E. Greene, G.H. Nickel, T.A. Oliphant and D. L. Weiss, "A Computational Model of Exploding Metallic Fuses for Multimegajoule Switching", J. Appl. Phys., 57(9), pp. 4447-4460 (1985).

[101] F.H. Webb, H.H. Hilton, P.H. Levine and A.V. Tollestrup, "The Electrical and Optical Properties of Rapidly Exploding Wires", Ref. 97, Vol. 2, pp. 37-74.

[102] T.J. Tucker and F.W. Neilson, "The Electrical Behavior of Fine Wires Exploded by a Coaxial Cable Discharge System", Ref. 97, Vol. 1, pp. 73-82.

[103] R.A. Damerow, J.C. Crawford, C.M. Fowler, R.S. Caird, K.J. Ewing, W.B. Garn, and D.B. Thomson, "An Explosive Generator Powered Theta-Pinch", Sandia Laboratories Report SCRR-6951 (1969).

[104] J.H. Goforth and S.P. Marsh, "Explosively Formed Fuse Opening Switches for Use in Flux Compression Generator Circuits", Ref. 5, pp. 515-526.

[105] J.H. Goforth and 37 other authors, "Procyon: 18MJ, 2μs Pulsed Power System", in Digest of Technical Papers, Tenth IEEE Pulsed Power Conference, IEEE Catalog No. 95CH35833, Eds. W.L. Baker and G Cooperstein, pp 478-483.

[106] V.K. Chernyshev, G.S. Volkov, V.A. Ivanov, and V.V. Vakhrushev, "Study of Basic Regularities of Formation of Multi-MA Current Pulses with Short Risetimes by EMG Circuit Interruption", Ref. 2, pp. 663-675.

[107] D.J. Erickson, R.S. Caird, C.M. Fowler, B.L. Freeman, W.B. Garn, and J.H. Goforth, "A Megavolt Pulse Transformer Powered by a Fast Plate Generator", Ref. 3, pp. 333-341.

[108] R.E. Reinovsky, R.G. Colclaser, J.M. Welby, and E.A. Lopez, "Energy Storage Transformer Power Conditioning Systems for Megajoule Class Flux Compression Generators", Ref. 4, pp. 575-582.

[109] R.E. Reinovsky. E. Lindemuth, and J.E. Vorthman, "High Voltage Power Condition Systems Powered by Flux Compression Generators", Proceedings of the Seventh IEEE Pulsed Power Conference, 1989, Monterey, CA, IEEE Catalog No. 89CH2678-2 , Eds. B. Bernstein and J. Shannon, pp 971-974 (June, ll-14).

[110] B.D. Khristoforov, I.I. Divnov, N.I. Zotov, and O.P. Karpov, "Experimental Research on Explosive-Driven Magnetic Generator Performance with Resistive-Inductive Load", Ref. 2, pp. 527-532.

[111] D.E. Christiansen, W.B. Garn, and C.M. Fowler, "Explosives Flux Compression Devices Project", DARPA Order Number 21619, Los Alamos Scientific Laboratory Report M-32, pp. 17-46 (August 1973).

[112] C.M. Fowler, R.S. Caird, D.J. Erickson, B.L. Freeman, and W.B. Garn, "Pulse Transformer Operation in Megagauss Fields", Ref. 2, pp. 275-285.

[113] R.E. Reinovsky, private communication.

[114] I. Bichenkov, V.S. Prokopiev, and A.N. Trubachev, "Magnetic Flux Transformation in Inductively Coupled Systems Using Magnetic Cumulation," Ref. 5, pp. 601-606.

[115] J.C. Martin, P.D. Champney, and D.A. Hammer, "Notes on the Construction Methods of a Martin High Voltage Pulse Transformer, 5.1", Rept. Cornell Univ. School of Electr. Eng., CU-NRL/2 (1967).

[116] B.L. Freeman, D.G. Rickel, A. Ramrus and B.E. Strickland "High-Voltage Pulsed Transformer Development" Ref 5, pp587-594.

[117] Coupling coefficients were measured as a function of frequency for a number of coaxial transformer configurations using different kinds of coaxial cables. Interested readers may contact the author for details.

[118] A.I. Pavlovskii, R.Z. Lyudaev, L.N. Pljashkevich, A.M. Shuvalov, A.S. Kravchenko, Yu.I. Pljashkevich, and V.A. Vasyukov, "Transformer Energy Output Magnetic Cumulative Generator," Ref. 2, pp. 611-626.

[119] C.M. Fowler and R.S. Caird, "The Mark IX Generator", Proceedings of the Seventh IEEE Pulsed Power Conference, Monterey, CA., IEEE Catalog No. 89CH2678-2, Eds. B. Bernstein and J Shannon, pp 475-479 (July 11-14,1989).

[120] J.E. Vorthman, C.M. Fowler, and R.F. Hoeberling, "A Battery Powered Flux Compression Generator", Ref. 5, pp. 437-440.

[121] See for example, Refs 13, 73, and 120.

[122] Ref. 11, pp. 365-367 gives a discussion of field diffusion through unslotted liners such as used in cylindrical implosion systems for more reproducible results.

[123] E.C. Cnare, R.J. Kaye, and M. Cowan, "An Explosive Generator of Cascade Helical Stages", Ref. 3, pp. 50-56.

[124] V.K. Chernyshev, E.I. Zharinov, V.E. Vaneev, A.I. Ionov, V.N. Buzin and Y.G. Bazanov, "Effective Comparison of Explosive Magnetic Cascade Systems", Ref 5, pp 355-365.

[125] J.C. Boydston, B.M. Freeman, and A.R. Luginbill, "Fast Helical Flux Compression Generator using a 50-mm Form Factor", ICOPS 2002, Alberta, Canada, (May, 2002).

[126] A.B. Prishchepenko. "Devices Build Around Permanent Magnets For Generating an Initial Current in Helical Explosive Magnetic Generators", Instruments and Experimental Techniques, Vol.38, №4, Part 2, pp. 515 - 520 (1995).

[127] D.M. Littrell, M.W. Heyse, K.A. Jamison, E.R. Parkinson, H. Zmuda, M.J. Matyac, and M.A. Cash, "Miniature Flux Compression Generators for Pulsed Telemetry", Proceedings of Megagauss IX, Moscow (2002), to be published.

[128] Andreas A. Neuber, Sergei I. Shkuratov, Thomas A. Holt, Evgueni F. Talantsev, James C. Dickens, John W. Walter, and Magne Kristiansen, "All-Explosive Pulsed Power Generator Systems", Proceedings of Megagauss IX, Moscow (2002), to be published.

[129] R.A. Marshall, "Railgunnery: Where Have We Been? Where are We Going?", IEEE Trans. On Magnetics, 37(1), Jan. 2001, pp.440 - 444.

[130] D.R. Peterson and C.M. Fowler, "Rail Gun Powered by an Integral Explosive Generator" in Proceedings of the Impact Fusion Workshop, 1979, pp 234-244. ed. A.T. Peaslee, Los Alamos National Laboratory report LA-8000-C.

[131] R.S. Hawke, A.L. Brooks, F.J. Deadrick, J.K. Scudder, C.M. Fowler, R.S. Caird and D.R. Peterson "Results of Railgun Experiments Powered by Magnetic Flux Compression Generators", IEEE TRANS-MAGN, MAG-18,1 (1982), pp 82-93.

[132] G.A. Shvetsov, Yu.L. Bashkatov, A.G. Anisisov, and I.A. Stadnichenko, "Flux Compression Generators for Railguns", Digest of Technical papers: 8 th IEEE International Pulsed Power Conference, Eds. K. Prestwick and R. White, IEEE Catalog No, 91CH30528 (1991), pp 465-471.

[133] E.L. Zimmermann, C.M. Fowler, E. Foley and J.V. Parker "Himass Electromagnetic Launches at Los Alamos" IEEE Trans Mag, 22, No. 6 (1986), pp 1823-1825.

[134] A.B. Prishchepenko, V.V. Kiseljov, I.S. and Kudimov, "Radio Frequency Weapon at the Future Battlefield", Proceedings of the European Electromagnetic International Conference on Electromagnetic Environments and Consequences, EUROEM 94, Bordeaux, France, Ed. D.J. Serafin, Gramat, France, p.p. 266 - 271 (May 30 - June 3, 1994).

[135] B.M. Novac and I.R. Smith, "Considerations of an Autonomous Compact Source for High-Power Microwave Applications", IEEE Transactions on Plasma Science (Special Issue on Pulsed Power Science & Technology), 28(5), pp 1620-1623, ISSN: 0093 3813 (October 2000).

[136] V.V. Mintsev, A.E. Ushnurtsev, V.E. Fortov, A.A. Leontyev, A.V. Shurupov, G.F. Kiuttu, "Multi-Stage Flux-Trapping Helical Flux Compression Generators" , Proceedings of the Conference "Pulsed Power Plasma Science 2001, Las Vegas, Nevada, June 17-22, 2001" Eds. R. Reinovsky and M Newton, IEEE Catalog No, 01CH37251, pp 994-997.

[137] E.I. Azarkevich, A.N. Didenko, A.G. Zherlitsin, Yu.V. Karpushin, A.A. Leontiev, G.V. Melnikov, V.B. Mintsev, A.E. Ushnurtsev, G.P. Fomenko, V.E. Fortov, V.I. Tsvetkov, V.B. Schneider, B.K. Yasel'ski, "Generation of electron flux and Pulses of Microwave Radiation by the Energy of Chemical Explosives", Teplofiz. Vys. Temp., 32(1), pp. 127-132 (1994).

[138] V.E. Fortov, A.N. Didenko, Y.V. Karpushin, A.A. Leontyev, V.B. Mintsev, A.E. Ushnurtsev, G.P. Fomenko, G.V. Melnikov, V.I. Tsvetkov, A.G. Zherlitsin, E.I. Azarkevich, V.B. Shneider, and B.K. Yaselski, "Generation of High Power Electron Beam and Microwave Radiation with the Aid of High Explosives", Ref 6, pp 939-946.

[139] B.L. Freeman, D.J. Erickson, C.M. Fowler, R.F. Hoeberling, J.C. King, P.J. Kruse, A.L. Peratt, D.G. Rickel, L.E. Thode, J.W. Toevs, and A.R. Williams, "Magnetic Flux Compression Generator Powered Electron Beam Experiments," Ref. 4, pp. 729-737.

[140] M. Kristiansen, P. Worsey, B.L. Freeman, and F. Stefani, Explosive-Driven Pulsed Power Generation (MURI 98), Report No. AFOSR MURI 00-2, (Sept. 1, 2000).

[141] Jason Baird, "Shock Wave Interactions at Explosive-Metallic Interfaces" Dissertation, University of Missouri, Rolla (July, 2001).

[142] B.L. Freeman, J. Rock, and L.L. Altgilbers, "25 mm Helical MCG", DEPS 4th DEW Conference, Huntsville, (November, 2001).

[143] A. Neuber, T. Holt, J. Hernandez, J. Dickens, and M. Kristiansen, "Geometry Impact on Flux Losses in MCGs," prepared for the Ninth International Conference on Megagauss Magnetic Field Generation and Related Topics, Moscow-St. Petersburg (July 7-14, 2002).

[144] B.M. Novac, I.R. Smith, H.R. Stewardson, P. Senior, P., V.V. Vadher, and M.C. Enache, "Design, Construction and Testing of Explosive-Driven Helical Generators", J Physics D, Applied Physics, 28, pp. 807-823, ISSN: 0022-3727 (April 1995).

[145] B.M. Novac, I.R. Smith, M.C. Enache, and H.R. Stewardson, "Simple 2D Model for Helical Flux-Compression Generators", Laser and Particle Beams, 15(3), pp. 379-395, ISSN 0263 0346 (October, 1997).

[146] M.C. Enache, B.M. Novac, I.R. and Smith, "3-Dimensional Modeling of Helical Flux-Compression Generators", IEE Symposium Pulsed Power '99, IEE, London, Oxford, UK, pp. 24/1-24 (April, 1999).

[147] T.G. Engel, J.E. Becker, and W.C. Nunnally, "Energy Conversion and High Power Pulse Production using Miniature Magnetic Flux Compressors", IEEE Transactions on Plasma Science, 28(5), October (2000).

[148] X. Gong, M. Cai, Y. Chen, S. Zhong, and C. Sun, "A Compact Magnetic Flux Compression Generator Driven by Explosives", Ref. 4, pp. 417-424.

[149] Q. Sun, C. Sun, X. Gong, W. Xie, Z. Liu, W. Dai, Y. Chi, and S. Fu, "An Effective Explosive Magnetic Flux Compression Generator with 102 nH Inductance Load", Preprint, Megagauss IX Conference, Russia (2002).

[150] M. Bavay, P. L'Eplattenier, C. Mangeant, F. Hamann, Ph. Monjaux, F. Lassalle, F. Bayol, D. Huet, G. Avrillaud, and B. Lalle, "The Magnetic Flux Compression Scheme as a Power Amplification & Pulse Shaping Stage", ICOPS 2002, Canada (2002).

[151] G. Staines, "Compact Sources for Tactical RF Weapon Applications" AMEREM 2002, Annapolis, Maryland (2002).

[152] "Rheinmetall Sets out Its Energy Weapon Stall", International Defense Review, Jane's International Group, Feb. 01, 2003.

[153] Geoff Turner, Nuclear Energy Corporation of South Africa, Private Communication (2003).

[154] J.W. Ahn, J.H. Kuk, J. Lee, J.S. Choi, C.H. Kim, and J.H. Ryu, "Output Characteristics of Serially Connected Magneto-Cumulative Generators", Preprint (2002).

[155] J.H. Kuk, J.W. Ahn, and H.H. Lee "Output Characteristics of the Cascade MCG System Consisting of Several MCGs Connected in Parallel", Preprint (2002).

[156] J.S. Choi, J. Lee, J. Ryu, and J.W. Ahn, "Explosive-Driven Ferromagnetic Generators as an Initial Energy Source of Compact Pulsed Power System", IEEE Preprint (2002).

[157] Gert Bjarnholt, FOI, Sweden, Private Communications.

[158] Institute of Electromagnetic Research, www.iemr.vl.net.ua.

[159] Code distribution is limited. Consult D.G. Tasker, Los Alamos National Laboratory, for details. E-mail: tasker@lanl.gov.

[160] J.B. Chase, D.Chato, G. Peterson, and P. Pincosy, "GAGEN: A Modern, PC Based Computer Modeling Tool for Explosive MCG Generators and Attached Loads", Proceedings of Megagauss VIII, Tallahassee (1998), to be published.

[161] M.G. Giesselmann, T. Heeren, A. Neuber, and M. Kristiansen, "Advanced Modeling of a Exploding Flux Compression Generator Using Lumped Element Models of Magnetic Diffusion," Proceedings of the IEEE Pulsed Power and Plasma Science Conference, Las Vegas, NV (June 17-22, 2001), Eds. R. Reinovsky and M. Newton, IEEE Catalog No. 0101CH37251, pp162-165.

[162] R. Parkinson, K.A. Jamison, J.B. Cornette, M.A. Cash, C.M. Fowler and J.D. Goettee, "Continued Benchmarking of an FCG Code" Proceedings of the 12th IEEE Pulsed Power Conference, Monterey, CA, IEEE Catalog No.99CH36358, Eds. C. Stallings and H. Kirbie pp.724-727 (June 27-30, 1999).

[163] L.L. Altgilbers, I. Merritt, M.D. Brown, and P. Tracy, "Semi-Empirical Model for the Resistance of Spiral Magnetocumulative Generators", Megagauss VIII, Tallahassee (1998), to be published.

[164] B.M. Novac, I.R. Smith, I.R., H.R. Stewardson, H.R., K. Gregory, and M.C. Enache, "Two-Dimensional Modeling of Flux-Compression Generators", IEE Symposium on Pulsed Power, IEE, London, pp 361-363 (April, 1998).

[165] B.M. Novac and I.R. Smith, "Fast Numerical Modeling of Helical Flux Compression Generators", Megagauss IX, Russia (July, 2002), to be published.

[166] Geoff Turner, Nuclear Energy Corporation of South Africa, Private Communication (2003).

[167] V.K. Chernyshev, G.I. Volkov, S.V. Pak, V.A. Ivanov, A.N. Skobelev, I.V. Morozov, V.P. Korchagin and A.N. Demin "Reduction of Extreme Conditions of Mago Chamber Operation by Changing the Shape of Pulse of Plasma Magnetization Current" in Pulsed Power Plasma Science 2001. R. Reinovsky and M. Newton, IEEE Catalog No. 01CH37251, pp 957-958.

[168] Tasker D.G., Fowler C.M., Goforth J.H., Keinigs R.K., Oona H., Reisman D.B., Springer P.T. and Cauble R.C. Isentropic Compression Experiments Using High Explosive Pulsed Power // in press, Proceedings of the 9-th Megagauss Conference.